

APPROVAL SHEET

Title of Dissertation: Effects of Urban Development on Groundwater Flow Systems and Streamflow Generation

Name of Candidate: Aditi Seth Bhaskar
Doctor of Philosophy, 2013

Dissertation and Abstract Approved: *Claire Welty*

Dr. Claire Welty
Professor
Chemical, Biochemical, and Environmental
Engineering

Date Approved: 2 Dec 2013

Curriculum Vitae

Name: Aditi Seth Bhaskar.

Degree and date to be conferred: Ph.D., 2013

Secondary education:

Montgomery Blair High School, Silver Spring, MD, June 2004.

Collegiate institutions attended:

Brown University
September 2004 – May 2008, Sc.B., 2008
Major: Geology-Physics/Math.

University of Maryland, Baltimore County
August 2008 – December 2013, Ph.D., 2013
Major: Environmental Engineering.

Professional Publications:

Bhaskar, A.S. and C. Welty. 2012. Water Balances along an Urban-to-Rural Gradient of Metropolitan Baltimore, 2001-2009. *Environmental and Engineering Geoscience*. 18(1), 37-50. doi: 10.2113/gseegeosci.18.1.37.

Bhaskar, A.S., J.W. Harvey, and E.J. Henry. 2012. Resolving hyporheic and groundwater components of streambed waterflux using heat as a tracer, *Water Resources Research*, 48, W08524, doi: 10.1029/2011WR011784.

Neupauer, R.M., J.L. Wilson, and A.S. Bhaskar. 2009. Forward and backward temporal probability distributions of sorbing solutes in groundwater, *Water Resources Research*, 45, W01420, doi:10.1029/2008WR007058.

ABSTRACT

Title of Document: EFFECTS OF URBAN DEVELOPMENT ON
GROUNDWATER FLOW SYSTEMS AND
STREAMFLOW GENERATION

Aditi Seth Bhaskar, Ph.D., 2013

Directed By: Dr. Claire Welty
Professor
Department of Chemical, Biochemical, and
Environmental Engineering

This work quantifies the impacts of urban development on groundwater storage and groundwater-surface water interactions using intensive data analysis and mathematical modeling. The monthly water balance for the period 2000-2009 for 65 Baltimore area watersheds was calculated using remote sensing data and the dense network of instrumented sites in this region. This analysis included estimation of spatially-distributed anthropogenic fluxes (water supply pipe leakage, lawn irrigation, and infiltration and inflow (I&I) of groundwater and stormwater into wastewater pipes) as well as natural fluxes of precipitation, streamflow, and evapotranspiration. Inflow fluxes of water supply pipe leakage and lawn irrigation were significant but small compared to precipitation, but I&I was approximately equal to gaged streamflow. Building on knowledge of the altered water balance, an integrated hydrologic model of the Baltimore metropolitan region was developed to quantify the impact of urban development on groundwater storage. The three-dimensional groundwater-surface water-land surface model ParFlow.CLM was implemented and a methodology to incorporate urban and hydrogeologic input

datasets was developed. Using the model, the impacts of reduced vegetative cover, impervious surfaces, I&I, and other anthropogenic discharge and recharge fluxes were isolated. Removal of I&I led to the largest change in storage, and removal of impervious surface cover had the smallest effect. To investigate the relationship between pre-event water proportion, storage, and streamflow at small watershed scales spanning a gradient of urbanization, chemical hydrograph separation, hillslope numerical experiments, and simple dynamical systems analysis were utilized. From analysis of high-frequency specific conductance data, the pre-event water proportion of stormflow was found to be greatest for storms with higher total precipitation. Using the simple dynamical systems approach, watersheds with larger percentages of impervious surfaces were found to have the largest sensitivity of streamflow to changes in storage. HydroGeoSphere, a three-dimensional groundwater-surface water flow and transport model, was implemented in an idealized hillslope and showed that the relationship between streamflow and storage was clockwise hysteretic. Overall this work demonstrates the importance of infrastructure leakage on urban hydrologic systems and shows that pre-event water contributions of stormflow are primarily related to precipitation and not initial storage in urban watersheds.

EFFECTS OF URBAN DEVELOPMENT ON GROUNDWATER FLOW
SYSTEMS AND STREAMFLOW GENERATION

By

Aditi Seth Bhaskar

Dissertation submitted to the Faculty of the Graduate School of the
University of Maryland, Baltimore County, in partial fulfillment
of the requirements for the degree of
Doctor of Philosophy
2013

UMI Number: 3609831

All rights reserved

INFORMATION TO ALL USERS

The quality of this reproduction is dependent upon the quality of the copy submitted.

In the unlikely event that the author did not send a complete manuscript and there are missing pages, these will be noted. Also, if material had to be removed, a note will indicate the deletion.



UMI 3609831

Published by ProQuest LLC (2014). Copyright in the Dissertation held by the Author.

Microform Edition © ProQuest LLC.

All rights reserved. This work is protected against unauthorized copying under Title 17, United States Code



ProQuest LLC.
789 East Eisenhower Parkway
P.O. Box 1346
Ann Arbor, MI 48106 - 1346

© Copyright by
Aditi Seth Bhaskar
2013

Acknowledgements

First, I would like to deeply thank my graduate advisor, Dr. Claire Welty, for her constant guidance, support, and mentorship over the past five years. I also appreciate the guidance of my committee members, Dr. Reed Maxwell, Dr. Keith Eshleman, Dr. Upal Ghosh, and especially Dr. Andrew J. Miller. I am grateful to my fellow graduate students in the Environmental Engineering program, in the IGERT program, and others I have interacted with at UMBC for their fellowship and camaraderie, and to all the ParFlow users who have helped with my model development issues. Last, I acknowledge my husband, Daniel Curl, for celebrating the high points, providing support at the low points, and always encouraging me through this journey.

Table of Contents

| | |
|--|-----|
| Acknowledgements..... | ii |
| Table of Contents..... | iii |
| List of Tables..... | v |
| List of Figures..... | vi |
| Chapter 1 : Introduction..... | 1 |
| 1.1 Motivation..... | 1 |
| 1.2 Research Questions..... | 3 |
| 1.3 Study Area..... | 4 |
| 1.4 Overview of Dissertation Chapters..... | 5 |
| Chapter 2 : Water Balances along an Urban-to-Rural Gradient of Metropolitan Baltimore, 2001-2009..... | 8 |
| 2.1 Introduction..... | 8 |
| 2.2 Study Area..... | 13 |
| 2.3 Methods..... | 17 |
| 2.4 Results..... | 22 |
| 2.5 Discussion..... | 37 |
| 2.6 Conclusions..... | 41 |
| 2.7 Acknowledgements..... | 43 |
| Chapter 3 : Untangling the effects of urban development on subsurface storage in Baltimore..... | 44 |
| 3.1 Introduction..... | 44 |
| 3.2 Methods..... | 49 |
| 3.2.1 Model geometry and boundary conditions..... | 49 |
| 3.2.2 Meteorological forcing and land surface model input data..... | 51 |
| 3.2.3 Processing and synthesis of material properties and urban flux input data 52 | |
| 3.2.4 Model initialization..... | 63 |
| 3.2.5 Model calibration of Manning's n..... | 65 |
| 3.2.6 Model development to isolate effects of different urban features..... | 67 |
| 3.3 Results..... | 68 |
| 3.3.1 Initialization..... | 68 |
| 3.3.2 Model comparison with observed data..... | 70 |
| 3.3.3 Isolation of urban features in model scenarios..... | 72 |
| 3.4 Discussion..... | 78 |
| 3.4.1 Model development..... | 78 |
| 3.4.2 Limitations..... | 80 |
| 3.4.3 Urban features..... | 82 |
| 3.5 Conclusions..... | 83 |
| 3.6 Acknowledgements..... | 86 |
| Chapter 4 : Urban watershed storage and streamflow generation..... | 88 |
| 4.1 Introduction..... | 88 |
| 4.1.1 Chemical hydrograph separation studies..... | 89 |
| 4.1.2 Stormflow generation mechanisms..... | 90 |

| | | |
|------------------------------|--|-----|
| 4.1.3 | Purpose..... | 95 |
| 4.2 | Methods..... | 96 |
| 4.2.1 | Hillslope numerical experiments | 96 |
| 4.2.2 | Simple dynamical systems to develop storage-streamflow relationship 101 | |
| 4.2.3 | Specific conductance measurements for use in chemical hydrograph separation | 107 |
| 4.2.4 | Question 1. Controls on pre-event water proportion | 107 |
| 4.2.5 | Question 2. Controls on storage-streamflow relationship | 109 |
| 4.2.6 | Question 3. Relationship between storage and pre-event water proportion..... | 110 |
| 4.3 | Results..... | 111 |
| 4.3.1 | Question 1. Controls on pre-event water proportion | 111 |
| 4.3.2 | Question 2. Controls on storage-streamflow relationship | 117 |
| 4.3.3 | Question 3. Relationship between storage and pre-event water proportion..... | 126 |
| 4.4 | Discussion..... | 126 |
| 4.4.1 | Precipitation amount as the primary control on pre-event water proportion..... | 126 |
| 4.4.2 | Controls on the storage-streamflow relationship | 128 |
| 4.4.3 | Storage as a secondary control on pre-event water proportion..... | 130 |
| 4.4.4 | Limitations of water balance based approach in an urban setting | 133 |
| 4.5 | Summary and implications | 134 |
| 4.6 | Acknowledgements..... | 137 |
| Chapter 5 : Conclusions..... | | 138 |
| 5.1 | Summary..... | 138 |
| 5.2 | Contributions..... | 143 |
| 5.3 | Recommendations for future work | 144 |
| 5.3.1 | Application to other cities..... | 144 |
| 5.3.2 | Implications for water quality..... | 145 |
| 5.3.3 | Consideration of infrastructure condition for urban water management 146 | |
| 5.3.4 | Need for improved urban water and evapotranspiration data..... | 147 |
| 5.3.5 | Data access and synthesis | 147 |
| Symbols..... | | 150 |
| Bibliography | | 151 |

List of Tables

| | |
|---|-----|
| Table 3.1. Anthropogenic discharge and recharge fluxes summed over the entire model domain (mm/day)..... | 64 |
| Table 4.1. Material properties used in hillslope model. Values shown are the base case model values, some of which are modified in numerical experiments (Table 4.3)..... | 100 |
| Table 4.2. Watersheds used for chemical hydrograph separation and simple dynamical systems analysis, along with drainage area and impervious surface cover..... | 104 |
| Table 4.3. Hillslope numerical experiments. | 106 |
| Table 4.4. Dead Run sub-watershed chemical hydrograph separation for storm events. | 113 |

List of Figures

- Figure 2.1. Locations of study watersheds relative to major river basins and political boundaries, with colors representing percentage watershed impervious area. Streams from the National Hydrography Dataset (NHD) are shown as solid black lines. USGS stream gage locations are shown as black dots. Watersheds were delineated by USGS or by UMBC/CUERE. Percent impervious surface area is from the National Land Cover Dataset (NLCD) 2006. Stream gages in reservoir-containing watersheds are designated by stars. 15
- Figure 2.2. Monthly means and standard deviations (SD) over all study watersheds of precipitation, streamflow and evapotranspiration (ET). 24
- Figure 2.3. Monthly means over all study watersheds, averaged for each season. Urban watersheds are those with 5% impervious area or greater. 24
- Figure 2.4. Regional annual means showing interannual variability, along with precipitation (P), streamflow (Q), evapotranspiration (ET) and water balance residual $P-Q^*-ET$, where Q^* indicates streamflow $Q +$ reservoir withdrawals W for the two reservoir-containing watersheds. 25
- Figure 2.5. GRACE (Gravity Recovery and Climate Experiment) storage and derived storage both normalized by subtraction of their respective means over 2003-2007, and shown monthly for the time period when the datasets overlap (April 2002 - September 2009). Derived storage represents the sum of $P-Q^*-ET$, and is given for the average of all watersheds (overall) and the urban and rural subsets. Breaks in the GRACE time series in early months are due to unavailable data (GRACE Tellus POET, 2011). 27
- Figure 2.6. Mean annual precipitation 2000-2009 from Parameter-elevation Regression on Independent Slopes Model (PRISM) monthly precipitation grids (PRISM Climate Group, 2011). 29
- Figure 2.7. Mean annual streamflow $Q +$ reservoir withdrawals W , where $Q^* = Q+W$. Mean annual streamflow 2000-2009 is from the USGS NWIS (U.S. Geological Survey, 2011). Reservoir withdrawals were estimated for Liberty Reservoir (Charshee, personal communication, 2010) and T. Howard Duckett Reservoir [*Prince George's County*, 2008]. 29
- Figure 2.8. Mean annual ET from GLDAS (Global Land Data Assimilation System)/Noah, available at the GES DISC (Goddard Earth Sciences Data and Information Services Center, 2011). 30
- Figure 2.9. Mean annual $P-Q^*-ET$, where the sources of P , Q^* and ET are as indicated in Figures 2.6-2.8. 30
- Figure 2.10. Logarithm of impervious area vs. $P-Q^*-ET$ (mm), where the size of the marker is proportional to watershed area. The division between urban and rural at 5% impervious is at 0.7 on the log-scale of the horizontal axis. 31
- Figure 2.11. Contributions of lawn irrigation (A) and water supply pipe leakage (B) in mm/mo over Baltimore City, the served area of Baltimore County and the watersheds contained in these areas. 33
- Figure 2.12. Infiltration and inflow in mm/year per sewershed from the Baltimore City Comprehensive Wastewater Monitoring Program [*Espinosa and Wyatt*,

| | | |
|--------------|--|----|
| | 2007; Espinosa, personal communication 2010]. The hatched areas are those for which I&I estimates are not available. Gwynns Run and Moores Run watersheds are indicated by heavy black boundaries. | 35 |
| Figure 2.13. | Comparison of the annual water balance components between the mean of 32 rural (impervious area < 5% and without reservoirs) and two urban watersheds in Baltimore City (Gwynns Run and Moores Run). The width of the arrows corresponds to the magnitude of the flows in mm/yr. Components were estimated separately (not by subtraction) so inflows do not necessarily equal outflows. | 36 |
| Figure 3.1. | Model input data required for surface-subsurface flow models (blue outlines) and input data specific to urban areas (black outlines). The arrows indicate data sources for the urban and hydrogeologic data sets needed. Numbers indicate urban data sets altered for scenarios, where 1 indicates the vegetated city scenario, 2 indicates the pervious city scenario, 3 indicates the no-I&I scenario, and 4 indicates the no-anthropogenic-discharge-or-recharge scenario. Modified from Figure 6.1 in <i>Welty et al.</i> [2007]. | 48 |
| Figure 3.2. | Map showing extent of model domain, stream gages and monitoring well locations, impervious surface coverage, physiographic provinces, and location within the Chesapeake Bay watershed. | 50 |
| Figure 3.3. | (a) Three slices through the three-dimensional model domain showing log (hydraulic conductivity in m/s). (b) Spatial distribution of upscaled soil SSURGO (http://soildatamart.nrcs.usda.gov/USDGSM.aspx) horizontal hydraulic conductivity (m/s). | 53 |
| Figure 3.4. | (a) Percentage of 500 m x 500 m model grid cell composed of grass/shrub based on the resampling of the University of Vermont Spatial Analysis Laboratory classification (http://128.118.47.34/chesapeakeview/MetadataDisplay.aspx?file=Landcover_2007_4county_baltmetro.xml&dataset=3152). (b) Total length of water supply pipes (m) in each model grid cell within the Baltimore water service area. (c) Number of residential private wells in each model grid cell outside of the municipal water service area derived using MdPropertyView 2009 (http://www.mdp.state.md.us/OurProducts/PropertyMapProducts/MDPropertyViewProducts.shtml). (d) Baltimore County and Baltimore City infiltration and inflow of groundwater and stormwater into wastewater pipes (combined for wet and dry weather) in each sewershed (mm/year). | 59 |
| Figure 3.5. | (a) Simulated subsurface storage summed over the model domain during the spin-up time period (black) and daily precipitation forcing over the same time period (blue). (b) Simulated daily change in subsurface storage during the spin-up time period (black) where positive values indicate an increase in subsurface storage compared to the previous day, as well as daily precipitation forcing (blue). | 69 |
| Figure 3.6. | Modeled and observed hydrographs over 1 January 2007 – 30 June 2007 at three example stream gages. These are Winters Run near Benson, MD (USGS 01581700), NW Branch Anacostia River near Colesville, MD (USGS 01650500), and Patuxent River near Bowie, MD (USGS 01594440). | 71 |

| | |
|---|-----|
| Figure 3.7. Base case daily water balance from 1 January 2007 – 30 June 2007. (a) Simulated subsurface storage in m (volumetric subsurface water storage in m^3 divided by surface area of domain) and model forcing precipitation; (b) simulated streamflow; (c) simulated evapotranspiration; and (d) model mass balance, where change in total model storage is compared to inflows minus outflows (precipitation – evapotranspiration – streamflow – anthropogenic withdrawals). Total anthropogenic withdrawals were 1.93 m/hour. | 73 |
| Figure 3.8. Percent difference between base-case subsurface storage and subsurface storage for each scenario compared to precipitation minus evapotranspiration summed over the simulation period (1 January 2007 – 30 June 2007). | 74 |
| Figure 3.9. Difference maps of land surface pressure head (m) for each scenario minus base-case land surface pressure head (m) at 30 June 2007. (a) Vegetated city scenario. (b) No-I&I scenario. (c) No-anthropogenic-discharge-or-recharge scenario. | 76 |
| Figure 4.1. Schematic of hillslope model domain and setup. Not to scale. | 99 |
| Figure 4.2. Map of watersheds used for simple dynamical systems analysis (Baisman Run, Delight, and Dead Run at Franklinton), and an inset showing the sub-watersheds of Dead Run that were used for the chemical hydrograph separation study (DRKR, DR1, DR2, DR3, DR4, and DR5). Red dots indicate stream gages, gray background indicates impervious surface cover, and blue lines represent hydrography (daylighted and buried streams). | 103 |
| Figure 4.3. Pre-event water proportion based on Table 4.1 using chemical hydrograph separation from Dead Run sub-watersheds. Color of marker corresponds to drainage area, indicated in km^2 in legend. Label indicates station name abbreviation. | 112 |
| Figure 4.4. Model domain to scale of hillslope with base-case parameters. Colors indicate contours of head (m) at 14000 s (37 minutes after rain event ends). | 114 |
| Figure 4.5. (a). Streamflow over time for model simulations given in Table 4.2. (b). Pre-event water proportion (Equation 4.4) for model simulations. Inset shows increased y-axis range of pre-event water proportion. (c). Subsurface storage calculated by Equation 4.5. Subsurface storage for each model is divided by its mean subsurface storage. | 116 |
| Figure 4.6. Subsurface storage vs. total and pre-event streamflow with base-case parameters in hillslope numerical experiments. Arrows indicate time, where rising limb indicates during the rain event, and falling limb indicates after the rain event. | 118 |
| Figure 4.7. Hydraulic head (m) at the land surface vs. distance from stream (m), shown for multiple time points. Before the storm, the hydraulic head was relatively constant, so the curve for 9000 s is directly underneath the curve for 10,000 s. | 119 |
| Figure 4.8. Hourly change in discharge vs. change in discharge on log and linear axes for the three study watersheds, along with bin means and bin fits. | 120 |
| Figure 4.8. Discharge sensitivity functions vs. discharge in linear (left) and logarithmic (right) axes, along with bins for three study watersheds and previously published work [Kirchner, 2009; Teuling et al., 2010]. | 122 |

| | |
|--|-----|
| Figure 4.9. Streamflow vs. watershed storage using the simple dynamical systems analysis, where storage is determined by integration, and therefore includes an unknown constant of integration (Equation 4.3)..... | 124 |
| Figure 4.10. Streamflow simulation for Dead Run, Delight, and Baisman during an 8-day period in February 2005 using simple dynamical systems approach..... | 125 |
| Figure 4.11. Pre-event water proportion and subsurface storage using base-case parameters in hillslope numerical experiments. Arrows indicate time, where before rain event indicates baseflow, rising limb indicates during the rain event, and falling limb indicates after the rain event. | 127 |
| Figure 4.12. Precipitation and stormflow during storm events in Dead Run at Franklinton (DRKR). Circle size is proportional to pre-event streamflow (baseflow). Stormflow was calculated from USGS streamflow records using the straight-line method for hydrograph separation, while maintaining equal pre- and post-storm baseflow values. Precipitation values were averaged over the watershed from bias-corrected Hydro-NEXRAD radar rainfall values [Smith et al., 2012]. Only isolated storm events were used, such that a direct response between a specific precipitation event and storm response could be manually identified. | 131 |

Chapter 1: Introduction

1.1 Motivation

Environmental systems are undergoing fundamental regime shifts from the dual forcing of human-caused climate change and land use change. Managing environmental systems under global change requires evaluation of the processes that lead to alteration in hydrologic fluxes, flowpaths, and stores, since we cannot simply rely on past records or envelopes of variability [Milly *et al.*, 2008; Wagener *et al.*, 2010] for predicting the future state of the system. In this work, I focus in particular on the impacts of land use change on the hydrologic cycle as a result of urban development. While there is still substantial uncertainty about the potential impact of climate change on most hydrologic systems, urban land use change has already led to considerable alteration of the water cycle.

There has been a migration of human populations to cities in the U.S. over the past century, and this migration is still underway in much of the world. Since 2007, most of the global population lives in cities [United Nations Population Division, 2011]. Cities are drivers of economic output and provide some environmental benefits through lower consumption of resources, such as fuel, due to greater population density [Grimm *et al.*, 2008]. Urban development alters all aspects of the hydrologic cycle, although the impacts on streamflow have been most studied. Led by the work of Leopold [1968], researchers have come to understand that urban streams have an altered flow regime compared to undeveloped systems. Urban streams are flashier, with shorter lag times between precipitation and peak flow, increased peak flows, increased storm flow volumes, and decreased recession times

[Leopold, 1968; Lull and Sopper, 1969; Rose and Peters, 2001; Beighley and Moglen, 2002]. Geomorphic changes in urban streams can be severe, including the piping, straightening, and incision of urban streams, leading to the disconnection of streams from riparian zones and floodplains, and the extension of the drainage network by storm drains and roads. Flow regime alteration, water quality degradation, and geomorphic changes are associated with outcomes such as increased flooding, increased channel erosion, polluted waterways [Paul and Meyer, 2001; Kaushal et al., 2005; Kaushal and Belt, 2012], altered biogeochemical processes [Mayer et al., 2010], and ecological degradation [Walsh, 2004], which together are referred to as the urban stream syndrome [Walsh et al., 2005].

Even with all that researchers have established about the environmental impacts of urban development, there are still significant gaps in our understanding about the effects on hydrologic systems. We generally do not have even the seemingly basic knowledge of the water balance of cities—how much water enters urban watersheds or aquifers in what form, how much is stored, and how much water leaves by what pathways [Pataki et al., 2011]. Quantifying urban groundwater storage and changes to that storage is needed for estimating water availability, elucidating groundwater-surface water interactions and biogeochemical processing, and preservation of baseflow in urban streams, but researchers have pointed out major knowledge gaps in this area [Kaushal and Belt, 2012; Hamel et al., 2013]. The impact of urban development (such as leaking water pipes or impervious surfaces) can lead to a wide variety of impacts on groundwater recharge and stream baseflow, but the isolated effects of the various components of development on groundwater are

generally unknown. This is exacerbated by the fact that groundwater-surface water modeling of urban areas is extremely complex and therefore usually not attempted. It is also not known how concepts describing the connection between groundwater and surface water systems, developed for more pristine environments, extend to urban areas. Examples include how groundwater contributes to stormflow in urban areas, and the applicability of the simple dynamical systems approach to relate storage and streamflow in cities. Urban areas may be used as an end-member to characterize hydrologic regimes where storage-discharge relationships and streamflow generation are affected by considerable hydrologic alteration.

1.2 Research Questions

The motivation for this dissertation is to address the knowledge gaps defined above. The goal is to quantify the effects of urban development on hydrologic systems in new ways. In particular, the focus is on the urban water balance, groundwater storage, and streamflow generation. The primary questions my research seeks to answer are as follows:

1. How does the water balance change along the urban-to-rural gradient, both in the forms and relative amounts of watershed inflows and outflows?
2. How do the magnitudes of human-induced (“urban”) water fluxes (water supply pipe leakage, wastewater infiltration and inflow, and lawn irrigation) compare to natural inflows (precipitation) and outflows (streamflow and evapotranspiration)? Which urban fluxes are most significant?
3. How do urban and rural water balances vary as a function of time, both seasonally and interannually?

4. How can spatially-and temporally-variable urban input data be best discovered, processed, and synthesized for incorporation into an integrated (surface-subsurface-land-atmosphere) hydrologic model?
5. How do reduced urban evapotranspiration, urban hardscapes, infiltration of groundwater into wastewater pipes, and other anthropogenic recharges and discharges affect subsurface storage on a regional scale?
6. What controls the pre-event water proportion of stormflow in urbanizing areas?
7. What controls the relationship between storage and streamflow along an urban-to-rural gradient?
8. What is the relationship between pre-event water proportion of stormflow and watershed storage in urban areas?

1.3 Study Area

Interactions between ecosystems and urban development have been evaluated through the Baltimore Ecosystem Study Long Term Ecological Research (BES LTER) project, one of two urban LTER sites in the U.S. (<http://www.lternet.edu>). As a result, Baltimore has become a hub of urban environmental research. A network of hydrologic instrumentation that supports the LTER provides a platform for place-based research, where watersheds are characterized in great detail from numerous previous studies and data collection efforts. This is the primary reason that my research focuses on the Baltimore area. My research spans scales ranging from a domain that encompasses the Baltimore metropolitan area (the model developed in

Chapter 3 spans 13,216 km²), to sub-watersheds of less than 2 km² and smaller hillslopes in Chapter 4.

1.4 Overview of Dissertation Chapters

I address research questions 1-3 in Chapter 2 by quantifying the water balance in the more urbanized portions Baltimore and comparing it to the water balance of undeveloped watersheds in the region. I used the time period 2001-2009 and estimated each component of the water balance for 65 watersheds in the Baltimore region. For natural water balance components, I used PRISM data for monthly precipitation, the land surface model GLDAS-Noah for evapotranspiration, and USGS stream gages for streamflow. I also estimated the piped components of the water balance that constitute additional inflows and outflows to urban watersheds. I included infiltration and inflow (I&I) of groundwater and stormwater into wastewater pipes in Baltimore City, water supply pipe leakage, and lawn irrigation. This I&I makes up about 68% of Baltimore City's wastewater demand. The study design and execution were primarily my responsibility. This work was published in a special issue on Hydrogeological Effects of Urbanization in *Environmental & Engineering Geoscience* in 2012.

The work presented in Chapter 2 shows how anthropogenic fluxes substantially affect the urban water balance in Baltimore, but the spatio-temporal effects of these fluxes on storage and in comparison to the effect of impervious surfaces cannot be determined from a water balance analysis alone. Chapter 3 addresses question 4 by presenting a methodology for development of an integrated groundwater – surface water – land surface hydrologic flow model applied to the

Baltimore metropolitan region. This chapter also addresses question 5 by implementing the built model and then exploring scenarios where four urban features are isolated to evaluate their effect on subsurface storage. The features evaluated were reduced urban evapotranspiration, urban hardscapes, infiltration of groundwater into wastewater pipes, and all other anthropogenic recharges and discharges (municipal and private well withdrawals, surface reservoir withdrawals, water supply pipe leakage, and lawn irrigation). The study area, model, and model gridding were selected by C. Welty as part of the NSF Coupled Human Natural Systems project, “Dynamic Coupling of the Water Cycle with Patterns of Urban Growth.” My contributions were primary responsibility for developing study questions beyond the scope of the original NSF project, study design, execution, and data interpretation.

Chapter 4 addresses questions 6-8 through a combination of numerical experiments using a coupled groundwater-surface water flow and transport model applied to an idealized hillslope, two-component chemical hydrograph separation during storm records collected in 5 small, nested urban watersheds, and simple dynamical systems analysis of hydrometric data to derive storage-discharge relationships along an urban-to-rural gradient in the Baltimore area. Chemical tracer records used for the chemical hydrograph separation were collected by C. Welty and her staff through the NSF project “Integrating Real-Time Chemical Sensors into Understanding of Groundwater Contributions to Surface Water in a Model Urban Observatory”. C. Welty performed the chemical hydrograph separation and processed streamflow records for use in the simple dynamical systems analysis. I had primary responsibility for generating the study questions, processing of precipitation

and evapotranspiration for the simple dynamical systems analysis, carrying out this analysis, designing and executing the numerical experiments, and interpretation of these results.

Chapter 5 summarizes the conclusions from the previous three chapters and answers the research questions. Remaining questions and directions for future work are also presented in Chapter 5.

Chapter 2: Water Balances along an Urban-to-Rural Gradient of Metropolitan Baltimore, 2001-2009

Aditi S. Bhaskar and Claire Welty

Environmental and Engineering Geoscience. 18(1), 37-50, 2012

2.1 Introduction

Quantitative information on how urbanization changes water balances and corresponding water availability is generally unknown. Yet knowledge of water availability is needed to manage ecosystem impacts, maintain in-stream flow requirements for biota, and manage water supply for potable consumption and potential reuse. Urbanization affects all components of the hydrologic cycle. The most readily observed impact is the response of urban streams to rainfall inputs, where urban streams are flashier with higher peak flow rates and greater total runoff volumes than their non-urban counterparts [e.g. *Leopold*, 1968]. Other well-known effects associated with urbanization include reduced infiltration caused by increased impervious surface coverage; contributions to groundwater recharge from leaking water supply pipes; changes to evapotranspiration (ET) due to decreases in vegetative land cover and increases in lawn irrigation [*Grimmond and Oke*, 1999; *Claessens et al.*, 2006a]; and increases in precipitation owing to the urban heat island effect [*Shepherd*, 2005]. These consequences can combine to alter the relative magnitudes of urban water balance components on a watershed basis compared to natural systems. The goal of this paper is to quantify the impacts of urbanization on

catchment-scale water balances using Baltimore as a case study. The novel aspect of this paper is the availability of spatially-detailed hydrologic data where water balance components are quantified along an urban-to-rural gradient of development.

Although often considered separately, engineered water and wastewater flows always interact with natural hydrologic flows. We refer to these engineered flows as piped flows. Piped flows include interbasin transfers of water and wastewater, leakage out of pressurized water supply pipes, and leakage into (infiltration) or out of (exfiltration) wastewater collection pipes. We define the water balance by setting the difference between inflows and outflows equal to the change in watershed storage, where the watershed defines lateral boundaries of a control volume. Our water balance equation for urban areas is given by:

$$P + I + L - ET - Q - W - I\&I = \Delta S \quad (2.1)$$

where P is precipitation, I is lawn and garden irrigation using piped water supply which is derived from outside the watershed (reservoir-supplied), L is water supply pipe leakage of municipal water which is derived from outside the watershed, ET is evapotranspiration, Q is streamflow, W is reservoir withdrawal, I&I is inflow and infiltration into wastewater collection pipes, and ΔS is change in storage. Inflows are positive and outflows are negative components of the left side of equation (2.1).

From I&I data available to us for the Baltimore region, we have evidence that although exfiltration from wastewater pipes occurs, on balance wastewater pipes act as a drain and as an additional watershed outflow. In other areas, however, wastewater pipes may predominantly act as sources of watershed inflow. In some cases, we group Q and W together, represented as Q^* . All quantities are given in

terms of average depth over a watershed per unit time. Changes in internal partitioning of water (e.g. increases in monthly storm runoff balanced by decreases in monthly baseflow that leave monthly streamflow volume unchanged) are not within the scope of this paper.

Consideration of piped and natural flows together as part of integrated urban water management [e.g. *Mitchell, 2006*] is rare. Studies that have quantified natural water budget inflows and outflows, as well as piped water and wastewater inflows and outflows, have been conducted for a variety of purposes. These include prediction of future water supplies [e.g. *Martinez et al., 2011*], quantifying groundwater recharge [e.g. *Birkle et al., 1998*], and determination of stormwater and wastewater contaminant loads [e.g. *Niemczynowicz, 1990*]. Previous studies provide comparisons of piped and natural flows in a variety of urban areas globally. Imported water is shown to exceed average precipitation in a few studies [*Vizintin et al., 2009*; *Martinez et al., 2011*]. More commonly, imported water makes up less than half of the total watershed input, with the remainder being precipitation [*Aston, 1977*; *Carlsson and Falk, 1977*; *Grimmond and Oke, 1986*; *van de Ven, 1990*; *Niemczynowicz, 1990*; *Stephenson, 1994*; *Binder et al., 1997*; *Birkle et al., 1998*; *Semádeni-Davies and Bengtsson, 1999*; *Eiswirth, 2001*; *Jia et al., 2002*; *Mitchell et al., 2003*]. These catchment water balance studies contrast with water balance studies focusing on groundwater, in which researchers have more commonly found precipitation to be a smaller source of recharge than leakage from water supply pipes [*Kim et al., 2001*; *Garcia-Fresca, 2006*].

There is no one form of outflow that is dominant across the spectrum of urban water balance studies. In some previous assessments, particularly in areas with combined sewer systems, the dominant outflow is wastewater [Niemczynowicz, 1990; van de Ven, 1990; Birkle et al., 1998; Jia et al., 2002; Vizintin et al., 2009; Martinez et al., 2011]. In others, streamflow or stormwater is the largest magnitude outflow [Aston, 1977; Grimmond and Oke, 1986; Semádeni-Davies and Bengtsson, 1999]. In still others, ET is dominant [Carlsson and Falk, 1977; Stephenson, 1994; Binder et al., 1997; Eiswirth, 2001; Mitchell et al., 2003]. Both large positive [e.g. Stephenson, 1994] and large negative [e.g. Niemczynowicz, 1990] changes in storage have been observed in urban water balance studies.

Only a few of the cited urban water balance studies compare natural and urban water balances to evaluate the differences between them. Stephenson [1994] and Grimmond and Oke [1986] both found that lawn irrigation led to greater or equal ET compared to corresponding rural sites. In our study, we are able to compare urban and nearby undeveloped water balances in the same climatic and hydrogeologic environment by evaluating a region with multiple watersheds ranging from urban to rural. This analysis of the spatial variability of urban to rural water budgets can also serve as a proxy for predicting the temporal evolution of water balances as an area becomes more urbanized.

Although yearly precipitation inputs exceed the volume of imported water for most previous studies, in some cases this is found to be dependent on annual climatic or seasonal variations. For example, Mitchell et al. [2003] evaluated multiple years in Canberra, Australia and found that in the driest year imported water exceeded

precipitation and exported wastewater exceeded streamflow, which was not the case in other years. To assess water availability impacts of urbanization, it is clear from the literature that a range of climatic conditions (multiple years) and seasonality should be considered.

None of the cited studies that address piped flows as well as natural flows have been carried out for cities in the northeastern U.S. Since the effects of urbanization on water balance depend on regional climate, studies from other climates are not clearly applicable to this area. In addition, the age and leakiness of the water system may play a significant role in determining how water budgets change with development in different cities. Baltimore, with a relatively old water and sewer system, may provide an analogue city for population centers in the northeastern U.S. or elsewhere with similar climate and water system age.

For the above reasons, we undertook a spatial and temporal analysis of the water balance of the Baltimore metropolitan area for Water Years 2001-2009. In this paper, we address the following questions:

- (1) The watersheds in our study area span a gradient from 0 to 60 percent impervious surface coverage. How does the water balance change along this gradient, both in the forms and relative amounts of watershed inflows and outflows?
- (2) How do the magnitudes of piped flows (water supply pipe leakage, wastewater infiltration and inflow, lawn irrigation, and reservoir withdrawals for water supply) compare to natural inflows (precipitation) and outflows (streamflow and ET)? Which piped flows are most significant?

(3) How do urban and rural water balances vary as a function of time, both seasonally and annually (wet years versus dry years)?

2.2 Study Area

The methodology used in this paper is completely general, and could be applied to a metropolitan region of any climate and infrastructure age. Baltimore was selected because of data availability in this region. The political jurisdictions that define the Baltimore metropolitan region include Baltimore City and Baltimore, Howard, Carroll, Harford, Anne Arundel, and Queen Anne's Counties (Figure 2.1). This study focuses on drainage from the counties on the western shore of the Chesapeake Bay and therefore excludes Queen Anne's County. The study area is approximately 4500 km² in size and contains a population of about 2.5 million.

The political boundaries fall within five U.S. Geological Survey 8-digit cataloging units: the Gunpowder-Patapsco, Severn, Patuxent, Monocacy, and Lower Susquehanna watersheds. The study watersheds lie predominantly within the Piedmont and Atlantic Coastal Plain physiographic provinces. Land surface elevations range from 0 – 360 m above sea level, with an abrupt change at the Fall Line, the zone of transition between the Piedmont and Coastal Plain. The Piedmont is composed of fractured and folded igneous and metamorphosed igneous and sedimentary rocks. Bedrock near the land surface is weathered to saprolite and valley floodplains typically are underlain by alluvium deposited by streams. The regolith (saprolite and alluvium) and fractured rock are viewed as two separate but interconnected flow systems owing to their difference in storage properties [Heath,

1984a]. The Atlantic Coastal Plain is composed of semi-consolidated to unconsolidated sediments (overlying saprolite and bedrock) consisting of silt, clay, and sand, with some gravel and lignite, dipping toward the ocean. Coastal Plain

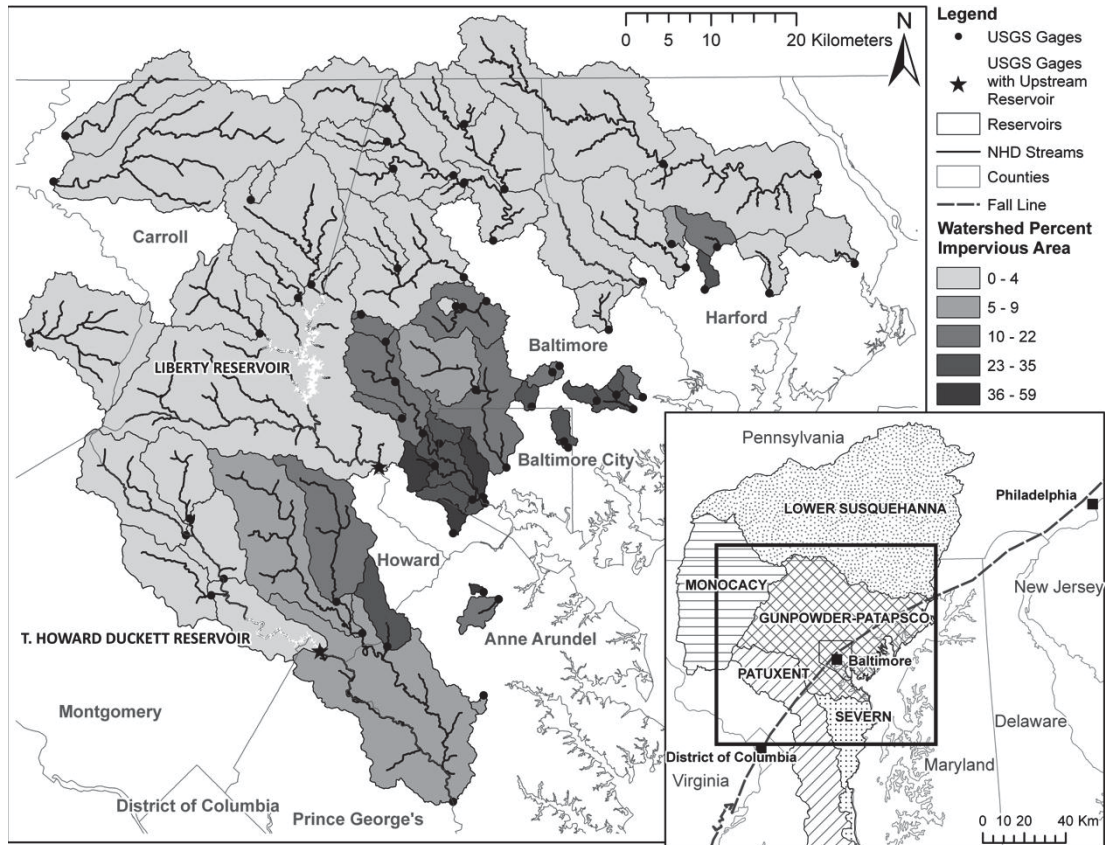


Figure 2.1. Locations of study watersheds relative to major river basins and political boundaries, with colors representing percentage watershed impervious area. Streams from the National Hydrography Dataset (NHD) are shown as solid black lines. USGS stream gage locations are shown as black dots. Watersheds were delineated by USGS or by UMBC/CUERE. Percent impervious surface area is from the National Land Cover Dataset (NLCD) 2006. Stream gages in reservoir-containing watersheds are designated by stars.

sediments range in thickness from a few meters along the Fall Line to as much as 2400 m along the Atlantic coast [*Trapp and Horn, 1997*].

The climate in Baltimore is characterized as humid subtropical, with average winter low and high temperatures of -2 C and 7 C and average summer lows and highs of 23 C and 33 C. The average annual precipitation is 1110 mm and is distributed nearly evenly throughout the year. The storm-event hydrologic response of some Baltimore watersheds has been studied by previous researchers [e.g. *Meierdiercks et al., 2010*].

Three water filtration plants in Baltimore City supply water to the Baltimore central water distribution system. The Ashburton Water Filtration Plant draws raw water from Liberty Reservoir located in the Patapsco River watershed. Montebello Nos. 1 and 2 Water Filtration Plants obtain raw water from the Loch Raven Reservoir, which is operated in conjunction with Prettyboy Reservoir, in the Gunpowder Falls watershed. The Baltimore system serves Baltimore City and portions of Baltimore, Howard, and Anne Arundel Counties. Wastewater from the Baltimore system is treated at two plants that discharge to the Back and Patapsco Rivers near their confluences with the Chesapeake Bay. The Washington Suburban Sanitary Commission, which serves the Maryland suburbs of the District of Columbia, provides some water to Howard County from the Patuxent Water Filtration Plant. The T. Howard Duckett and Triadelphia Reservoirs on the Patuxent River are operated together to serve as the raw water source for this plant. Municipal wastewater from the western part of the Howard County service area is treated at the Little Patuxent Water Reclamation Plant. Several smaller surface water systems

supply portions of Harford and Carroll Counties. Municipal wells supply most of Anne Arundel County and portions of Harford and Carroll Counties. Outside of the service areas, private wells and septic systems are predominantly used for water supply and wastewater disposal.

2.3 *Methods*

We collected and analyzed datasets from a wide variety of sources for use in this study. In this section, we describe how each component of the water balance was derived. We obtained the percentage of impervious land cover, shown in Figure 2.1, from the 30 m resolution 2006 National Land Cover Dataset (NLCD) [Xian *et al.*, 2009]. For this and other gridded data sets evaluated, the zonal statistics tool in ESRI ArcGIS software was used to calculate areal means over each watershed. Nested watersheds were analyzed independently. Means of water balance components over the entire region were weighted by watershed area. To compare the hydrologic inflow-outflow behavior of urban and rural watersheds over this time period, we split the 65 study watersheds into two groups. The group referred to as rural includes watersheds characterized by less than 5% impervious land cover. The urban group is characterized by 5% impervious land cover or greater. Thirty-four watersheds comprised the rural group and 31 made up the urban group.

We used PRISM (Parameter-elevation Regression on Independent Slopes Model) monthly precipitation grids (PRISM Climate Group, 2011) to estimate the precipitation component of water balances. PRISM uses point precipitation measurements and other climate and landscape parameters to generate monthly gridded precipitation at 2.5 arc minute resolution (~ 4 km). We obtained monthly

streamflow data at U.S. Geological Survey gages from National Water Information System (NWIS) (U.S. Geological Survey, 2011). Only watersheds gaged by the U.S. Geological Survey for at least one Water Year during our study period were included. Streamflow and other volume-based water data were divided by watershed area so that all water balance components were comparable as units of depth.

We obtained evapotranspiration (ET) estimates for the region from the Noah land surface model [Ek *et al.*, 2003], forced by GLDAS (Global Land Data Assimilation System) [Rodell *et al.*, 2004b]. The GLDAS/Noah model outputs are available in monthly and 0.25 degree (~22 km) resolutions globally at the GES DISC (Goddard Earth Sciences Data and Information Services Center, 2011). The finer resolution NLDAS-Mosaic was not used in our analysis because of its high modeled ET values. Mueller *et al.* [2011] exhaustively compared global ET estimates and found that both GLDAS/Noah and NLDAS-Mosaic had higher ET globally than a reference dataset, but that the GLDAS/Noah estimate was closer to the reference dataset.

We used GRACE data to provide a regional estimate of water storage. GRACE (Gravity Recovery and Climate Experiment) is a twin satellite mission launched in 2002 by NASA and the Deutsche Forschungsanstalt für Luft und Raumfahrt. The purpose of the mission is to map variations in the earth's gravitational field at approximately monthly and 400 km grid scales by making accurate measurements of the distance between two satellites using GPS and a microwave ranging system [Tapley, 2004]. GRACE data has been used to estimate changes in water storage at regional and global scales [Rodell *et al.*, 2004a]. We used

a Level-3 data product created by the Jet Propulsion Laboratory (GRACE Tellus POET, 2011) that consists of a monthly scaled time-series of storage minus mean monthly storage calculated over 2003-2007 [Swenson and Wahr, 2006]. The time series is a smoothed spatial average over the domain of interest, which overlaps with 4 pixels, each of 1 degree (~86 km) resolution. To compare our time series of monthly natural water balance changes in storage (P-Q*-ET) to GRACE data, we summed monthly P-Q*-ET to get an estimate of total storage as a function of time, which we term “derived storage”. We then subtracted the mean value of 2003-2007 derived storage from the entire derived storage time series to obtain derived storage normalized to 2003-2007.

When quantifying piped flows, we focused on areas served by imported water and exported wastewater. Because private well intakes, septic disposal systems and stormwater drainage largely keep water within a watershed, these flows are not modifications to the overall water balance. Municipal groundwater is used in some jurisdictions (Harford and Anne Arundel Counties) and may cross watershed boundaries, but this was not investigated.

For reservoir-containing watersheds, which are shown as starred gages in Figure 2.1, we calculated water withdrawals (W) in million gallons per day (MGD) and mm/mo. This amount was an additional monthly export for these two watersheds. The watershed containing Loch Raven reservoir was not gaged downstream of the reservoir during our study time period, thus the water balance for this basin could not be calculated. The source of information for water withdrawals consisted of records of raw water inputs to corresponding filtration plants. We

obtained data on the combined volume of raw water inputs to all Baltimore water treatment plants from 2000-2009, as well as data on water inflows to only the Ashburton Water Filtration Plant from October 2003 – September 2004 (Charshee, personal communication, 2010). We assumed that the proportion of raw water flowing to the Ashburton Water Filtration Plant of the total raw water flowing to all filtration plants was the same over the decade as it was during the 2004 Water Year. The mean volume of water withdrawn from the Patapsco River between Water Years 2001 and 2009 was 86 MGD or 157 mm/yr when scaled by watershed area. For the Patuxent watershed, the reported average value withdrawn from the T. Howard Duckett Reservoir was 50 MGD, or 201 mm/yr [*Prince George's County*, 2008]. This amount was used in our water balances throughout the study period.

Leakage from water supply pipes was calculated for the municipal water service areas of Baltimore City and Baltimore County to illustrate the effects of including pipe leakage on a subset of urban water balances. Leakage from the water distribution system of Baltimore is about 23% of flow [*McCord*, 2009a]. According to City of Baltimore [2006], 204.7 MGD of finished water is supplied to Baltimore City and County. We obtained a GIS coverage of the water supply pipe layers, and since the distribution of pipe leaks and ages of pipes was unknown, we assumed the leakage rate to be distributed equally per unit length of pipe within the service area. We calculated watershed inflows from supply pipe leakage for Baltimore City and County service areas, as well as for study watersheds within this area.

To estimate water inflows from lawn irrigation, we calculated lawn area using a 2007 land cover classification developed by the University of Vermont Spatial

Analysis Laboratory. UVM derived this 0.63 m land cover classification using LiDAR data, color infrared aerial imagery, building footprints, and road and water polygons for Baltimore City and Baltimore, Howard, and Anne Arundel Counties. The grass/shrub land cover class may overestimate lawns in areas where fields and shrubs are included in the class, and it may underestimate lawns in areas where tree canopy shades lawns and where lawns may therefore be classified as forest cover. We assumed that 25% of the area classified as grass/scrub is irrigated at a rate of 1 in (25.4 mm) per week for 4 months of the year [Law et al., 2004b; Milesi et al., 2005a; Claessens et al., 2006a].

As in many older cities where infrastructure is aging, the Baltimore wastewater collection system can be dominated by groundwater infiltration and rainwater inflow under high water table or wet weather conditions. Groundwater and rain water entering wastewater pipes through cracks or improper connections, such as stormwater draining to wastewater pipes, is commonly termed “infiltration and inflow” or “I&I”. Between May 2006 and May 2007, Baltimore City conducted a comprehensive wastewater monitoring program that involved metering wastewater flows and quantifying infiltration and inflow [Espinosa and Wyatt, 2007], delineated on a per sewer basin basis (Espinosa, personal communication, 2010). The Town of Hampstead in Carroll County conducted an I&I study of its sewer system from February to June 2009 [Carroll County, 2009]. Howard County conducted a Sewer System Evaluation Survey of the Little Patuxent sewershed from March to July 2001 and March to June 2003 [Howard County, 2005]. Other municipalities in the region have not conducted recent I&I surveys. Because of the difficulty of extrapolating

from available I&I studies, we only considered I&I exports from Baltimore City sewersheds, Baltimore City as a whole, and study watersheds that fall within Baltimore City, as case studies.

2.4 Results

Figure 2.2 shows the mean and standard deviation over all study watersheds of the inflows and outflows of the natural hydrologic cycle— monthly precipitation, streamflow, and ET. The seasonal cycle of ET is evident with peaks in summer months that sometimes exceeded monthly precipitation inflows. As expected, precipitation showed a high degree of variability from month to month and streamflow peaks generally corresponded to precipitation but showed comparatively less variability. Monthly precipitation, streamflow, and ET were averaged by season over the 9-year record (Figure 2.3). For both urban and rural sites, ET was the dominant outflow except in winter months. Precipitation was similar between urban and rural sites (92 mm/mo for urban; 94 mm/mo for rural), but streamflow was consistently higher in urban watersheds and ET was consistently lower, especially in the summer. In rural watersheds, average summer ET exceeded precipitation by 14 mm/mo. The ET peak in summer led to the well-known effect of decreased summertime streamflow.

To evaluate interannual variability, mean monthly inflows (P) and outflows (Q and ET) over rural and urban watersheds were each summed over water years and plotted in Figure 2.4. Precipitation averaged 1118 mm/yr for the region with an annual mean range of 820 to 1635 mm/yr. Precipitation and streamflow both showed

more interannual variability compared to ET. Mean annual ET was relatively constant,

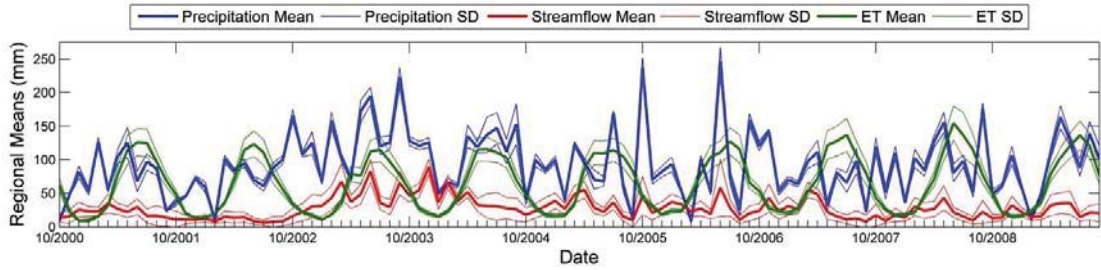


Figure 2.2. Monthly means and standard deviations (SD) over all study watersheds of precipitation, streamflow and evapotranspiration (ET).

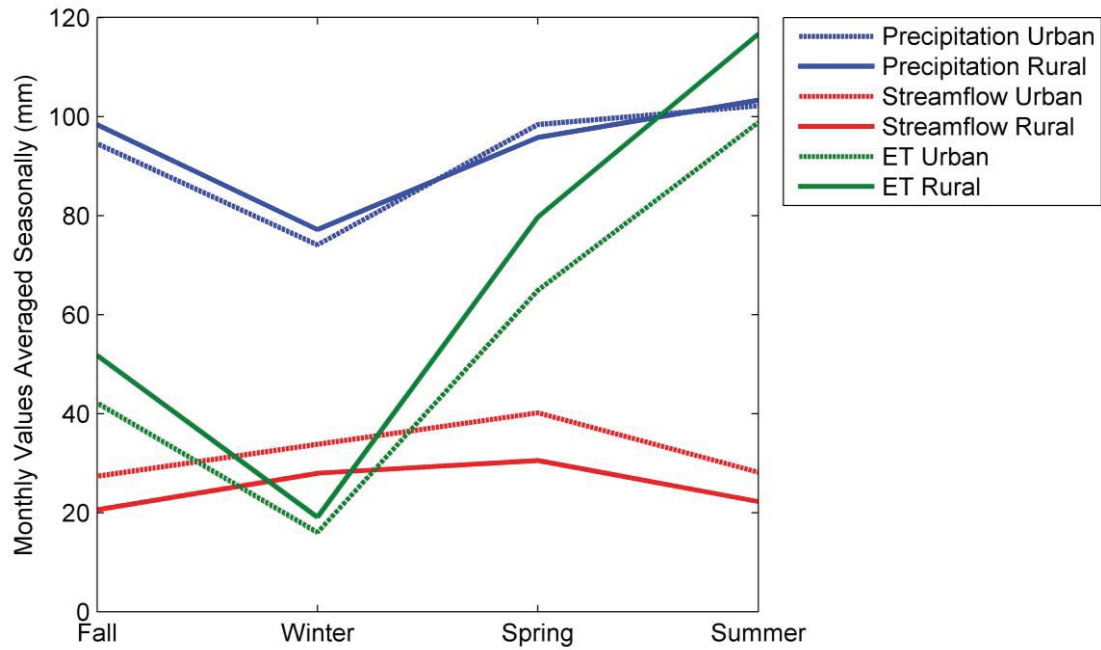


Figure 2.3. Monthly means over all study watersheds, averaged for each season. Urban watersheds are those with 5% impervious area or greater.

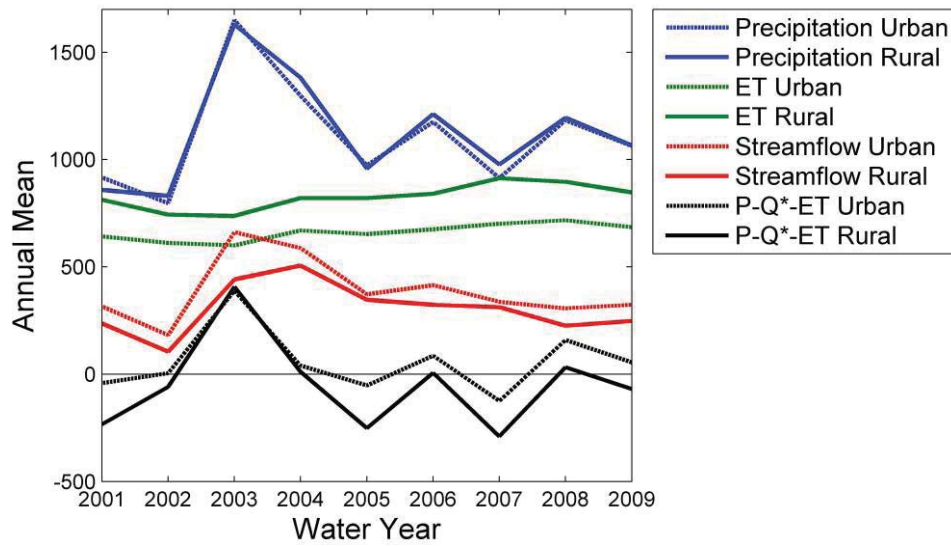


Figure 2.4. Regional annual means showing interannual variability, along with precipitation (P), streamflow (Q), evapotranspiration (ET) and water balance residual $P-Q^*-ET$, where Q^* indicates streamflow $Q +$ reservoir withdrawals W for the two reservoir-containing watersheds.

ranging from 695 to 848 mm/yr, and was generally greater than mean streamflow (128 to 531 mm/yr). Mean ET in urban watersheds was 164 mm/yr less than rural ET while mean urban streamflow was 64 mm/yr greater than rural streamflow. Again, there was little difference between urban and rural precipitation. Figure 2.4 also shows mean annual inflows minus outflows ($P-Q^*-ET$) over the nine years, where we included streamflow Q and reservoir withdrawals W together as Q^* for the two reservoir-containing watersheds. Generally, the reduced ET in urban areas led to a greater residual $P-Q^*-ET$ value compared to the rural $P-Q^*-ET$. The difference between urban and rural streamflow increased during the wettest year (2003), which led to a convergence of the urban and rural $P-Q^*-ET$ toward the same value. The annual difference between natural watershed inflows and outflows ($P-Q^*-ET$) was on average negative for rural areas (-108 mm/yr) and positive for urban areas (19 mm/yr).

We evaluated our calculated storage changes by comparison to GRACE data. GRACE data over our study region showed that mean storage changed little between 2002 and 2009 (Figure 2.5). The GRACE storage and $P-Q^*-ET$ derived storage curves showed annual cycles that were similar in timing. Storage in both curves peaked during spring months, declined with high ET during summer, and started increasing again in the fall. Following the increase in storage with the wet year of 2003 however, the rural $P-Q^*-ET$ storage curve exhibited a negative trend for the remainder of the study period whereas the GRACE curve showed little trend. Urban derived storage had the opposite trend, it increased over time compared to GRACE storage. Monthly changes in GRACE storage were calculated by subtracting the

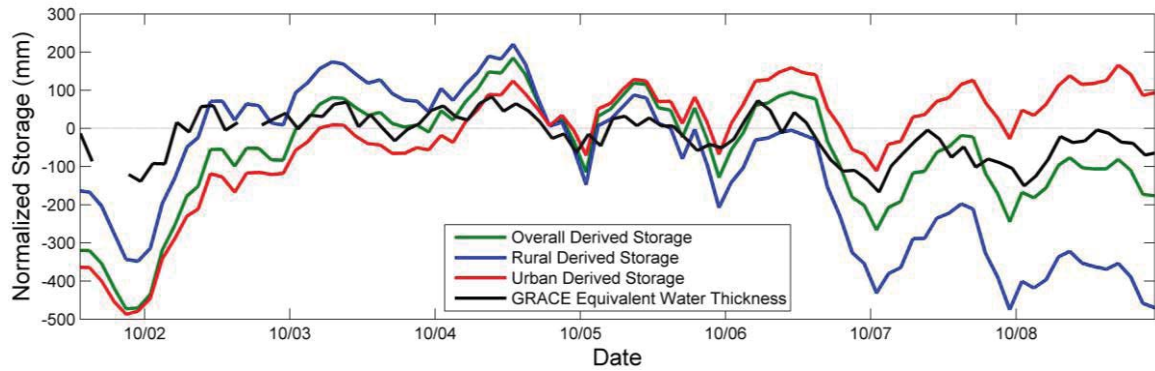


Figure 2.5. GRACE (Gravity Recovery and Climate Experiment) storage and derived storage both normalized by subtraction of their respective means over 2003-2007, and shown monthly for the time period when the datasets overlap (April 2002 - September 2009). Derived storage represents the sum of $P-Q^*-ET$, and is given for the average of all watersheds (overall) and the urban and rural subsets. Breaks in the GRACE time series in early months are due to unavailable data (GRACE Tellus POET, 2011).

previous month's storage value from the current. Over the same time period (4/2002 to 9/2009), the mean change in storage from GRACE was 0.84 mm/mo. The change in storage from the normalized derived storage for rural areas (-2.8 mm/mo) was less than GRACE change in storage, while the corresponding urban value (5.5 mm/mo) was greater.

Figure 2.6 shows the spatial pattern of mean annual PRISM precipitation by watershed. As discussed in detail by *Smith et al.* [2012], there is a clear spatial pattern in precipitation over the Baltimore region. The northeastern-most watersheds received over 100 mm/yr more precipitation than western watersheds. Mean annual streamflow + withdrawals (Q^*) is shown in Figure 2.7. Urban watersheds were characterized by greater runoff (427 mm/yr) compared to rural watersheds (363 mm/yr). There was also greater streamflow in the northeast part of the study region, which appears to correspond to the high precipitation region. The range in streamflow was much greater than that of precipitation. Figure 2.8 shows the mean annual ET where urban watersheds generally had lower ET.

The mean annual $P-Q^*-ET$ (mm) is shown in Figure 2.9. $P-Q^*-ET$ is plotted versus percent impervious area in Figure 2.10, where the size of the marker is proportional to watershed area. The logarithm of percent impervious area was used because many of the watersheds have close to zero percent impervious area. Figure 2.10 shows generally that watersheds with the lowest values of percent impervious area are associated with negative values of $P-Q^*-ET$. As the percent impervious area increases, there is a larger spread in $P-Q^*-ET$ values, with most urban watersheds characterized by an increase in $P-Q^*-ET$ compared to the rural baseline.

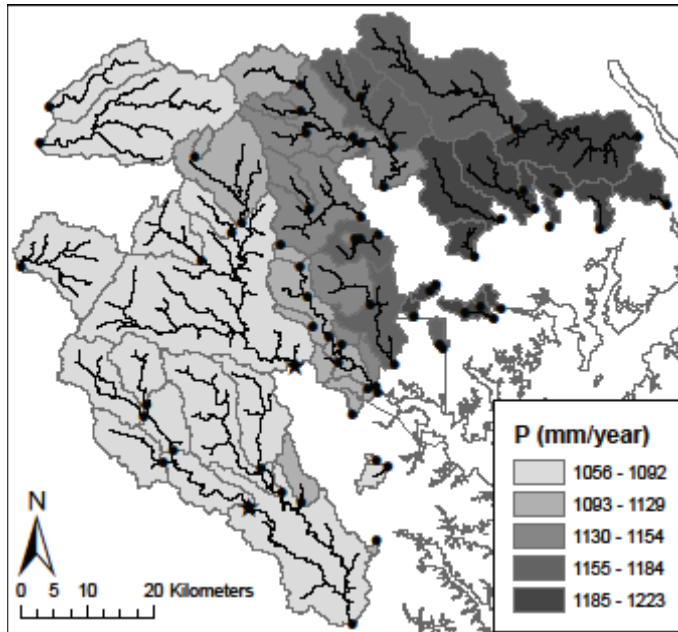


Figure 2.6. Mean annual precipitation 2000-2009 from Parameter-elevation Regression on Independent Slopes Model (PRISM) monthly precipitation grids (PRISM Climate Group, 2011).

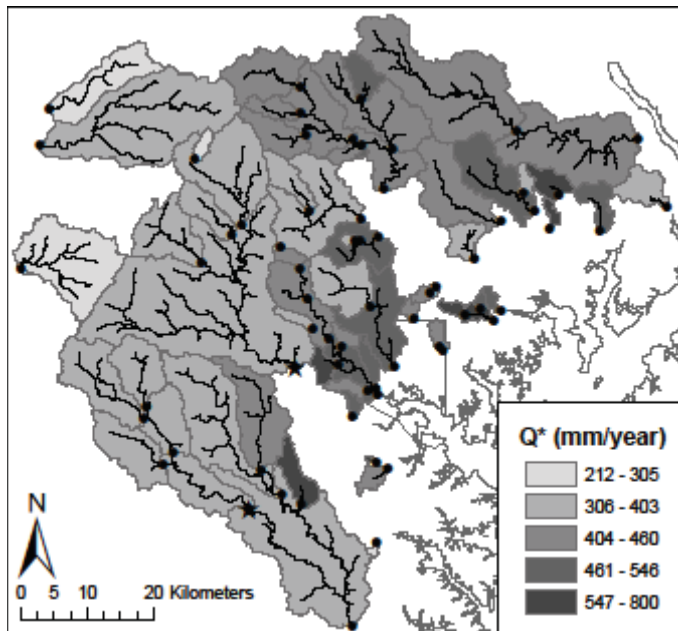


Figure 2.7. Mean annual streamflow Q + reservoir withdrawals W , where $Q^* = Q+W$. Mean annual streamflow 2000-2009 is from the USGS NWIS (U.S. Geological Survey, 2011). Reservoir withdrawals were estimated for Liberty Reservoir (Charshee, personal communication, 2010) and T. Howard Duckett Reservoir [*Prince George's County*, 2008].

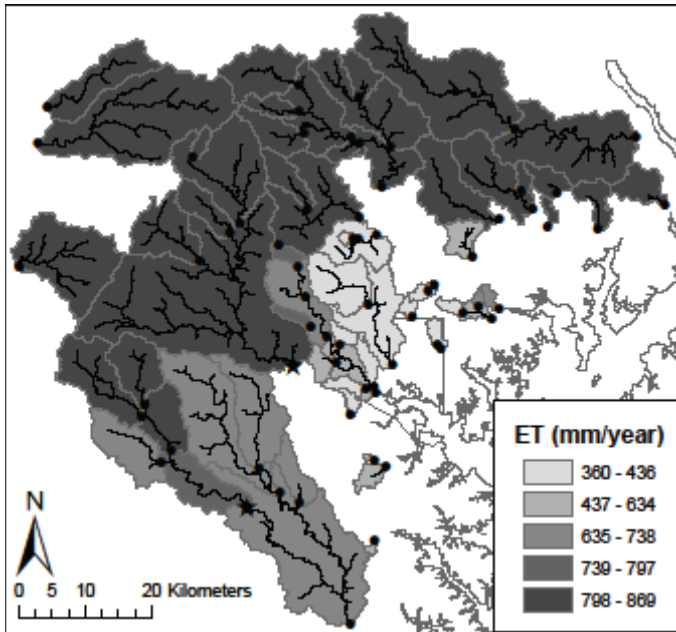


Figure 2.8. Mean annual ET from GLDAS (Global Land Data Assimilation System)/Noah, available at the GES DISC (Goddard Earth Sciences Data and Information Services Center, 2011).

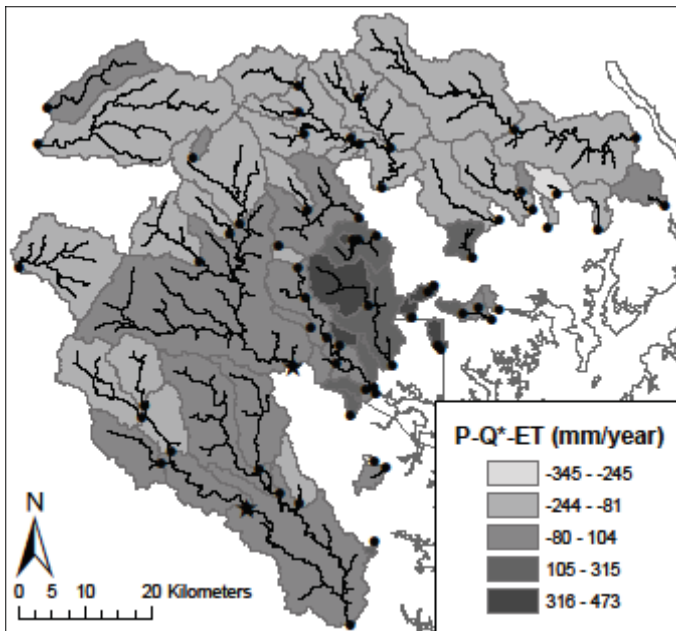


Figure 2.9. Mean annual P-Q*-ET, where the sources of P, Q* and ET are as indicated in Figures 2.6-2.8.

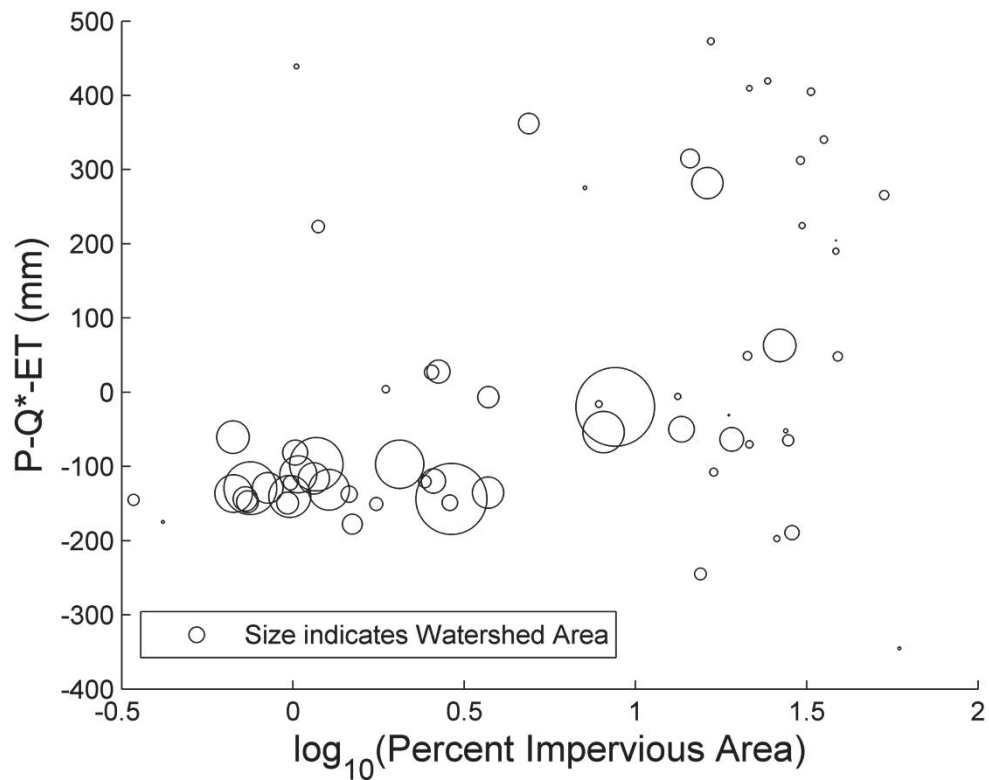


Figure 2.10. Logarithm of impervious area vs. P-Q*-ET (mm), where the size of the marker is proportional to watershed area. The division between urban and rural at 5% impervious is at 0.7 on the log-scale of the horizontal axis.

The three piped water balance terms we considered were lawn irrigation, supply pipe leakage, and infiltration and inflow. The supply of treated water to Baltimore City in FY 2005 was 107.25 MGD or 707 mm/yr [*City of Baltimore, 2006*]. The metered water in FY 2010 was 90.6 MGD (598 mm/yr) (Espinosa, personal communication, 2010). We proportionally allocated wastewater between Baltimore County and Baltimore City by population served, which resulted in estimated wastewater demand of 101 MGD for Baltimore City in FY 2000 (669 mm/yr) [*City of Baltimore, 2006*]. Instead of presenting overall numbers for watershed potable water imports and wastewater exports, we believe it is more relevant to water budget calculations to quantify the interactions between piped and natural systems.

We found water was served to Baltimore City and County through a total length of 6.5×10^6 m of water supply pipes. We assumed that leakage was 23% of water supply flow [*McCord, 2009a*], and this 47 MGD of leakage was equally distributed per pipe length. This was calculated to be 7 gallons per day of leakage per meter of pipe. Watersheds within the served area of Baltimore City and County ranged between 20% and 80% grass/shrub. Overall, Baltimore City and served Baltimore County were characterized by 21% and 26% of land area in the grass/shrub class, respectively. Estimates of the spatial distribution of supply pipe leakage and lawn irrigation are provided in Figures 2.11A and 2.11B. Only watersheds within service areas of Baltimore City and County are shown, along with overall estimates for the city and county served areas. Pipe leakage was related to density of water

supply pipes. Thus, leakage generally increased with impervious surface coverage, as they

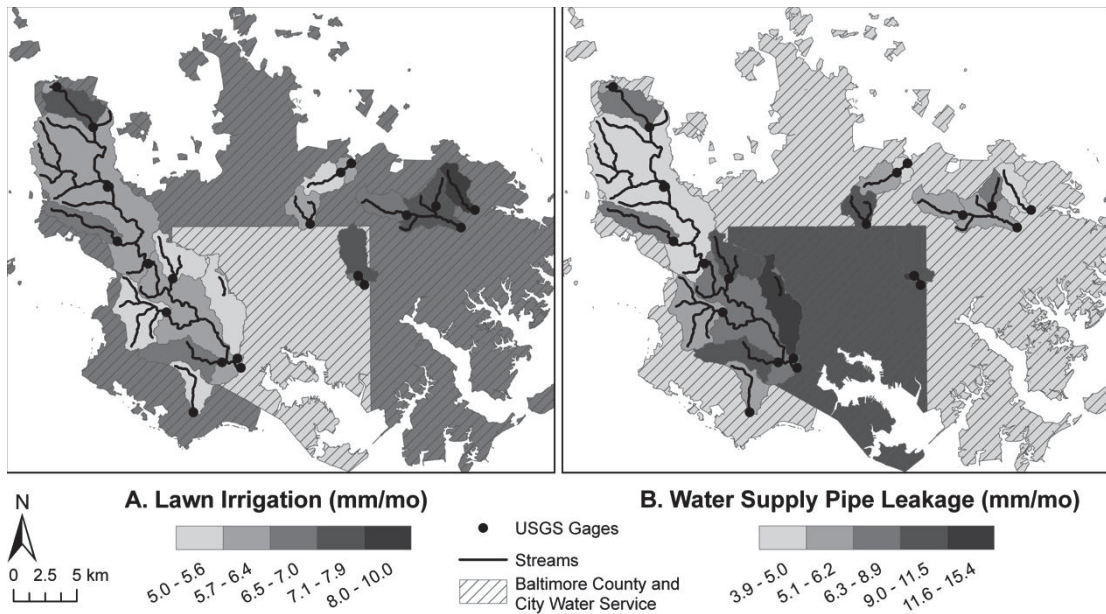


Figure 2.11. Contributions of lawn irrigation (A) and water supply pipe leakage (B) in mm/mo over Baltimore City, the served area of Baltimore County and the watersheds contained in these areas.

are both estimators of degree of urbanization. Lawn irrigation was correlated to lawn area, which was inversely correlated with impervious surface cover within the service area. The sum of supply pipe leakage and lawn irrigation ranged between 11 and 20 mm/mo, or assuming that leakage occurred for 12 months of the year and lawn irrigation for 4 months/yr, between 84 and 203 mm/yr. Over Baltimore City, the sum was 160 mm/yr.

I&I for Baltimore City (Figure 2.12) was estimated to be 92 MGD (606 mm/yr), and was dominated by groundwater-derived infiltration during dry weather conditions. I&I was approximately 90% of the wastewater demand, which is high but not unheard of in the region. In the Howard County I&I study, the percentage of metered sewer flow from I&I in different sewersheds ranged from 41% to 94%. Within the town of Hampstead in Carroll County, 49% of dry-day wastewater flow was from groundwater infiltration alone. I&I export from Baltimore City was greater than average streamflow for gaged urban watersheds (427 mm/yr).

We used two watersheds within Baltimore City as case studies for comparison of I&I and other water balance components. These watersheds, Gwynns Run and Moores Run (shown in Figure 2.12), had spatially averaged I&I of 670 mm/yr and 460 mm/yr, respectively. In Figure 2.13, we present the average of the water balances for these two watersheds, including all piped and natural components, along with the mean rural water balance. The urban water balance exhibits less ET, more streamflow and much more outflow in the form of I&I as compared to the rural water balance. Urban pipe leakage and lawn irrigation are minor compared to inflows by precipitation. The components shown in this figure were estimated separately (not by

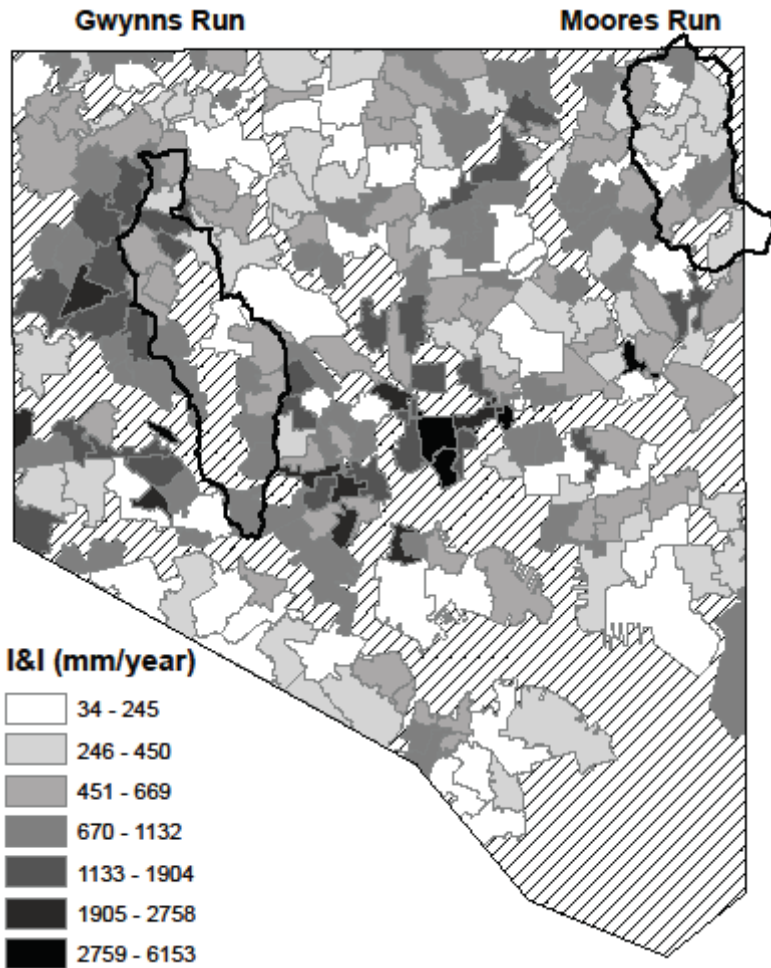


Figure 2.12. Infiltration and inflow in mm/year per sewer from the Baltimore City Comprehensive Wastewater Monitoring Program [Espinosa and Wyatt, 2007; Espinosa, personal communication 2010]. The hatched areas are those for which I&I estimates are not available. Gwynns Run and Moores Run watersheds are indicated by heavy black boundaries.

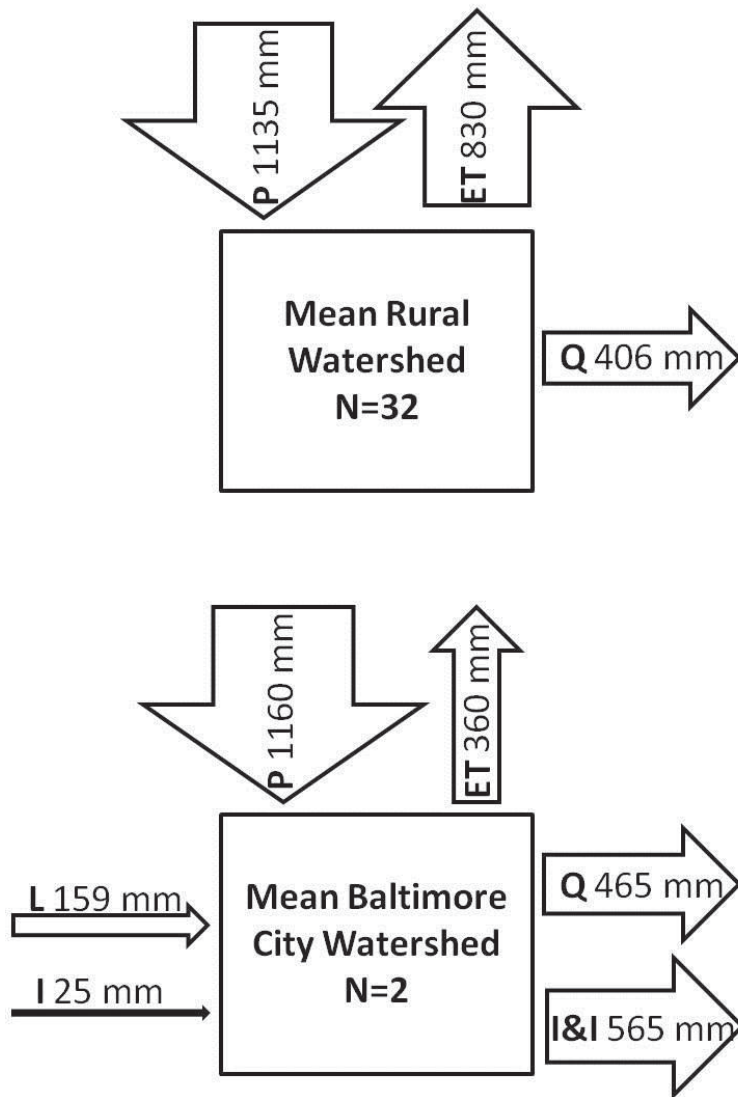


Figure 2.13. Comparison of the annual water balance components between the mean of 32 rural (impervious area < 5% and without reservoirs) and two urban watersheds in Baltimore City (Gwynns Run and Moores Run). The width of the arrows corresponds to the magnitude of the flows in mm/yr. Components were estimated separately (not by subtraction) so inflows do not necessarily equal outflows.

subtraction), and therefore inflows do not necessarily equal outflows. In the case of average of rural watersheds (excluding the two reservoir-containing watersheds), the inflows minus outflows was -101 mm/yr whereas for urban watersheds the inflows minus outflows was -46 mm/yr.

2.5 *Discussion*

In comparing GRACE data and the residual between natural water balance terms ($P-Q^*-ET$), we expected that we would need to include piped components for urban areas, but that we would have well characterized rural inflows and outflows. If we had accurately estimated flows in rural areas, and there was no annual change in storage, we would predict the difference between inflows and outflows ($P-Q^*-ET$) to be zero. Instead, we found that the $P-Q^*-ET$ in rural watersheds was negative. On the other hand, GRACE data, which is an evaluation of an integrated signal of water storage over the region, did not show declining storage. The monthly change in GRACE storage was greater than that found using rural $P-Q^*-ET$. This leads to a decreasing derived $P-Q^*-ET$ storage curve over time for rural watersheds as compared to that of GRACE data.

We suspect that the negative monthly rural change in storage ($P-Q^*-ET$) is due to bias in one or more of the water balance components. For example, if ET, the most uncertain natural water balance term, is regionally overestimated by the land surface model, undeveloped $P-Q^*-ET$ would be negative. This would lead to an apparent declining storage trend, when actual storage is relatively stable. For urban watersheds, our calculated mean monthly change in storage is greater than the GRACE change in storage. If GLDAS/Noah overestimated ET throughout the

region, then $P-Q^*-ET$ for urban areas would be even more positive. Lawn irrigation in water service areas is not included in the forcing of GLDAS/Noah however, so actual urban ET might be higher than the ET modeled by GLDAS/Noah. Urban excess water, when considering only natural water balance components, can be explained by including piped components. For Baltimore City, the net watershed export due to piped components ($I\&I - L - I$) was found to be 446 mm/yr (606 mm/yr of $I\&I - 160$ mm/yr of $I + L$). Correspondingly, for Gwynns Run and Moores Run, the net watershed exports due to piped components were 466 and 297 mm/yr, all of which are greater than the discrepancy between urban and rural water balances. The high levels of $I\&I$ measured by Baltimore City occurred before planned upgrades were made to the wastewater system, and therefore the water balance of the Baltimore region will change as cracked pipes are repaired.

Although the mean $P-Q^*-ET$ value was greater for urban compared to rural watersheds, there is a larger spread in $P-Q^*-ET$ for urban watersheds (Figure 2.10). This may be related to, among other things, the spatial variability in piped water balance terms. The net contribution of piped components may change dramatically over small distances. For example, $I\&I$ per sewershed ranged from 0 mm/yr to 6150 mm/yr with the highest $I\&I$ values located in downtown Baltimore (Figure 2.12). This range means that for an individual sewershed, the net effect of piped components ($I\&I - L - I$) on the water balance may be positive or negative regardless of the mean for Baltimore City. Lawn irrigation and pipe leakage might also have similar spatial heterogeneities, although we do not have the data to quantify these components. Pipe leakage is likely not distributed equally per pipe length, but rather highly

concentrated among a few water main leaks. Similarly, homeowners of some watersheds could be irrigating their lawns well above landscaping industry recommendations, which would lead to higher lawn irrigation inputs than we have assumed in some areas. Depending on the relative rates of I&I, pipe leakage and lawn irrigation, urban watersheds may have a range of positive or negative net contributions to the water balance from piped components, which can lead to the spread among urban watersheds shown in Figure 2.10.

Since each component of the water balance in Figure 2.13 is estimated separately (not by subtraction), neither of the example watersheds is balanced in terms of inflows and outflows. The rural watersheds have negative values for inflows minus outflows. The average of two Baltimore City watersheds shown in Figure 2.13 has a small negative value of inflows minus outflows. We do not have strong evidence to indicate that the apparent imbalance between inflows and outflows is caused by a progressive cumulative change in annual storage for either rural or urban watersheds. The regionally flat trend of GRACE data and the heterogeneous distribution of net water balance values for individual watersheds, all of which are characterized by uncertainty, suggest that these apparent discrepancies may be caused by errors in one or more of the components of the water balance.

Some of the challenges for this study included obtaining accurate ET estimates, as well as resolving the spatial mismatch of datasets. We used land surface models to obtain ET estimates. This procedure is less than ideal for urban areas because (1) the resolution of land surface model output is far too coarse to precisely describe ET in cities and (2) the forcing dataset, which includes gridded precipitation

used to drive the land surface models, does not properly reflect urban water inflows from irrigation and supply leakage. One alternative would be use of a finer resolution satellite product, such as the newly released MODIS ET product (MOD16) [Mu *et al.*, 2011]. This product does not however include urban areas because of the lack of good leaf area index satellite estimates (Mu, personal communication, 2010). Flux towers can provide good point estimates of ET in urban areas but a sparse network may not be reasonably extrapolated to entire cities. Modeling approaches [e.g. Bou-Zeid *et al.*, 2009] can be used to calculate urban ET, but require distributed meteorological inputs that are not commonly available. Accurate, fine-scale, spatially-variable estimates of ET over cities are currently lacking but are crucial to water budget closure. This is an important area of future work for those interested in understanding the quantity and distribution of water for both natural and engineered urban systems.

As is often the case for urban areas, it is a complex task to integrate the spatial boundaries required, such as watersheds, counties, and water and wastewater service areas. For example, streamflow was measured for watersheds, pipe leakage was estimated over water service areas, and sewer infiltration was measured over sewersheds within one of the area municipalities. This leads to limitations in the comparison of piped and natural water balance components for all of the developed watersheds. Data from municipalities, necessary for quantifying piped components of the water balance, are often scarce compared to the availability of natural component data.

2.6 Conclusions

1. Our analysis has shown that in the Baltimore region, natural inflows minus outflows ($P-Q^*-ET$) increase along a rural to urban gradient. When we solely considered natural water balance components, we found excess water in many urban watersheds due to decreased ET compared to rural sites. We did not have evidence to suggest that the magnitudes of total inflows and outflows were different between urban and rural watersheds or that there were systematic increases or decreases in storage over time. Nevertheless, the forms of inflows and outflows were certainly different, since urbanization introduces a number of additional water balance components, including leakage from supply pipes, lawn irrigation, and infiltration and inflow into wastewater collection pipes. There was a much greater proportion of water exiting urban watersheds by wastewater pipes or streamflow as compared to ET-dominated rural watersheds. Precipitation was still the largest inflow to urban watersheds, although lawn irrigation and water supply pipe leakage both contributed additional water.

2. Using estimates of piped components, we compared their magnitudes to natural water balance components. We found that I&I for two Baltimore City watersheds were 131% and 110% of watershed mean annual streamflow. Within the Baltimore City and County water service areas, lawn irrigation and water supply pipe leakage together accounted for 11 – 21% of monthly precipitation inputs. Annually, for the average of two Baltimore City watersheds, lawn irrigation and pipe leakage were 14% of total watershed inflows and I&I was 41% of total watershed outflows. Reservoir withdrawals upstream of gages were 64% (Liberty Reservoir) and 100%

(T. Howard Duckett Reservoir) of annual streamflow in reservoir-containing watersheds. On average, the most significant piped flows were I&I, but piped components were extremely spatially heterogeneous. The net effect of pipe leakage can change within relatively small distances, and led to an observed broad range of natural inflows minus outflows in urban areas.

3. We observed that $P-Q^*-ET$ in urban areas was greater than in rural areas for dry years (e.g. 2001, 2002, 2005, 2007), whereas the urban and rural $P-Q^*-ET$ values converged in the wet year of 2003. The wet year behavior could be attributed to urban streamflow increases relative to rural streamflow while the ET difference stayed about the same compared to other years. Rural areas showed more seasonal variability in ET than urban areas. On average, there were some modest variations in precipitation and streamflow by season, but ET was by far the largest control of seasonal variations in the water balance, leading to corresponding seasonal storage cycles.

4. Our understanding of water balances would benefit from expanded data collection by municipalities as well as continued development of gridded national and global data products such as those provided by precipitation models, land surface models, and remote sensing. On regional scales, gridded data products would help close the water budget for even data-sparse areas. For understanding of urban areas however, finer-scale data are needed, particularly for ET, to constrain water budgets. Municipalities could collect data to help increase the accuracy of urban water balance components. For example, municipalities could estimate I&I by improving communication and data sharing between water and wastewater agencies and

comparison of volumes between their systems. Assessments of temporal changes (e.g., seasonal) in I&I could be used to determine times of concentrated groundwater infiltration. Municipalities could also document water supply and wastewater collection pipe leakage through existing meter records in many cases. Improved knowledge of the significant components of urban water balances can be used for a variety of purposes including the development of urban hydrologic surface and subsurface models.

2.7 *Acknowledgements*

The authors thank Roxanne Sanderson and Michael P. McGuire for their significant contributions to data processing and spatial data analysis; Andrew J. Miller, Jack Sharp, Gary Fisher, and one anonymous reviewer for their helpful comments on the manuscript; and Carlos Espinosa for providing access to Baltimore City water and I&I data. This research was supported by National Science Foundation (NSF) Grants DGE-0549469, EF-0709659, and DEB- 0948944. In addition, this work builds upon field and data infrastructure supported by the NSF Long- Term Ecological Research (LTER) Program under NSF Grants DEB-0423476 and DEB-1027188.

Chapter 3: Untangling the effects of urban development on subsurface storage in Baltimore

Aditi S. Bhaskar, Claire Welty, Reed M. Maxwell, Andrew J. Miller

Submitted to Water Resources Research

3.1 Introduction

The percentage of people living in urban areas globally was 13% in 1900, 52% in 2011, and is expected to grow to 67% by 2050 [United Nations Population Division, 2011]. The accelerating migration of human populations to densely settled areas has led to profound alteration of urban hydrologic systems. Urban streamflow is flashier, with shorter lag times between precipitation and peak flow, increased peak flows, increased stormflow volumes, and decreased recession times [Leopold, 1968; Lull and Sopper, 1969; Rose and Peters, 2001; Beighley and Moglen, 2002]. The impacts of these hydrologic alterations can be far-reaching, from increased flooding and channel incision, to decreased capacity to process contaminants and degradation of urban aquatic habitat [Paul and Meyer, 2001; Pickett et al., 2001; Walsh et al., 2005]. The well-documented impacts of urban development on hydrologic systems have been mostly focused on surface water systems, whereas there has been little focus on groundwater systems [Kaushal and Belt, 2012; Hamel et al., 2013].

Previous studies of the effects of urbanization on base flow or groundwater recharge have reported a variety of effects [Meyer, 2005; Price, 2011]. Observed

decreases in groundwater recharge or base flow with urban development have been attributed to factors such as reduced infiltration due to connected impervious surfaces [Ku et al., 1992; Konrad et al., 2005; Hardison et al., 2009], increased groundwater withdrawals [Roach et al., 2008], export of locally supplied water to wastewater treatment plants [Pluhowski and Spinello, 1978; Simmons and Reynolds, 1982], or infiltration of groundwater into wastewater collection systems. Other studies have observed increases in groundwater recharge or base flow with urbanization that is credited to water supply pipe leakage [Lerner, 2002], reduced evapotranspiration, focused recharge of storm water infiltration [Ku et al., 1992; Appleyard, 1995; Stephens et al., 2012; Hogan et al., 2013], recovery from industrial groundwater pumping [Vázquez-Suñé et al., 2005], or discharge of wastewater from imported or confined water supply [Burns et al., 2005; Townsend-Small et al., 2013]. Where a range of these features was present and the increases and decreases nearly balanced out, or the effects on urban development were small compared to pre-development recharge, little effect was observed from urban development on groundwater recharge or base flow [Ferguson and Suckling, 1990; Barringer et al., 1994; Yang et al., 1999; Kim et al., 2001; Trowsdale and Lerner, 2003; Brandes et al., 2005; Meyer, 2005; Roy et al., 2005].

Urban development can impact groundwater flow systems even where overall water levels remain relatively constant. Although Trowsdale and Lerner [2003] found the increase in groundwater withdrawals to be balanced by recharge from leaking water mains with development in Nottingham, England, the groundwater flow system shifted from being dominated by regional flow to numerous local systems

controlling flow paths. Changes in the spatial distribution of recharge and discharge resulting from urban development, even without changes in magnitude, could alter fate and transport of contaminants in the subsurface and groundwater-surface water interactions.

Both increases and decreases in subsurface storage from urban development may lead to negative consequences. Falling water tables may lead to reductions in water availability or land subsidence. An associated decline in base flow can affect the survival of aquatic biota and diminish the connection between the stream channel and riparian vegetation, in turn reducing biogeochemical processing [Groffman *et al.*, 2002]. Rising water tables can lead to deleterious effects on urban infrastructure, such as structural property damage, flooding of underground structures (basements, tunnels, and parking structures), groundwater leakage into wastewater pipes, vegetation damage from over-saturation, and pollutant mobilization [Göbel *et al.*, 2004; Vázquez-Suñé *et al.*, 2005].

The conversion of land to urban use and need for improved management of urban hydrologic systems is ongoing, yet typically our understanding of urban groundwater is incomplete. The most commonly assumed effect of urbanization on the subsurface, reduced groundwater recharge, is based almost entirely on the most visible aspect of urban development, impervious surface coverage. As discussed above, previous studies have found evidence that contradicts this understanding, including increases in groundwater recharge and base flow with urban development. This suggests that evaluating a single aspect of urbanization may be too simplistic to explain observed effects of cities on groundwater systems. The effect on

groundwater is commonly attributable to the combination of many different characteristics of urban development, with varied impacts on groundwater recharge. In hydrologic monitoring of streamflow or groundwater levels, all impacts of urban development are usually observed in aggregate and therefore individual contributions cannot easily be discerned.

The objective of this paper is to evaluate the effects of individual features of urban development on subsurface storage, by isolating the impact of each aspect on the whole system. We use the Baltimore, Maryland, USA metropolitan region as a case study, where the water balance has been found to be significantly altered by anthropogenic discharges and recharges [Bhaskar and Welty, 2012a]. We develop a methodology to process and synthesize numerous urban discharge and recharge fluxes into an integrated hydrologic model. The urban features assessed for effects on subsurface storage are as follows, indicated in Figure 3.1.

1. reduced urban evapotranspiration;
2. urban hardscapes;
3. infiltration of groundwater into wastewater pipes; and
4. all other anthropogenic recharges and discharges (municipal and private well withdrawals, surface reservoir withdrawals, water supply pipe leakage, and lawn irrigation).

To achieve this objective, we implement and analyze the results from a three-dimensional groundwater-surface water-land surface hydrologic model. We compare the subsurface storage resulting from each scenario to isolate the effects of the features listed above.

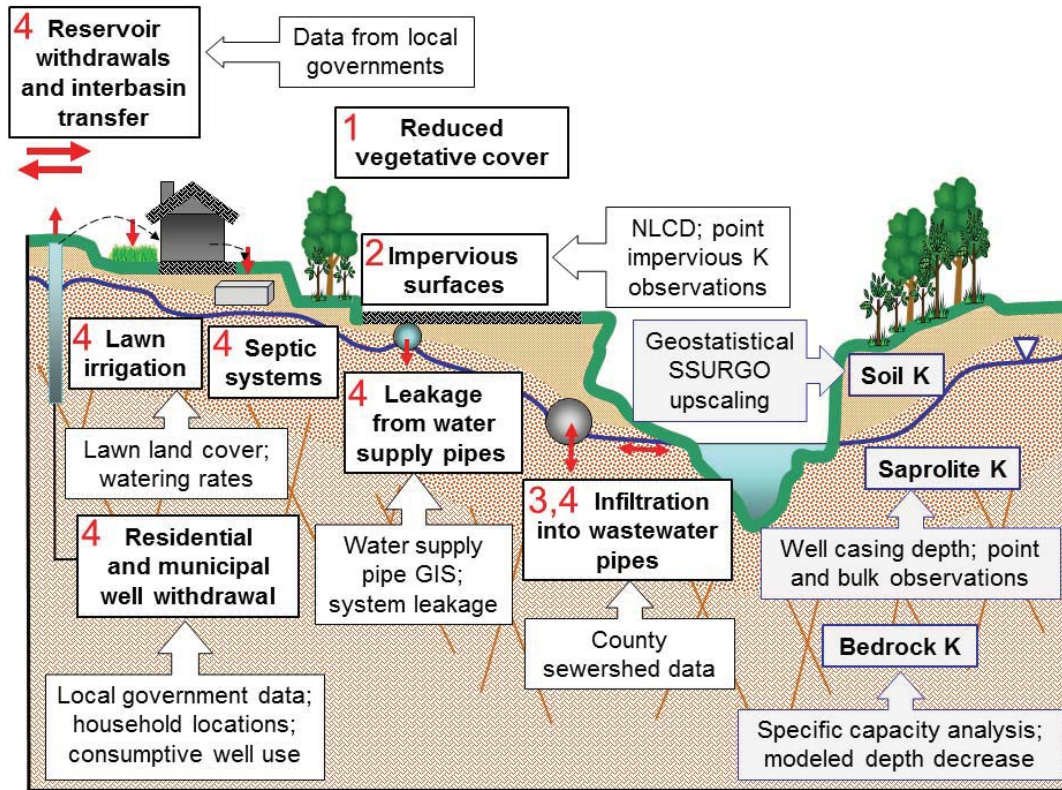


Figure 3.1. Model input data required for surface-subsurface flow models (blue outlines) and input data specific to urban areas (black outlines). The arrows indicate data sources for the urban and hydrogeologic data sets needed. Numbers indicate urban data sets altered for scenarios, where 1 indicates the vegetated city scenario, 2 indicates the pervious city scenario, 3 indicates the no-I&I scenario, and 4 indicates the no-anthropogenic-discharge-or-recharge scenario. Modified from Figure 6.1 in *Welty et al.* [2007].

3.2 Methods

We used the model ParFlow as a tool to achieve our research objectives. ParFlow is a three-dimensional, finite-difference, parallel hydrologic flow model developed by Lawrence Livermore National Laboratory and Colorado School of Mines [Ashby and Falgout, 1996; Jones and Woodward, 2001; Kollet and Maxwell, 2006, 2008]. It couples surface flow and variably-saturated subsurface flow using the continuous variable of pressure head. ParFlow has also been coupled with a number of other models, including the land surface model CoLM [Common Land Model; Dai *et al.*, 2003; Maxwell and Miller, 2005] (referred to as ParFlow.CLM), allowing interaction between subsurface soil moisture and simulated evapotranspiration.

We focused on the Baltimore metropolitan area with a 13,216 sq km model domain that includes Baltimore City and the five surrounding counties to the west of the Chesapeake Bay (Figure 3.2). The region is underlain by the Piedmont and Atlantic Coastal Plain physiographic provinces. Baltimore City has a population of 621,342 [US Census Bureau 2012 estimate, 2013], and receives an average precipitation of 1060 mm/year. The hydrology of the metropolitan area is well characterized by a dense network of hydrologic instrumentation and data collection.

3.2.1 *Model geometry and boundary conditions*

Because the regional model covers a large area, we used a horizontal grid cell discretization of 500 m x 500 m. A vertical discretization of 5 m was chosen to capture regional unsaturated flow dynamics. The maximum domain thickness was 1080 m, with subsurface thickness ranging from 200 m in the Piedmont physiographic province to 745 m in the Coastal Plain. The resulting total number of

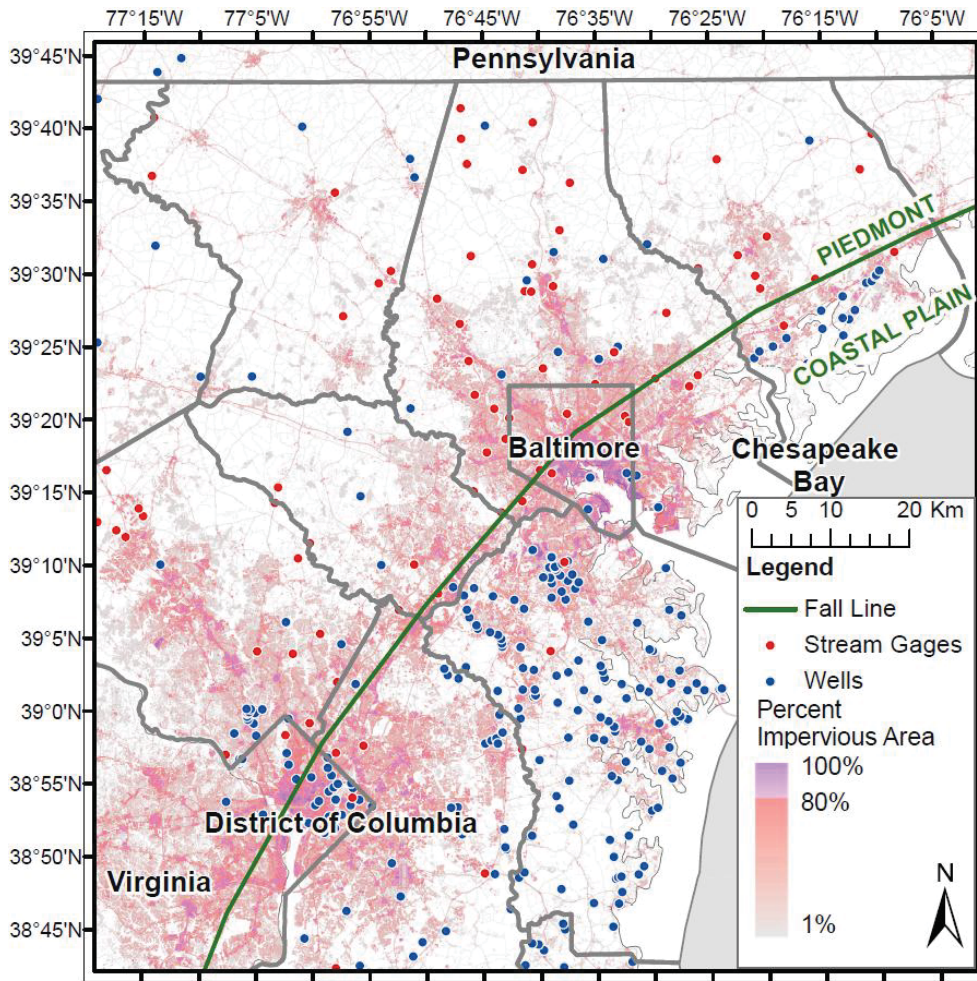


Figure 3.2. Map showing extent of model domain, stream gages and monitoring well locations, impervious surface coverage, physiographic provinces, and location within the Chesapeake Bay watershed.

active grid cells was 2,869,549. In order to minimize simulation times with this number of model grid cells, parallel simulations were carried out. Most of the simulations were conducted using 324 processors on the National Institute of Computational Sciences (NICS) Kraken system.

Because of the large extent of the model domain in comparison with the development footprint of the metropolitan area, no-flow boundary conditions were applied to the lateral and bottom boundaries. An overland flow boundary condition was applied to the surface that allowed surface flow to exit the domain based on topographic slope. Surface slopes derived from topographic data were required to define the land surface geometry and for use in the model overland flow component. We resampled a 30-m National Elevation Dataset (NED) Digital Elevation Model (DEM) (<http://ned.usgs.gov>) for the 500-m grid cells. Topographic data thus obtained required further manipulation to ensure smooth surface drainage and removal of pits, especially since the model domain had some flat and complicated topography, as is often the case for urban areas. ParFlow uses four-directional overland flow surface drainage. We used a global slopes enforcing method to ensure hydrologic connection and smooth drainage for four-directional overland flow [Barnes *et al.*, 2012].

3.2.2 Meteorological forcing and land surface model input data

Precipitation and evapotranspiration boundary condition fluxes at the surface are handled by the coupling between ParFlow and the land surface model CoLM [Maxwell and Miller, 2005]. CoLM requires meteorological forcing data, which was obtained from hourly North American Land Data Assimilation System Phase 2 (NLDAS-2) primary forcing data (FORA0125) (available online at NASA Goddard

Earth Sciences Data and Information Services Center Mirador, <http://mirador.gsfc.nasa.gov/>). Forcing included precipitation, temperature, solar radiation, wind speed, specific humidity, and atmospheric pressure and was spatially variable, derived by bilinear interpolation of NLDAS 1/8th degree grids to 500-m model grids. Other input data to CoLM included land cover derived from MODIS (Moderate Resolution Imaging Spectroradiometer) Land Cover Type 1 2007 using the International Geosphere-Biosphere Programme (IGBP) classification (Oak Ridge National Laboratory Distributed Active Archive Center, Oak Ridge, Tennessee, available online at http://webmap.ornl.gov/wcsdown/wcsdown.jsp?dg_id=10004_31). The land cover data were mapped from the original resolution to our model grid resolution by evaluating the dominant land cover type in each grid cell and assigning that land cover type to the cell. Urban areas were combined together in this land cover dataset and mapped to the bare soil land cover vegetation properties in CoLM. The standard ParFlow.CLM time step of 1 hour was used.

3.2.3 *Processing and synthesis of material properties and urban flux input data*

3.2.3.1 Subsurface and surface material properties

3.2.3.1.1 Fractured rock and saprolite

The Piedmont consists of fractured crystalline rock overlain by soil and saprolite; the Atlantic Coastal Plain is composed of semi-consolidated and unconsolidated sediments that dip toward the Atlantic Ocean and thicken seaward (Figure 3.3a), overlying saprolite and bedrock. We used specific capacity data from the Maryland Department of the Environment (MDE) Well Database [D. Swatzbaugh, MDE, personal communication, 2008] to estimate fractured-bedrock

hydraulic

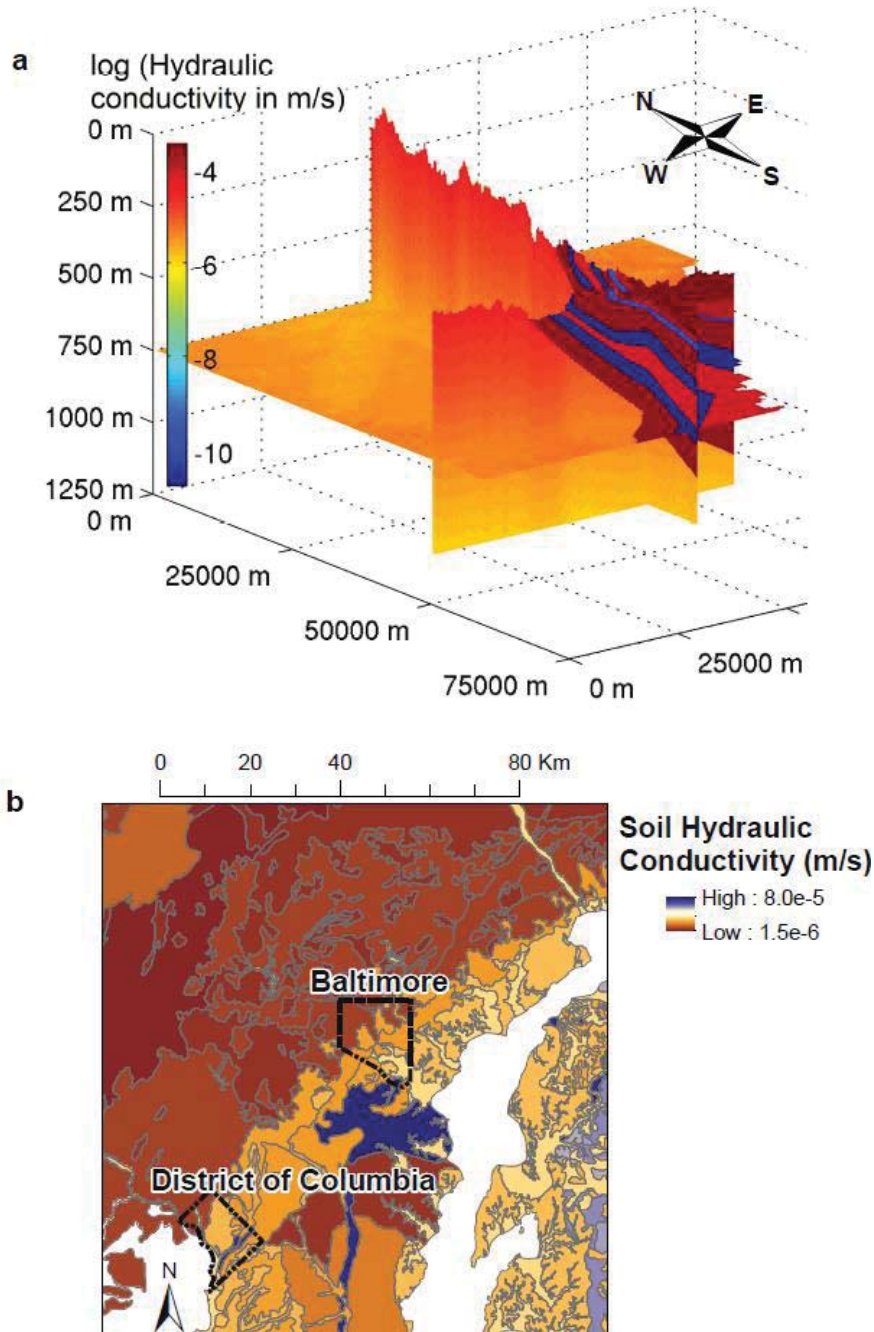


Figure 3.3. (a) Three slices through the three-dimensional model domain showing log (hydraulic conductivity in m/s). (b) Spatial distribution of upscaled soil SSURGO (<http://soildatamart.nrcs.usda.gov/USDGSM.aspx>) horizontal hydraulic conductivity (m/s).

conductivity (K) in the Piedmont. We estimated median K using 575 specific capacity values from wells less than 20 m deep using the method of *Theis et al.* [1963]. Because specific-capacity-derived hydraulic conductivity provides only sparse information for the deeper parts of the model domain, the shallowest specific-capacity-derived hydraulic conductivity value (3×10^{-5} m/s) was used as the hydraulic conductivity of the top of the bedrock. We used an exponential decrease of hydraulic conductivity with depth to describe bulk properties (exponential decay constant of 0.004 1/m [*Saar and Manga, 2004*]). Point observational values [*Stewart, 1962; Heath, 1984b*] were used to define total porosity (1%) for fractured rock grid cells.

Well casings are required for boreholes drilled through soil and saprolite, whereas the borehole portion in fractured rock is typically left as an open hole [*Daniel, III et al., 1997; Low et al., 2002*]. The well casing information provided by the MDE well database was used to estimate the combined soil and saprolite thickness in the Piedmont. Saprolite thickness was averaged for each location and interpolated among locations using kriging. Depth-averaged and depth-profile point observations of saprolite hydraulic conductivity were used to define hydraulic conductivity as a function of saprolite thickness [*Nutter and Otton, 1969; O'Brien and Buol, 1984; Simpson, 1986; Schoeneberger and Amoozegar, 1990; Amoozegar et al., 1991; Vepraskas and Williams, 1995; Rasmussen et al., 2000*]. Where saprolite was only one model grid cell thick, a bulk K value was used (10^{-6} m/s). For multiple saprolite cells in the vertical, the top-most cell was assigned a lower K value (10^{-7} m/s) with a linear increase with depth to the shallowest bedrock K value. Point observational values [*Stewart, 1962; Heath, 1984b*] were used to define total porosity

at 40% for all saprolite grid cells.

3.2.3.1.2 Atlantic Coastal Plain aquifers and confining units

For the Atlantic Coastal Plain, we used aquifer and confining unit altitudes derived from borehole analyses and reported in the Maryland Coastal Plain Aquifer Information System, MCPAIS (J. Raffensperger, USGS, personal communication, 2012). The aquifer geometry was translated to model horizontal gridding by resampling and to model vertical gridding using stair-step approximations. The hydraulic conductivity values for Coastal Plain aquifers and confining units were based on results from previous pump tests conducted in wells screened in various aquifers. The hydraulic conductivity was assigned as 3.5×10^{-4} m/s in the surficial aquifer [Andreasen and Fewster, 2001], 1.4×10^{-4} m/s in the Magothy aquifer [Andreasen and Fleck, 1996], 2.1×10^{-4} m/s in the Upper Patapsco aquifer [Achmad, 1991], 7.4×10^{-4} m/s in the Lower Patapsco aquifer [Andreasen, 1999], and 2.5×10^{-4} m/s in the Patuxent aquifer [Andreasen, 1999]. The hydraulic conductivity was set to 2.5×10^{-10} m/s in the Magothy-Patapsco confining unit [Mack and Mandle, 1977], 2.1×10^{-11} m/s in the Patapsco confining unit [Mack and Mandle, 1977], and 1.8×10^{-11} m/s in the Arundel Clay confining unit. The hydraulic conductivities of the dipping aquifers and confining units, along with the hydraulic conductivity decreasing exponentially with depth in the Piedmont bedrock are illustrated in a three-dimensional view of the model domain (Figure 3.3a). Point observational and reference values [Freeze and Cherry, 1979; Chapelle, 1986; Fleck and Vroblesky, 1996; McFarland, 1997] were used to define total porosity for aquifers (40%) and confining units (50%) .

3.2.3.1.3 Soil properties

The National Resources Conservation Service (NRCS) Soil Survey Geographic (SSURGO) data set provides saturated hydraulic conductivity (K) values at fine spatial scales (<http://websoilsurvey.nrcs.usda.gov/>). SSURGO “map units” (4000 – 40,000 m²) are characterized by representative saturated hydraulic conductivity in the dominant soil component for layers up to about 3 m below land surface. One approach to upscaling SSURGO data is to use geostatistical analysis [Journal and Huijbregts, 1978; Deutsch and Journel, 1998] to calculate experimental variograms of ln(K) from SSURGO data and incorporate best-fit variogram parameters into theoretical expressions [e.g., Gelhar and Axness, 1983] to calculate an effective hydraulic conductivity tensor at the scale of a chosen larger spatial unit. This methodology has been applied previously to sand and gravel aquifers [e.g. Sudicky, 1986; Hess et al., 1992; Sudicky et al., 2010].

To upscale SSURGO data using geostatistical analysis, we calculated the horizontal correlation scale, vertical correlation scale, sill for both directions, and a nugget for the horizontal variogram by fitting a negative exponential variogram model to experimental variograms of SSURGO map unit data using nonlinear least squares. The fit of the exponential model to the experimental variograms revealed a clear anisotropy structure in saturated ln(K), with calculated horizontal correlation lengths on the order of meters to tens of meters and vertical correlation lengths on the order of centimeters. We incorporated the best-fit variogram parameters into the theory of Gelhar and Axness [1983; Eq. 59] to calculate an effective hydraulic conductivity tensor at the scale of a NRCS STATSGO2

(<http://websoilsurvey.nrcs.usda.gov/>) unit. We utilized the larger STATSGO2 map units as a way to group the region's SSURGO polygons in order to define areas over which to calculate effective, anisotropic hydraulic conductivity of the soils. The soil hydraulic conductivities calculated are shown in Figure 3.3b. We assumed a total porosity value of 40% because of the relatively small range in hydraulic conductivities for soil grid cells (based on sand value in *Freeze and Cherry* [1979]).

3.2.3.1.4 Impervious surfaces

Urban hardscapes such as roads, parking lots, and buildings are characterized by a range of finite permeabilities and therefore should not be thought of as being completely impervious to water, although this is commonly assumed to be the case. We used the average observational K value of 10^{-7} m/s from infiltration tests of fractured roads [*Wiles and Sharp*, 2008] and a total porosity value of 5% based on point observation values [*Liu and Guo*, 2003]. These values were applied to surfaces designated as “impervious” or hard surfaces. Because many cells contained a mixture of surface cover types, we resampled impervious surface coverage from the 30-m National Land Cover Dataset [NLCD 2006; *Fry et al.*, 2011] (Figure 3.2), resulting in model cells with a designated percent “impervious” area. Since a model grid cell can only be assigned a single hydraulic conductivity value, cells with “impervious” percentage exceeding 50% were assigned hard-surface hydraulic conductivity and total porosity values.

3.2.3.2 Urban water fluxes

As demonstrated above, application of a coupled groundwater-surface water model to any area requires intensive data processing. The challenge is compounded

when applying such a model to an urbanized area, where there are numerous anthropogenically-caused recharge and discharge fluxes (Figure 3.1). Precise data on these fluxes can be challenging to obtain. Here we present our methodology to find and process urban input datasets, estimate these fluxes from available data, and synthesize data into our hydrologic model.

3.2.3.2.1 Lawn irrigation

Irrigation of lawns and gardens using public water supply can provide anthropogenic recharge to the subsurface. Grass/scrub land cover has been mapped at 0.63-m resolution in the Baltimore region by the University of Vermont Spatial Analysis Laboratory (http://128.118.47.34/chesapeakeview/MetadataDisplay.aspx?file=Landcover_2007_4county_baltmetro.xml&dataset=3152). Using this fine-scale lawn coverage, we calculated the area of lawn in each model grid cell within the municipal water service area (Figure 3.4a). We assumed 25% of the lawn area to be irrigated at a rate of one inch (25.4 mm) per week for four months of the year [Law *et al.*, 2004a; Milesi *et al.*, 2005b; Claessens *et al.*, 2006b]. We modeled the water applied over the four-month irrigation period as being distributed uniformly over the year to be consistent with our representation of wells as having constant recharge or discharge rates during the same period of time. The estimated lawn irrigation ranged from 10^{-4} to 10^2 mm/year/model grid cell.

3.2.4.2.2 Water supply pipe leakage

Water supply pipes are pressurized and deteriorate over time, leading to leakage of between 5 and 60 percent of their flow [Garcia-Fresca and Sharp, 2005].

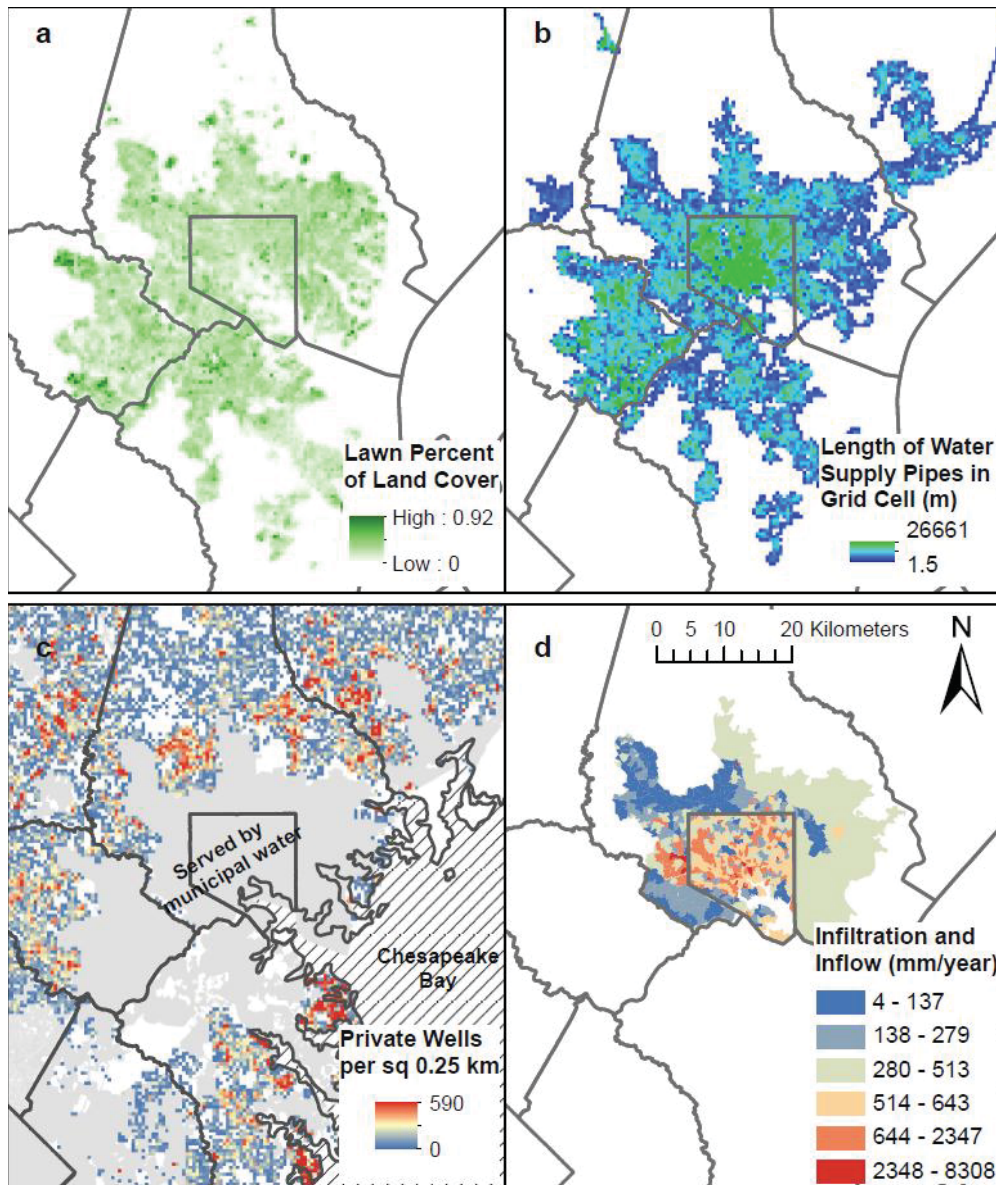


Figure 3.4. (a) Percentage of 500 m x 500 m model grid cell composed of grass/shrub based on the resampling of the University of Vermont Spatial Analysis Laboratory classification

(http://128.118.47.34/chesapeakeview/MetadataDisplay.aspx?file=Landcover_2007_4county_baltmetro.xml&dataset=3152). (b) Total length of water supply pipes (m) in each model grid cell within the Baltimore water service area. (c) Number of residential private wells in each model grid cell outside of the municipal water service area derived using MdPropertyView 2009

(<http://www.mdp.state.md.us/OurProducts/PropertyMapProducts/MDPropertyViewProducts.shtml>). (d) Baltimore County and Baltimore City infiltration and inflow of groundwater and stormwater into wastewater pipes (combined for wet and dry weather) in each sewershed (mm/year).

The total amount of flow in the Baltimore water system is 204.7 MGD, and 23% of this water becomes leakage [McCord, 2009b; Bhaskar and Welty, 2012a]. We used spatial data sets of regional water supply pipes to calculate the total length of pipe in each model grid cell (Figure 3.4b). Since information on leak locations was unknown but the overall leakage rate in the system was known, we distributed the leakage in proportion to water supply pipe density. Calculated pipe leakage ranged from 10^{-2} to 290 mm/year/model grid cell. Pipe leakage was implemented as an injection at surface model grid cells.

3.2.3.2.3 Residential private wells

In areas outside public water supply systems, consumptive use from residential private wells constitutes a groundwater withdrawal. Total annual water use per person on residential private water was estimated from USGS Water Use Reports [Kenny *et al.*, 2009]. The average household size in each county from the US Census [United States Census Bureau, 2007] was used to convert water use per person (approximately 80 gallons/person/day) to water use per household. The percentage of total water use per residential well that is consumptive has been estimated to be 18% [DeSimone, 2004] because aside from summer irrigation use, most water is returned to the subsurface via septic disposal. The number of private wells in each model grid cell was assumed to be all residential properties outside of municipal service areas and was identified using the state tax assessment system, MdProperty View (<http://www.mdp.state.md.us/OurProducts/PropertyMapProducts/MDPropertyViewProducts.shtml>). Since the exact well location within a residential parcel is usually

unknown, we assigned the location of the well to the centroid of the residential parcel. The consumptive use per household multiplied by the number of private wells in each model grid cell provided an estimate of private consumptive well use (Figure 3.4c). Private wells were assigned a depth of 72 m, with the screened portion starting at a depth of 58 m below land surface (Atlantic Coastal Plain) or 15 m below land surface (Piedmont). These values were based on the mean drinking water well casing depth and well screening information from the MDE Well Database (D. Swatzbaugh, MDE, personal communication, 2008). The estimated consumptive use by private wells ranged from 0 to 125 mm/year/model grid cell.

3.2.3.2.4 Infiltration and inflow

The dominant direction of leakage into or out of wastewater pipes depends on the position of the water table relative to the wastewater pipes. In cities where exfiltration out of wastewater pipes is dominant, contaminant flux balances or application of Darcy's law to sewer defects have been used as methods to quantify leakage rates [Yang *et al.*, 1999; Eiswirth, 2001; Eiswirth *et al.*, 2004; Morris *et al.*, 2007]. In other cities, groundwater infiltrating into wastewater pipes forms an important groundwater discharge [Kim *et al.*, 2001; Wolf *et al.*, 2007; Rodriguez *et al.*, 2008; Bhaskar and Welty, 2012a]. This infiltration and inflow (I&I) of groundwater and stormwater into the wastewater system occurs via cracks and improper connections [American Public Works Association, 1971; Heaney *et al.*, 2000].

Information on net I&I was provided by two local wastewater utility I&I studies [D. Bayer, Baltimore County Bureau of Engineering, personal communication

(2012); C. A. Espinosa, KCI Technologies, personal communication (2010); *Espinosa and Wyatt, 2007*]. In some cases, the studies only provided rainfall-derived I&I (RDII) on a design-storm basis. We made an assumption that RDII scales linearly with precipitation to calculate RDII on an annual basis, by multiplying RDII by the inverse of the fraction of average annual rainfall used in the 24-hour design storm. I&I was reported as millions of gallons per day per sewershed. We converted to millimeters per year by scaling by sewershed area then calculating area-weighted values for model grid cells. In areas within the Baltimore wastewater system where I&I data were not available (38% of the region), we assumed the average respective Baltimore City or County area-weighted average I&I rate. I&I was represented in the model as a near-surface withdrawal. Figure 3.4d shows the sum of wet and dry I&I (both storm and baseflow periods) in each sewershed. Baltimore has separate stormwater and wastewater systems; however, Figure 3.4d shows that because of infrastructure deterioration, the stormwater system is indirectly connected to the wastewater system.

3.2.3.2.5 Municipal public wells and reservoir withdrawals

Municipal well data (discharge values and well lengths) were in some cases available in local government reports or were provided through communication with local government agencies [J. Glass, Westminster Department of Public Works, personal communication (2012); D. Nott, Manchester Department of Public Works, personal communication (2012); J. Barrington, Freedom Bureau of Utilities, personal communication (2012); F. Schaeffer, New Windsor Town Manager, personal communication (2012); K. Henry, Anne Arundel County Department of Public

Works, personal communication (2012); J. Caudil, Bel Air Public Works, personal communication (2012); *Andreasen, 2007; Harford County Department of Public Works, 2007; Carroll County Government, 2009*]. Where data on screened or open well lengths were incomplete or unknown, the value was based on a representative length in the area. Where the total well depth was not provided, nearest available well-depths were used. We assumed temporally constant well pumping equal to the average pumping rate. Average reservoir withdrawals were also typically available from county reports or through communication with local agencies, and were included as withdrawals at the land surface at the location of the reservoir. We assumed temporally constant reservoir withdrawal equal to reported average reservoir withdrawal over time. Table 3.1 shows the total withdrawal of each type of net recharge or discharge represented in the model. The surface water reservoir withdrawal was the largest total withdrawal type in this region, and was followed by infiltration of groundwater into the wastewater system. Residential well pumping was the smallest total flux.

3.2.4 *Model initialization*

Model initialization requires an assumed starting water table depth at every surface grid cell, followed by a spin-up period in order to reach an equilibrium state consistent with model inputs and boundary conditions. We started by placing the water table 10 m below the land surface everywhere. We used homogeneous hydrogeologic properties (e.g. hydraulic conductivity of 5.556×10^{-5} m/s and total porosity of 0.4), without including the input data discussed in section 2.3. We ran the model for over 11 months without precipitation input to allow the water table to

Table 3.1. Anthropogenic discharge and recharge fluxes summed over the entire model domain (mm/day).

| Anthropogenic discharge or recharge | Total discharge flux (m/hour) |
|---|-------------------------------|
| Lawn irrigation | -0.15 |
| Water supply pipe leakage | -0.18 |
| Surface water reservoirs | 1.14 |
| Residential wells | 0.02 |
| Municipal wells | 0.18 |
| Infiltration and inflow (I&I) into wastewater pipes | 0.88 |

equilibrate based on topography, with the result that the water table became shallower in the valleys and deeper at higher elevations relative to the initial condition of constant depth below land surface. Following this step, coupling with the Common Land Model along with associated meteorological forcing was introduced. This period featured transient spin-up, an initialization procedure in which multiple years of forcing were applied. During this period, the water table equilibrated based on meteorological and topographic forcing. The aim of the transient spin-up was to reach a dynamic equilibrium where subsurface storage responded primarily to meteorological conditions and not in response to the initial state. The spin-up time period using ParFlow.CLM was 1 October 2000 – 31 December 2006.

3.2.5 *Model calibration of Manning's n*

Using the final output from the initialization time period as an initial condition, 1 January 2007 – 31 March 2007 was then simulated with hydrogeologic and urban model inputs included (described in section 2.3). This was used as a calibration period for Manning's n , the roughness coefficient relating pressure head (a model output) to volumetric streamflow through Manning's equation. Because of the large horizontal grid resolution (500 m), stream cells had much greater width and much shallower depth than would occur in a real stream draining a watershed of comparable size. Therefore there is no physical relation between field estimates and the modeled Manning's n value, which should be considered a fitted parameter. No other parameters were calibrated because our purpose was not to force observed and modeled streamflow or water table elevations to match at specific locations.

Calibration of a single Manning's n was performed by minimizing the root mean squared error between observed and modeled hourly streamflow, summed for all stream gages in the domain not having dams directly upstream (78 stream gages), over a range of Manning's n values. Manning's n was used in two steps in the application of ParFlow: (1) in the model input files for use in simulation and (2) in post-processing for the conversion of the ParFlow output of pressure head to volumetric streamflow. In order to avoid the lengthy wall-clock time that would be required to repetitively simulate three months to calibrate the Manning's n value used for both the simulation and for post-processing, the calibration was done using an iterative procedure for the two steps, described in detail as follows.

A series of 10 short simulations was run (1 day each) for 10 different values of Manning's n, where the input value of Manning's n was used in post-processing to calculate the streamflow output from the pressure field. A "default" value of n ($5.52 \times 10^{-6} \text{ hr} \cdot (\text{m}^{-1/3})$) was then used as input and the resulting pressure field was converted to the streamflow previously obtained for each of the 10 simulated cases through the use of 10 different n values. A tight nonlinear relation was found relating these post-processed n values to the original input values for the set of 10 simulations. Then this relation was used to choose an n value to post-process the pressure head data generated from the simulation for the calibration period (1 January – 31 March 2007) where the "default" value had been used as input, such that modeled streamflow data matched observed data by minimizing root mean squared error (RMSE). This Manning's n value was then used as both the input and post-processing value for the production simulation starting on 1 January 2007.

3.2.6 *Model development to isolate effects of different urban features*

The base case simulation is the one described above, in which the initialized water table, hydrogeologic and urban model inputs, and calibrated Manning's n value were incorporated. The base case simulation was carried out for the period 1 January 2007 to 30 June 2007. Modeled streamflow and water levels in wells were compared to observed values over the base case time period. This length of time was used in order to compare growing season and dormant months. In order to isolate the effects of individual urban features, we simulated other scenarios having only one modification from the base case. These scenarios do not represent possible policy outcomes. Rather they are used to explore the sensitivity of the hydrologic system to aspects of urban features. The four scenarios that were compared to the base case are:

1. Vegetated city scenario. The areas represented as urban land cover (areas greater than 70% impervious surface cover) were converted to the land cover type of natural vegetation mosaic in the Common Land Model for calculation of evapotranspiration.
2. Pervious city scenario. The impervious (hardscaped) surface cover in urban areas was removed and background soil hydraulic conductivities were used instead.
3. No-I&I scenario. The infiltration and inflow (I&I) of groundwater and storm water into wastewater pipes was removed.
4. No-anthropogenic-discharge-or-recharge. All anthropogenic discharges or recharges were removed, including infiltration into wastewater pipes, reservoir withdrawals, municipal and private well withdrawals, water

supply pipe leakage, and lawn irrigation. Since these fluxes were represented as well injections or withdrawals in ParFlow, requiring that the total porosity of these grid cells be set equal to 1 in the base case, in this scenario the wells were still included (keeping the total porosity the same as the base case), but the fluxes were reduced to zero.

These scenarios were run for the same time period as the base case (beginning 1 January 2007) and using the same initial conditions for both ParFlow and CoLM. They were also simulated through 30 June 2007 using the same meteorological forcing as the base case. With the same initial conditions, boundary conditions, and only one change in the representation of urban features, the impact of each of these features was effectively isolated.

3.3 *Results*

3.3.1 *Initialization*

During the transient spin-up period, we evaluated model outputs to ensure a dynamic equilibrium was reached. Figure 3.5a shows simulated total subsurface storage over the spin-up time period. Total subsurface storage was calculated by summing the volume of water over all cells in the domain subsurface for each day. Precipitation in 2002 was 5% lower than average, and this was reflected in the draining of subsurface storage over this year. Subsequently, subsurface storage recovered as precipitation volumes returned to higher values. During the spin-up period, base flow followed the expected seasonal pattern with smaller values in the summer, higher values in winter, and peaks in streamflow corresponding to storm events.

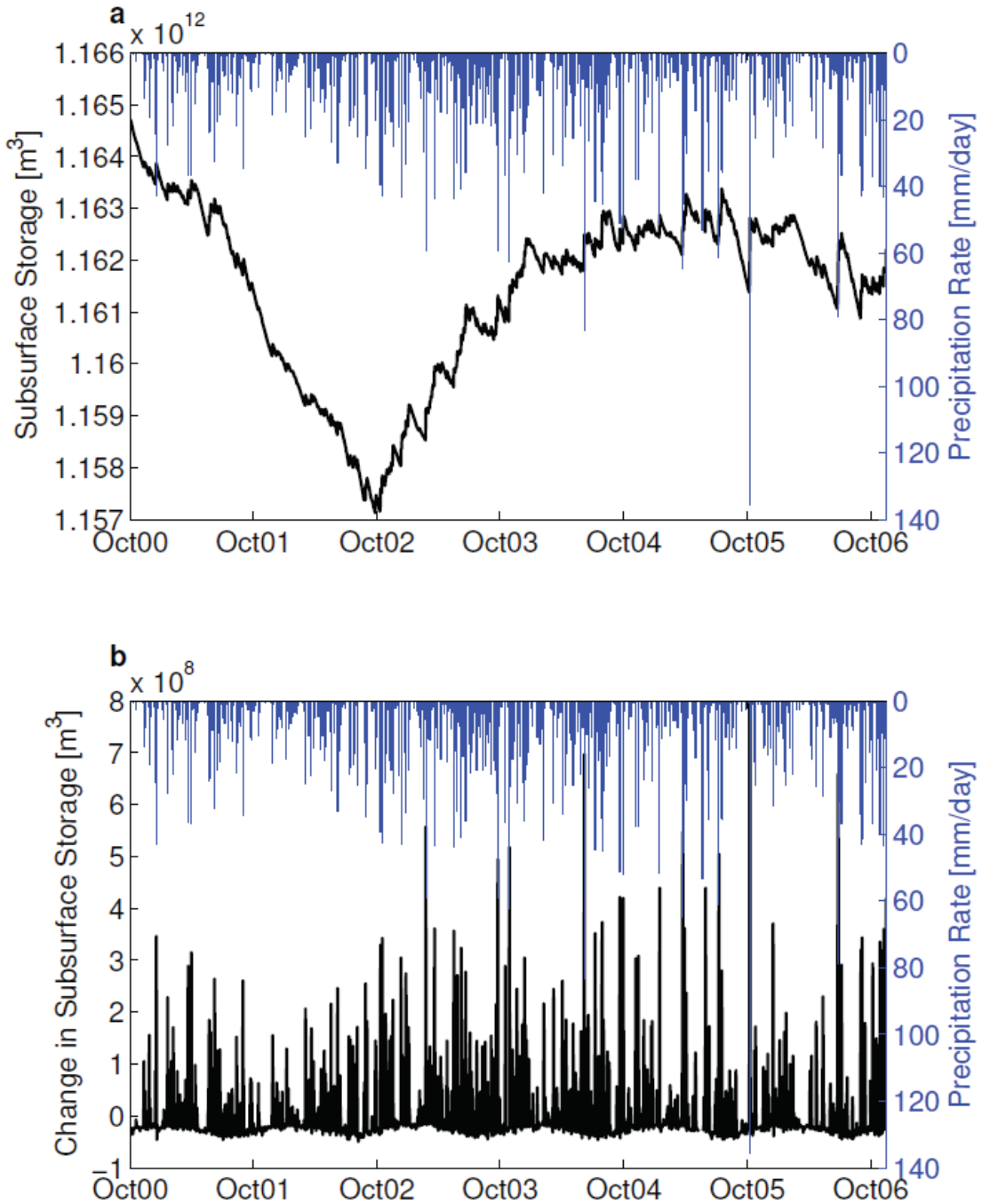


Figure 3.5. (a) Simulated subsurface storage summed over the model domain during the spin-up time period (black) and daily precipitation forcing over the same time period (blue). (b) Simulated daily change in subsurface storage during the spin-up time period (black) where positive values indicate an increase in subsurface storage compared to the previous day, as well as daily precipitation forcing (blue).

The difference in subsurface storage between a given day and the previous day is shown in Figure 3.5b. The change in subsurface storage was negative on most days, meaning subsurface storage decreased from the previous day due to the lack of precipitation inflow and continued evapotranspiration and stream outflow. During precipitation events there were large increases in subsurface storage, leading to positive values of change in subsurface storage. There was also a seasonal cycle of change in subsurface storage during dry days (shown by the lower part of the curve in Figure 3.5b). The daily change in subsurface storage was most negative during summer when evapotranspiration was higher, removing more water from storage. The change in subsurface storage was largest (less negative and closer to zero) in the winter when evapotranspiration was smaller. These plots of model output during spin-up show that there was no consistent upward or downward trend in these data and therefore the system could be assumed to have reached a dynamic equilibrium.

3.3.2 *Model comparison with observed data*

The next step was to calibrate Manning's n and compare modeled output with observations. The calibrated Manning's n coefficient was $5 \times 10^{-8} \text{ hr} \cdot (\text{m}^{-1/3})$. The calibration procedure ensured that the mean modeled vs. mean observed streamflow over the calibration time period (1 January 2007 – 31 March 2007) was fit by a 1:1 line. Three example observed and modeled hydrographs over the simulation period which showed the range of hydrologic responses are presented in Figure 3.6. We calculated Nash-Sutcliffe efficiencies to quantify the performance of the model at 78 stream gages. We found that the efficiencies ranged from -14 to 1. Well hydrographs are not shown because most wells that had records over this time period were

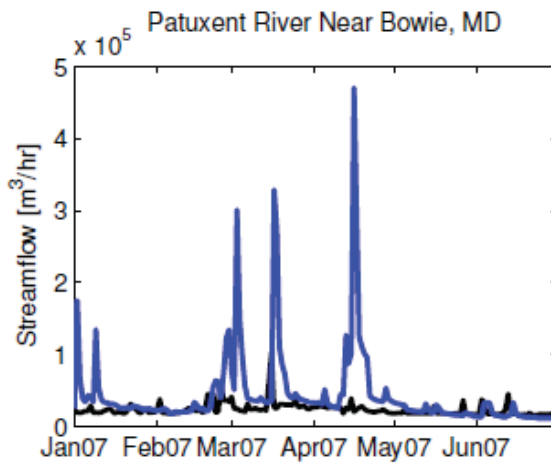
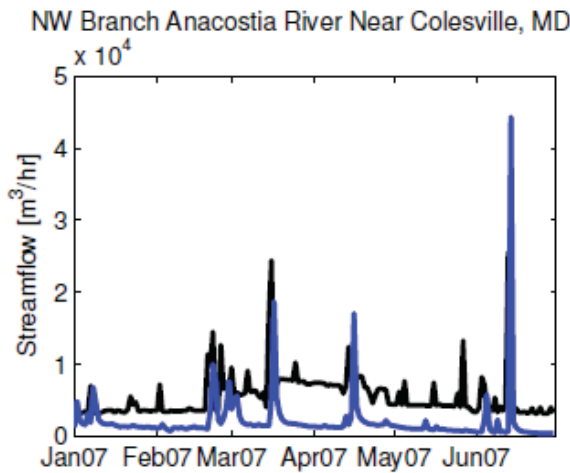
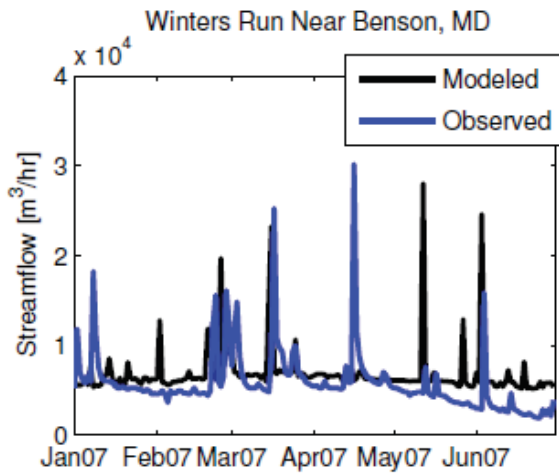


Figure 3.6. Modeled and observed hydrographs over 1 January 2007 – 30 June 2007 at three example stream gages. These are Winters Run near Benson, MD (USGS 01581700), NW Branch Anacostia River near Colesville, MD (USGS 01650500), and Patuxent River near Bowie, MD (USGS 01594440).

measured monthly and the six measurements did not change substantially over this period.

3.3.3 Isolation of urban features in model scenarios

The base case water balance is shown in Figure 3.7. Subsurface storage decreased gradually during periods without precipitation, and increased sharply after precipitation events, as expected. Change in storage was well matched by inflows minus outflows (precipitation – streamflow – evapotranspiration – urban withdrawals), as we would expect based on mass balance. Figure 3.8 shows the percent difference in subsurface storage between each model scenario and the base case as compared to the difference between precipitation and evapotranspiration. The difference between precipitation and evapotranspiration (P-ET) over the six-month simulation period can be considered the water available for natural recharge. The same relative magnitudes of scenario results were seen when comparing changes in subsurface storage to the total volume of subsurface storage, but since the total volume of subsurface storage is so large (on the order of 10^{17} m³), even large changes over six months had little effect on the total volume.

The pervious-city scenario had nearly no change in subsurface storage compared to the base case. The change in subsurface storage was positive, meaning that subsurface storage in the pervious city scenario was higher than that in the base case, as might be expected due to increased infiltration through urban areas with higher permeability. However, the magnitude of the percentage increase in subsurface storage was negligible (4×10^{-4} %) compared to the magnitude of difference in the other scenarios. The vegetated-city scenario had less subsurface

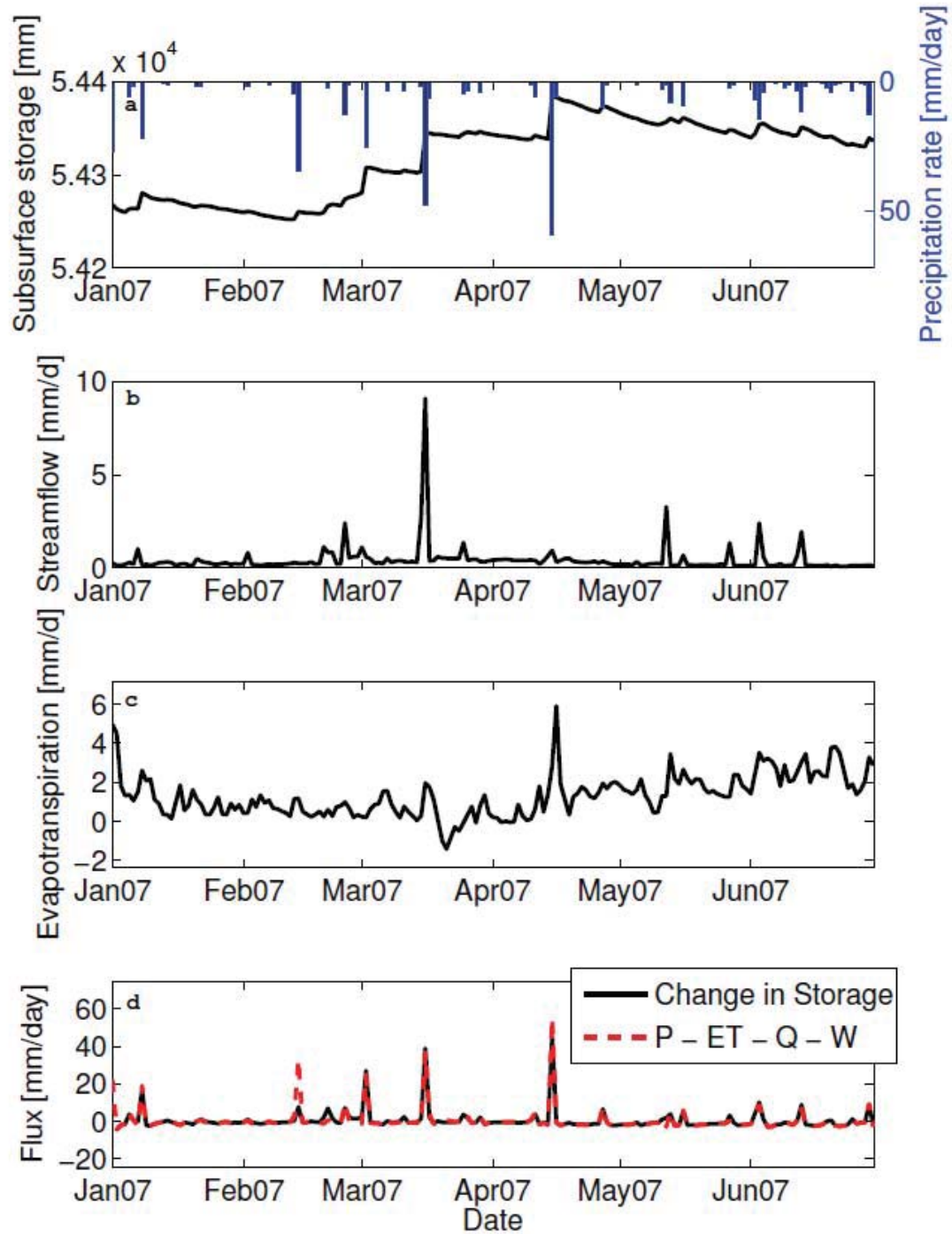


Figure 3.7. Base case daily water balance from 1 January 2007 – 30 June 2007. (a) Simulated subsurface storage in m (volumetric subsurface water storage in m^3 divided by surface area of domain) and model forcing precipitation; (b) simulated streamflow; (c) simulated evapotranspiration; and (d) model mass balance, where change in total model storage is compared to inflows minus outflows (precipitation – evapotranspiration – streamflow – anthropogenic withdrawals). Total anthropogenic withdrawals were 1.93 m/hour.

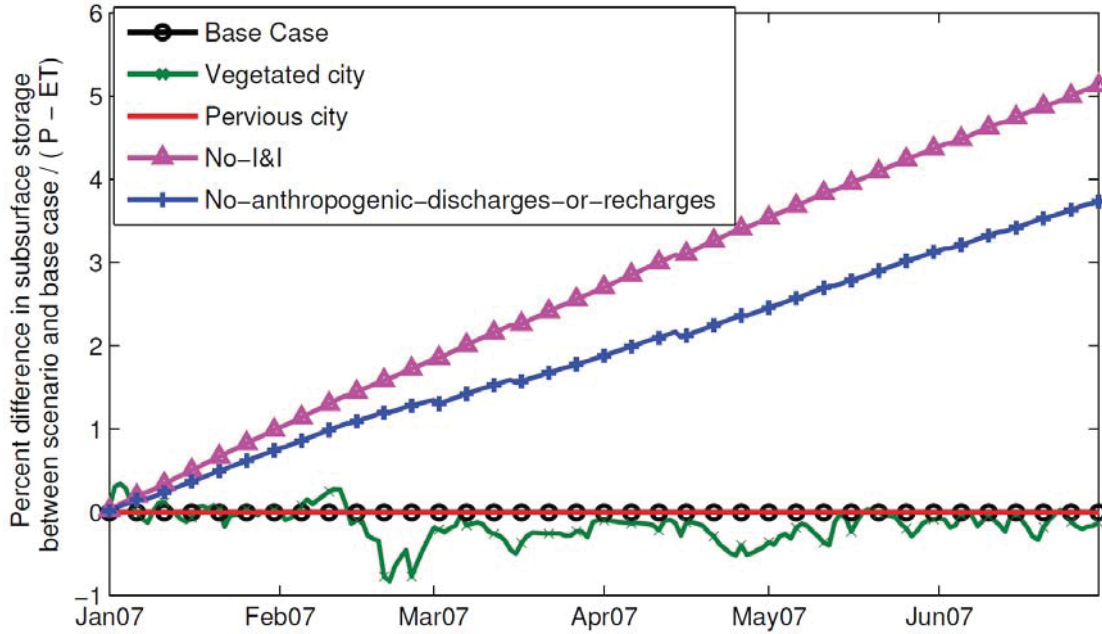


Figure 3.8. Percent difference between base-case subsurface storage and subsurface storage for each scenario compared to precipitation minus evapotranspiration summed over the simulation period (1 January 2007 – 30 June 2007).

storage and greater evapotranspiration compared to the base case (0.13% less than the base case compared to P-ET). The no-I&I scenario had subsurface storage that increased at a constant rate compared to the base case, and was 5.1% greater after six months relative to P-ET. The no-anthropogenic-discharge-or-recharge scenario showed a smaller subsurface storage than the no-I&I scenario, and had subsurface storage 3.7% greater than the base case as compared to P-ET. This means the total recharge removed (lawn irrigation and pipe leakage) was outweighed by the net effect of water exported through leakage into wastewater pipes, but was still larger than the total discharge removed (e.g. due to private and municipal well withdrawals). Figure 3.8 as discussed above presents a spatially summed view of temporal changes in subsurface storage for each of the scenarios. Another way to examine the scenarios is to look at spatial changes due to the differences among scenarios at one point in time.

Figure 3.9 presents the spatial difference in pressure head at the land surface between the scenario value and the base case at 1 July 2007. The depth to water is related to pressure head at the land surface. Depth to water, while more intuitive to interpret than pressure head, does not show much variation even over the six months of simulation. This is because the vertical grid discretization was 5 m, and therefore only depth to water changes in multiples of 5 m can be discerned. Positive values in Figure 3.9 indicated that the pressure head was greater in the scenario, whereas negative values indicated pressure head was greater in the base case.

Figure 3.9a demonstrates that the base case was characterized by greater pressure head in the more populated areas as compared to the vegetated-city scenario. This behavior is consistent with the decrease in subsurface storage seen in the

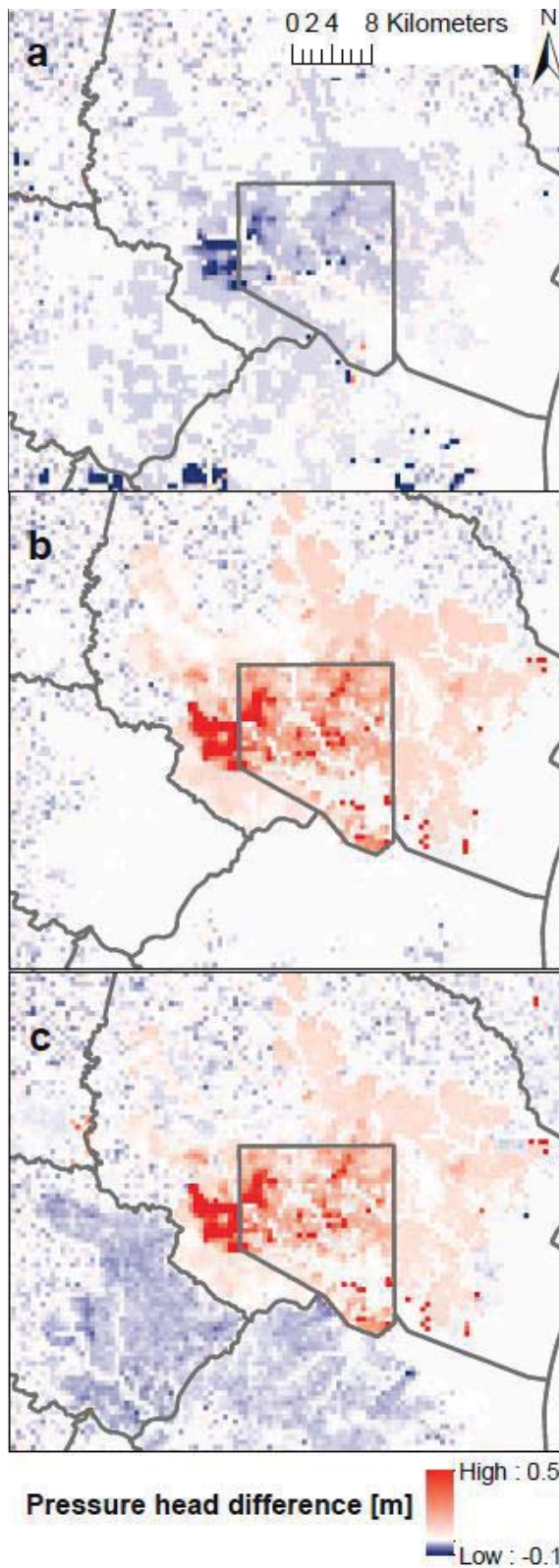


Figure 3.9. Difference maps of land surface pressure head (m) for each scenario minus base-case land surface pressure head (m) at 30 June 2007. (a) Vegetated city scenario. (b) No-I&I scenario. (c) No-anthropogenic-discharge-or-recharge scenario.

vegetated-city scenario (Figure 3.8), which results from greater evapotranspiration with the transformation from bare soil to natural vegetation mosaic land cover. Figure 3.9b shows the changes in pressure head between the no-I&I scenario and base case. This scenario led to the largest positive change in subsurface storage over time as depicted in Figure 3.8. Figure 3.9b shows that this increase in pressure head is concentrated primarily within Baltimore City and Baltimore County. This is the area in which I&I values were included, and therefore these are the areas where the removal of I&I led to increases in pressure head.

Figure 3.9c presents the spatial difference in pressure head between the no-anthropogenic-discharge-or-recharge scenario and the base case. The pattern of positive pressure head in Baltimore City and County is similar to that shown in Figure 3.9b, which is presumed to result from removed I&I discharge. The removed recharge leads to the negative values (decreases in pressure head in the scenario as compared to the base case) in other parts of Howard and Anne Arundel Counties. These areas are served by public water where additional recharge is provided by lawn irrigation and leaking water supply pipes.

The portion of the land surface area that changed in surface pressure head by more than 25 cm between the scenario and the base case varied among the urban features. For the vegetated city scenario, this land surface area was 7.8% of the surface area of the domain (13,216 km²), $5.7 \times 10^{-3}\%$ for the pervious city scenario, 0.45% for the no-I&I scenario, and 0.39% for the no-anthropogenic-discharge-or-recharge scenario. This can be compared to the original amount of land surface area of the model where the input data was altered by the scenario. For the vegetated city

scenario, 21% of the land cover in the model was changed from urban to natural vegetation mosaic. In the pervious city scenario, 4.2% of the land surface was changed from impervious surface hydraulic conductivity to soil hydraulic conductivity. In the no-I&I scenario, I&I fluxes were removed from grid cells making up 6.6% of the surface area of the model domain. The no-anthropogenic-discharge-or-recharge scenario removed fluxes applied at 43% of model surface area.

3.4 *Discussion*

3.4.1 *Model development*

The method of model initialization required long simulation times, but this approach prevented the arbitrary initial condition from having undue influence on model results. This was done by providing a buffer period during model spin-up (shown in Figure 3.5) when the model state moved away from the initial condition and towards a dynamic equilibrium with meteorological forcing. The synthesis of urban and hydrogeologic input data required a large amount of data collection and processing, as well as a number of assumptions to derive required information from incomplete data. ParFlow is a complex, parallel, integrated hydrologic model and the combination of material properties required for all applications and the urban discharge and recharge fluxes required incorporation of numerous heterogeneous datasets. This combination of urban fluxes included in an integrated model is unique and involved calibration of Manning's n . A formal calibration of multiple parameters of this complex model involving millions of model grid cells was infeasible, and would not have furthered our goal of understanding the impact of individual features of urban development.

No single value of Manning's n was ideally suited for all periods of simulation. The period used for model calibration had greater precipitation than the overall simulation period (227 mm during 1 January 2007 – 31 March 2007 vs. 195 mm during 1 April 2007 – 30 June 2007). During drier conditions, calibration of Manning's n led to a smaller value, whereas calibration during wetter periods resulted in a higher value. During low base flow periods, stream stage dropped considerably, requiring a smaller Manning's n value to increase the volumetric streamflow to be closer to the observed condition. The values of Manning's n that resulted from different calibration periods indicated that the contrast in stream stage between average and low base flows was greater in the model than in observed streamflow.

In addition to the limitations in applying one Manning's n value over different streamflow conditions, there are also limitations in applying a single n value to all streams in the model domain (Figure 3.6). In terms of Nash-Sutcliffe efficiencies, the best-modeled values of streamflow were for small drainage areas, whereas efficiencies were poorest for large drainage areas. However, because the distribution of drainage areas of USGS gaged watersheds for this region is skewed toward smaller watersheds, the calibrated Manning's n was presumably weighted to better fit overland flow for smaller watersheds. Also, different basin sizes would be expected to have different hydraulic radii and different water flow depths. There is no clear way to calibrate Manning's n for individual basins because the basins are nested within each other, and furthermore, matching observed hydrographs was not the main goal of this work. Calibration of Manning's n to multiple observed records over space and time is an issue that should be explored in future research.

Unlike streamflow, depth to water table had no calibration performed. The relationship between observed and modeled water table depth shifted during different time periods. The simulated time period was drier than average, and the model dried to a greater extent as compared to well observations. This is particularly the case in the Piedmont as the elevations are higher and therefore the depths to water table in both the model and in observations were deeper; this may be related to representations of hydraulic conductivity, which were based on the best available data but are not fully known throughout the subsurface.

3.4.2 Limitations

Small stream systems periodically became unsaturated during dry periods in the summer of 2007 in the model. This behavior did not occur in the observed flow record during this period. Based on previous experience with ParFlow, this seems to be primarily related to the model grid resolution [Kollet and Maxwell, 2008; Ferguson and Maxwell, 2010]. The 500-m model grid size defined the width of all streams. To maintain the volumetric streamflow for stream widths sometimes 500 times larger than observed, the modeled stream stage was necessarily much smaller than observed. Owing to the ease with which the resulting small depth (a thin film of water) is evaporated compared to deeper observed channel flow, this resulting geometry of streams was not conducive to the streams staying saturated and flowing throughout the simulation. The result was in many cases that positive pressure heads could not be maintained at a low flow conditions. In these cases, saturation dropped just below 100%, pressure head would become slightly negative, and the stream would cease to be fully connected and flowing. Given current computational

limitations even using parallel processing, this is a model design issue (for finite difference methods requiring constant grid spacing) that could be remedied by focusing on smaller model domains where model grid size approaches the size of actual stream channels or through the development of upscaled equations and parameters to relate small-scale hydrologic and urban behavior to larger-scale model representation.

Another limitation having to do with model resolution is that this model only crudely represents stormwater management as it does not include hydraulic modeling of pipe flow and stormwater management facilities and the associated re-routing of surface flow that can result. The effect of storm drains can be represented by directly connecting impervious surfaces with streams in ParFlow [Barnes *et al.*, 2013], but these methods are not generally applicable at the scale of the present model. Storm drains are numerous and much smaller than the model resolution, so representing storm drains using 500 m x 500 m grid cells is not feasible. The 500 m grid resolution was used in order to represent the entire metropolitan area, ranging from rural to urban and privately served to publicly served water supply. Without storm drains, impervious surfaces in our model are only directly connected to streams via other impervious surface grid cells. This is an underestimation of the connection of impervious surfaces to streams, and therefore, the effect of impervious surfaces is likely underestimated in our study. For example, precipitation that does not infiltrate at an impervious surface grid cell in the model may flow as surface runoff to a downslope neighboring cell and infiltrate at that location, whereas in reality the water

may take a path directly from the impervious surface through storm drains to the stream without infiltration in between.

3.4.3 *Urban features*

Our results (Figure 3.8) show that in the Baltimore metropolitan area, impervious surface coverage is a smaller factor in changing subsurface storage than is infiltration of groundwater into wastewater pipes, water supply pipe leakage, and reduced vegetative cover. The effects of urban fluxes on subsurface storage were shown to accumulate over time, although the simulation period was orders of magnitude shorter than that over which cities have been developed. Therefore, the cumulative effect on subsurface storage over decades of urban fluxes such as infiltration of groundwater into the wastewater system will likely lead to large-scale depletion of the groundwater reservoir and profound alteration in groundwater flow paths.

We found that changes in subsurface storage are in most cases spatially concentrated in more populated areas (Figure 3.9). The spatial extent of alterations in urban features is not necessarily proportional to the resulting change in pressure head due to those alterations. The no-anthropogenic-discharge-or-recharge scenario altered fluxes at more surface grid cells than the no-I&I scenario, but resulted in fewer surface grid cells with a pressure head difference of more than 25 cm from the base case. The change in subsurface storage was found to be largest in the no-I&I scenario, although only 6.6% of the surface grid cells were altered.

3.5 Conclusions

Other researchers [*Lerner, 2002; Price, 2011*] have pointed out that presence of impervious surfaces does not necessarily lead to decreased base flow and recharge in urban areas. Our work demonstrates the importance of considering multiple aspects of urban development on groundwater, beyond the effects of impervious surfaces. Major conclusions are as follows.

1. Using the coupled subsurface-surface-land surface hydrologic model, ParFlow.CLM, applied to the Baltimore metropolitan area, we quantified the individual impact of each of four urban features on subsurface storage. The features investigated, in order of increasing magnitude of change to subsurface storage, were: removal of infiltration and inflow (I&I) of groundwater into wastewater pipes (“no-I&I scenario”); removal of water supply pipe leakage and other anthropogenic recharge and discharge fluxes; replacement of urban land cover with vegetative cover (“vegetated city scenario”); and removal of impervious surface coverage (“pervious city scenario”). After six months of simulation, removing I&I led to 5.1% greater total subsurface storage, removing all anthropogenic fluxes led to 3.7% greater subsurface storage, the vegetated city scenario had a 0.13% decrease in subsurface storage, and the pervious city scenario had a 4×10^{-4} % increase in subsurface storage, all referenced to the base case subsurface storage normalized to precipitation minus evapotranspiration.
2. The spatial extent and magnitude of the effects of alteration in urban features did not necessarily correspond to the area over which these features

were applied. For example, we applied I&I over 6.6% of the model domain, yet this urban feature was found to have the largest magnitude of effect on total model subsurface storage. Conversion of urban land cover to vegetative cover applied to 43% of the model domain led to smaller magnitude but more spatially extensive changes in land surface pressure head. The vegetated city scenario resulted in lower pressure heads (less storage) in Baltimore compared to the base case, whereas the no-I&I scenario resulted in higher pressure heads (greater storage). The pervious city scenario had little change from the base case, and the no-anthropogenic-discharge-or-recharge had a combination of the no-I&I scenario increase in pressure head in Baltimore City and County, and a decreased pressure elsewhere within the urban region due to the removed recharge from leaking water supply pipes.

3. The relative magnitude of effects of individual features will likely vary according to location, and therefore the results found here are not directly applicable to other urban regions. Infrastructure condition and climate will play a role in determining the significance of each feature for other areas. However, this work points to the importance, particularly in older cities, of considering infrastructure leakage as important features of urban systems, and illustrates a methodology for quantifying these effects.

4. Synthesis of input data for distributed hydrologic modeling of undeveloped areas is a challenging task, and is made much more complicated when evaluating urban regions. Model representation of urban development requires a number of non-standard and difficult-to-obtain data sets. We have

developed a methodology for the synthesis of disparate hydrogeologic and urban data sets for the purpose of incorporation into distributed hydrologic models. In addition to considerations required for any land use type (estimation of soil, saprolite, fractured bedrock, and sedimentary aquifer hydraulic conductivity values and processing of surface slopes), addressing aspects specific to urban areas was needed. This included representations of impervious surfaces, lawn irrigation using public water supply, water supply pipe leakage, residential and municipal well pumping, reservoir withdrawals, and infiltration and inflow of groundwater and stormwater into the wastewater system.

Recent trends in stormwater management have focused on on-site infiltration and storage of stormwater to mitigate the impact of urban development. This is often done through small-scale green infrastructure, such as bioinfiltration basins, green roofs, pervious pavements, vegetated swales, and rain barrels. One of the stated goals of this type of infrastructure, sometimes referred to as Low-Impact Development (LID), is to restore groundwater recharge to near-natural conditions. However, for the goal of restoring groundwater fluxes to pre-development conditions, focusing only on impervious surfaces while there are significant infrastructure leaks will not be effective. This method for watershed management largely ignores the centralized infrastructure of wastewater and water pipes that may be leaking in or out, and the large impacts this infrastructure may have on subsurface storage and overall water balance. Infrastructure maintenance should be incorporated into efforts to develop new ways of managing urban hydrologic systems.

3.6 Acknowledgements

This research was supported by National Science Foundation (NSF) Grants DGE-0549469, EF-0709659, DEB-0948944, CBET-1058038, CBET-0854307, EEC-1028968, and NOAA Grant NA10OAR431220. In addition, this work builds upon field and data infrastructure supported by the NSF Long-Term Ecological Research (LTER) Program (Baltimore Ecosystem Study) under NSF Grants DEB-0423476 and DEB-1027188. The study used a number of computational resources, including the UMBC High Performance Computing Facility (HPCF). This facility is supported by NSF through the MRI program (Grants CNS-0821258 and CNS-1228778) and the SCREMS program (Grant DMS-0821311), with additional substantial support from UMBC. The study also utilized the Extreme Science and Engineering Discovery Environment (XSEDE), which is supported by NSF grant number OCI-1053575, and simulations were conducted on Kraken at the National Institute for Computational Sciences. NLDAS-2 forcing data used in this study were acquired as part of the mission of NASA's Earth Science Division and archived and distributed by the Goddard Earth Sciences (GES) Data and Information Services Center (DISC). This work benefited from data queried by Wendy McPherson (USGS). We are grateful for the assistance of Joshua Cole, Roxanne Sanderson, Kelsey Weaver, Thomas Myers, Cynthia Ward, and Dakota Smith of the Center for Urban Environmental Research and Education at UMBC in obtaining and processing model input data. We had beneficial discussions with Jeff Raffensperger (USGS) and Dean Cowherd (Maryland NRCS). David Bayer (Baltimore County), Carlos A. Espinosa (KCI), and Gould

Charshee (BMC) helpfully provided data. The modeling work also benefited from discussions with Michael Barnes and Alimatou Seck.

Chapter 4: Urban watershed storage and streamflow generation

Aditi S. Bhaskar and Claire Welty

Prepared for submission to Water Resources Research

4.1 *Introduction*

Elucidating groundwater-surface water interactions over a range of flow conditions has been a growing area of research over the past two decades [*Winter et al.*, 1998]. Coupling of groundwater and streamflow under storm conditions has been investigated using a wide variety of techniques. Many studies in undeveloped areas have found that pre-event water dominates stormflow [*Buttle*, 1994; *Genereux and Hooper*, 1999]. Pre-event water, also termed old water, is present in the watershed before a precipitation event, and is isotopically or chemically distinct from event (precipitation or new) water. In his commentary about the future of isotopic stormflow hydrograph separation, *Burns* [2002] asks, “What about catchments in which people live and work?” Many assume that urban areas are one of the only places in which infiltration-excess (Hortonian) overland flow is the main stormflow generation process [*Freeze*, 1974; *Nolan and Hill*, 1990; *Buttle*, 1994; *Burns*, 2002; *Spence*, 2010], meaning that impervious surfaces generate stormflow and the subsurface is unimportant. Yet significant pre-event water proportions have been observed in urban watersheds [*Nolan and Hill*, 1990; *Buttle et al.*, 1995; *Gremillion et al.*, 2000; *Pellerin et al.*, 2008; *Meriano et al.*, 2011], exposing our lack of understanding about where and how stormflow is generated.

4.1.1 Chemical hydrograph separation studies

Studies that have investigated chemical or isotopic hydrograph separation in urban watersheds have found a wide range of pre-event water contributions (0-89%), sometimes within the same watershed. Some investigations in urban areas use specific conductance (primarily reflective of chloride concentrations) to perform hydrograph separations. The concentration of chloride is often significantly higher in urban groundwater as compared to rainwater, due to years of accumulated road salts [Gelhar and Wilson, 1974]. Buttle et al. [1995] examined an Ontario catchment with 14% of the watershed as hydraulically-connected impervious area, and found that 45-52% of stormflow due to snowmelt was pre-event water. Sidle and Lee [1999] used deuterium to separate hydrographs in a first-order stream near Cincinnati, Ohio, and found that 62-76% of the stormwater was pre-event water. Gremillion et al. [2000] found that the pre-event water proportion of a developed watershed was 47%, as compared to 76% in the upstream, less developed, portion of the Florida stream. Pellerin et al. [2008] analyzed a Massachusetts basin with 25% impervious area, and found 22-82% of stormflow was pre-event water, and was related to the antecedent stream streamflow over multiple storms. Meriano et al. [2011] studied a 75% urbanized watershed in Ontario and found that 23-30% of stormflow was pre-event water. Nolan and Hill [1990] found that 57-89% of stormflow in an “urban” watershed in California was pre-event water, where 14% of the watershed area was delineated as a limestone quarry, and 6% was designated as impervious surface cover. The authors suggested that the cause was in-channel (pre-event) water being displaced downstream soon after rainfall by additional event water from the channel

upstream. This explanation does not appear to be generally applicable, however, because the time of elevated pre-event water observed in many storms is longer than the few minutes they calculated for the travel time of the in-stream flood wave.

4.1.2 Stormflow generation mechanisms

Isotopic hydrograph separation distinguishes between temporal origins of streamflow (pre-event and event water), which is not the same as streamflow separation by source (groundwater, unsaturated flow, overland flow) or flow paths [Sklash and Farvolden, 1979]. For example, rainwater infiltrating into the subsurface and quickly discharging to streams may retain the chemical signature of event water although it travelled to the stream by a subsurface pathway. The converse, pre-event water appearing at the surface, can occur due to mixing between surface and subsurface water at saturated patches. Kienzler and Naef [2008], and others cited within, found variations in the percentage of stormflow resulting from subsurface flow made up of pre-event water, sometimes dropping as low as 20%. Nevertheless, some researchers refer to pre-event and event water as groundwater and surface water, respectively [Buttle *et al.*, 1995]. Isotopic hydrograph separation has well served the purpose of time source separation, but does not provide information on the source areas, pathways, or mechanisms of streamflow generation. It is still an open question in hydrology precisely how pre-event water, which is thought to largely be slow-moving subsurface flow, responds so quickly and significantly to precipitation events in moving from the subsurface to a stream channel. Kirchner [2003] called this the ‘rapid mobilization of old water’ paradox.

There have been a number of conceptualizations of how stormflow is generated, with some hypotheses falling out of favor over time. The streamflow generation process of variable source area has been updated with the suggestion that areas contributing to overland flow are not necessarily contiguous, continuous, or centered on the stream network [McDonnell, 2003; Spence, 2010]. It is not clear, however, how the variable source area process could lead to pre-event water dominating hydrographs. Subsurface flow resulting from a storm, also called subsurface stormflow, has been suggested by a number of researchers, including those utilizing isotopic hydrograph separation [e.g. Kienzler and Naef, 2008], to be an important process. Some conceptualizations of how subsurface stormflow is activated are discussed below.

From detailed field measurements at the Panola research site in the Georgia Piedmont, *Tromp-van Meerveld and McDonnell* [2006] found the dominant mechanism by which subsurface flow was generated by storms was lateral flow at the soil-bedrock interface. They called this the fill and spill mechanism because saturation connectivity and filling of bedrock topography is a necessary threshold before spilling, or connected subsurface flow leading to streamflow, can occur. Below the 55 mm precipitation threshold they observed for significant subsurface stormflow, saturation at the soil-bedrock interface was patchy. Once this precipitation threshold was crossed, subsurface stormflow was generated because the bedrock topographic lows were filled and connected to the hillslope outflow and excess water spilled out. Yet, the subsurface stormflow measured at the Panola hillslope site was relatively small (maximum of 7 mm for a 60 mm storm), and not

observed at a watershed scale to determine whether significant streamflow was produced through this subsurface flow generation mechanism.

Modeling studies of hydrologic response have been developed to investigate the sensitivity of subsurface stormflow generation to various hillslope factors. These studies have found that specific yield [*Weiler and McDonnell*, 2004], bedrock permeability [*James et al.*, 2010], bedrock leakage [*Tromp-van Meerveld and Weiler*, 2008], catchment slope angle and bedrock topography contributing area [*Hopp and McDonnell*, 2009] are important in controlling subsurface hydrologic response. These hillslope modeling studies have a number of limitations, however. None of them include overland flow, which is important to include in cases where this phenomenon may be important (for example, urban areas). *Weiler and McDonnell* [2004] performed numerical chemical hydrograph separation using a solute transport model, focusing on comparison of results using two values of specific yield. This approach is not common, possibly because in systems other than urban, almost all water is pre-event water.

Graham and McDonnell [2010] compared two streamflow-generation hypotheses using numerical experiments to implement a conceptual mathematical model. The “fill and spill” (bedrock detention storage) hypothesis postulates that streamflow generation is controlled by bedrock permeability and subsurface storage volume. The pre-storm moisture-deficit hypothesis states that streamflow generation is controlled by antecedent moisture and potential evapotranspiration. The results of the numerical experiments showed that antecedent moisture controlled the precipitation threshold for subsurface streamflow generation to occur, and that

bedrock permeability and subsurface storage volume controlled the slope of the precipitation – streamflow relationship after the threshold is reached. This research makes explicit the theorized connection between watershed storage and streamflow generation.

Watershed storage is difficult to measure and has received little attention compared to measurement and analysis of streamflow and precipitation. Nevertheless, the relationship between streamflow and storage has long been sought [Beven, 2006]. Storage has also been proposed as a component of a catchment classification framework [McDonnell and Woods, 2004; Wagener et al., 2007; McNamara et al., 2011]. Furthermore, some researchers have suggested that storage may control streamflow and have called for a greater understanding of the storage dynamics of watersheds [Spence, 2010; Sayama et al., 2011]. The emerging paradigm of streamflow generation processes is that of “threshold-mediated, connectivity-controlled processes” in which storage is crucial [Spence, 2010]. Threshold behavior in the relationship between streamflow and precipitation has been observed by researchers in diverse hydrogeologic and climatic settings [Tromp-van Meerveld and McDonnell, 2006; McGuire and McDonnell, 2010; Graham and McDonnell, 2010; Sayama et al., 2011]. The precipitation value at which this threshold occurs is storage dependent [Graham and McDonnell, 2010], meaning that precipitation alone is not necessarily a predictor of streamflow. Threshold behavior has also been observed between storage or antecedent moisture, and runoff response [Sidle et al., 2000; Spence, 2007; Detty and McGuire, 2010; Teuling et al., 2010].

Both the precipitation-streamflow and storage-streamflow thresholds may be explained by precipitation first filling available storage reservoirs with little streamflow response. After a threshold in storage is reached, such as bedrock topographic lows being filled, stormflow generation is activated and subsequent precipitation leads to large changes in streamflow. This was observed by *Sayama et al.* [2011] in the storage and streamflow of 17 watersheds in the Pacific Northwest. Using water balance methods, they found that watersheds had variable maximum storage volumes, ranging from 200 – 500 mm. The maximum watershed storage was most correlated with mean watershed topographic gradient, which they attributed to the hydrologically active bedrock zone hypothesis.

Kirchner [2009] proposed a methodology to develop the relationship between storage and streamflow in which watersheds are treated as simple dynamical systems. During periods of low precipitation and evapotranspiration, changes in storage are assumed to be primarily related to streamflow. This methodology has been applied to watersheds in Plynlimon, Wales [*Kirchner*, 2009] and the Swiss prealpine [*Teuling et al.*, 2010]. This method assumes that streamflow is solely related to storage, and as *Kirchner* [2009] states, this method may not work for watersheds in which there is significant overland or bypassing flow. The method has not yet been tested in any urban watersheds, and therefore the limits to the method are not known. It is not clear how urban development (impervious cover, compacted fill, pipes) may affect the relationship between storage and streamflow. Since this relationship describes the continuum of hydrologic response, from baseflow to storms, knowledge of how the

storage-streamflow relationship changes with development would provide information on both shifts in baseflow and stormflow.

4.1.3 Purpose

Thresholds and connectivity of watershed storage behavior have been suggested as controlling streamflow generation from subsurface sources [Spence, 2010; Sayama *et al.*, 2011]. However, the controls on the relationship between storage and stormflow and the role of storage thresholds in stormflow generation are not well known, especially in urban areas. With their wide range of pre-event water responses, urban areas can be viewed as endmember watersheds that can be used to investigate controls on stormflow generation. It is also important to have tools to quantify the subsurface contribution to flashy stormflow that could contribute to improved management of urban streams [Walsh *et al.*, 2005].

This work seeks to better quantify the controls on and relationship between pre-event water proportion and watershed storage in urban areas. Specifically, we seek to answer the following questions:

1. What controls the pre-event water proportion of stormflow in urbanizing areas?
2. What controls the relationship between storage and streamflow along an urban-to-rural gradient?
3. What is the relationship between pre-event water proportion of stormflow and watershed storage in urban areas?

The controls investigated were percent impervious surface coverage, storm size, and initial watershed storage, and were evaluated using a combination of idealized numerical experiments and analysis of field data from the Baltimore area.

4.2 *Methods*

We approached these research questions using a combination of three methods. First, we developed a coupled groundwater-surface water flow and transport model of an idealized hillslope. Using this model, we conducted numerical experiments to explore changes in pre-event water proportion and the relationship between storage and streamflow (section 4.2.1). We utilized the model HydroGeoSphere [Therrien *et al.*, 2010] to carry out model-based tracer hydrograph separation [Jones *et al.*, 2006; Park *et al.*, 2011]. Second, we applied the simple dynamical systems approach to developing the storage-streamflow relationship [Kirchner, 2009] to existing hydrometric data from three watersheds along an urban-to-rural gradient in the Baltimore area (section 4.2.2). The last tool we employed was chemical hydrograph separation in which we analyzed specific conductance data to separate pre-event and event contributions to stormflow for a set of six small, nested, urban watersheds (section 4.2.3).

4.2.1 *Hillslope numerical experiments*

With field observations, it is nearly impossible to alter most watershed characteristics to observe the effects of these changes. Numerical modeling is well suited to address these limitations. Although mathematical models are simplified representations of reality, they allow watershed characteristics to be systematically varied in order to better understand the interactions and factors that control

hydrologic behavior. This type of analysis can be viewed as conducting “virtual experiments” [Weiler and McDonnell, 2004; Hopp and McDonnell, 2009], where understanding of patterns and controls across watersheds, instead of cataloguing the functionality of an individual watershed, can be advanced [McDonnell, 2003].

We utilized HydroGeoSphere as a tool to evaluate the controls on pre-event water proportion of an idealized watershed. HydroGeoSphere uses a control volume finite-element scheme to solve the coupled three-dimensional surface-subsurface fluid flow and solute transport equations [Therrien *et al.*, 2010]. We developed an implementation of the model to represent an idealized hillslope in order to examine the effect of changes to hillslope properties. We focused on storm simulations using small, adaptive timesteps (between 1×10^{-6} s and 100 s). The simulations were generally 200,000 s (2.3 days) long, except for the simulation with impervious surface cover (described in section 4.2.4.2), which was run for double this amount of time because of the slow return to baseflow conditions. The modeled pre-event water was assigned a conservative solute concentration distinct from that in event (rain) water, and the solute concentration in the modeled stormflow was used to partition streamflow between pre-event and event water. We used chloride as the conservative solute because of its distinct signature in groundwater in urban areas where there is accumulation of chloride in the subsurface from road salt application such that the concentration of chloride in groundwater greatly exceeds the chloride concentrations in rain.

The idealized domain was designated as 39.9 m in the horizontal direction perpendicular to the stream (y-axis), 0.9 m parallel to the stream (x-axis), and ranged

from 10.006 m to 12.4 m in thickness (z-axis) (Figure 4.1). We assumed isotropic local dispersivity of 1 cm in all three directions. To keep the grid Peclet number less than 10 (to minimize numerical dispersion and spurious oscillations), the discretization was set to less than 0.1 m in all dimensions. Specifically, dx was 0.09975 m, dx was 0.09 and dz varied between 0.08 and 0.1 according to y position since there were 124 layers regardless of the total model thickness. Therefore, the number of model grid cells was 400 x 10 x 124, or 496,000. The land surface had a constant slope of 0.06. The material property values used in the base case model are listed in Table 4.1. The “dual nodes” option in HydroGeoSphere was chosen for coupling subsurface with surface flow and tables were generated to approximate the unsaturated zone functions.

The surface flow boundary condition at the line of stream cells was a zero-depth hydraulic gradient boundary with the bed-slope equal to the land surface slope of 0.06. The boundary condition at the up-gradient face of the domain was specified as a hydraulic head value of 10.406 m. The transport boundary condition at the up-gradient face was a specified third-type condition with a solute concentration of 0.2 kg/m³ and fluid flux based on the head solution. The top of the model domain, which was designated as an overland flow zone, had a specified rainfall flux boundary condition of 5.555 x 10⁻⁶ m/s for 30 minutes. This rainfall had an associated specified third-type boundary condition concentration of 1 x 10⁻⁵ kg/m³ imposed from 10000 s to 11800 s.

To initialize the model, we first ran a steady-state simulation with an initially linear water table hydraulic gradient defined by hydraulic head values specified as

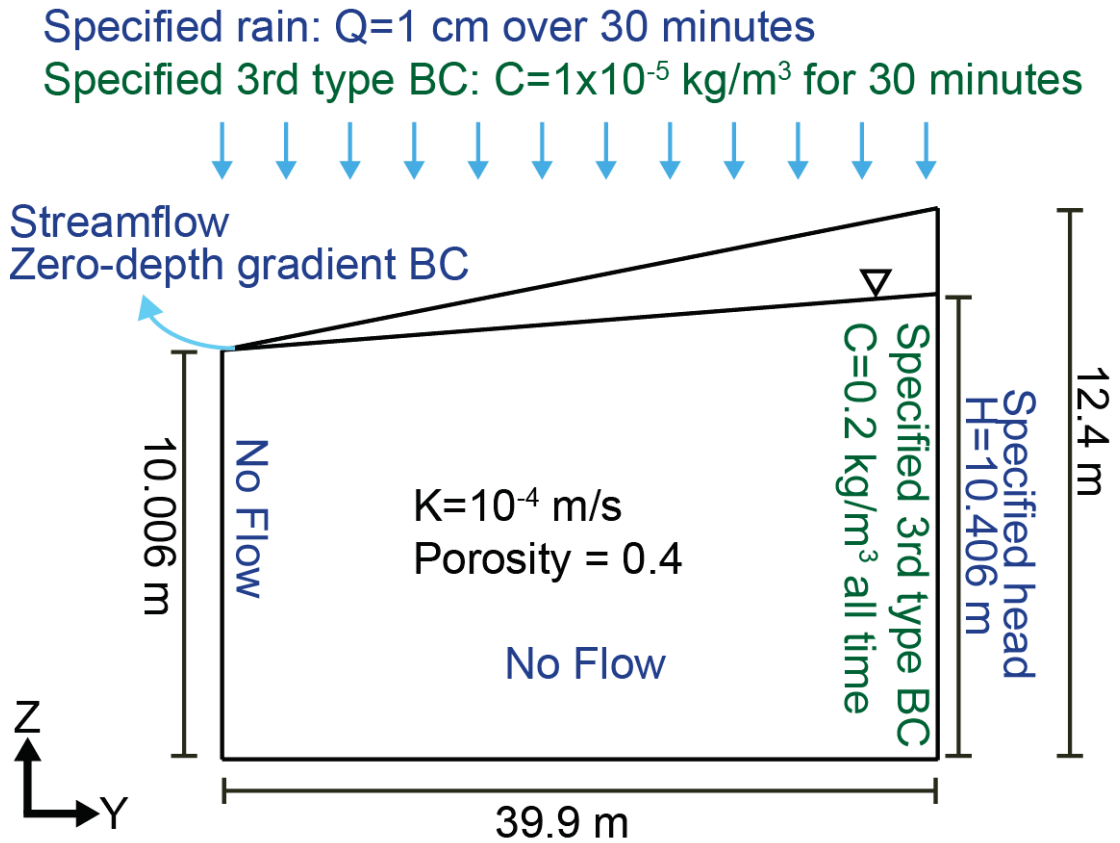


Figure 4.1. Schematic of hillslope model domain and setup. Not to scale.

Table 4.1. Material properties used in hillslope model. Values shown are the base case model values, some of which are modified in numerical experiments (Table 4.3).

| Property | Value |
|--|------------------------|
| Total orosity | 0.4 |
| Hydraulic conductivity | 1×10^{-4} m/s |
| Specific storage | 1×10^{-6} 1/m |
| Tortuosity | 0.05 |
| van Genuchten parameter α | 2 m^{-1} |
| van Genuchten parameter β | 2 |
| Residual saturation | 0.1 |
| Unsaturated zone minimum pressure head | -50 m |

10.006 m at the stream cells to 10.406 m at the up-gradient face of the domain, and flow boundary conditions as described above. The hydraulic head output from the steady-state simulation was used as the initial condition for the transport model, which was transient and ran for 200,000 seconds (2.3 days). In the transient transport simulation, precipitation was introduced as well as a groundwater background chloride concentration of 0.2 kg/m^3 , with transport boundary conditions as described above. The head and concentration output from this transient simulation were used as initial conditions for the numerical experiments described in sections 4.2.4.2 and 4.2.5.1. A summary of the material properties, model domain, and boundary conditions used in the base case of the numerical experiments is shown in Figure 4.1.

4.2.2 Simple dynamical systems to develop storage-streamflow relationship

We used the simple dynamical systems approach by *Kirchner* [2009] to develop storage-streamflow relationships for three Baltimore watersheds characterized by a range of urbanization. The method used a water balance formulation where the water entering storage (S) was from precipitation (P), and water left storage through evapotranspiration (ET) and streamflow (Q; also termed discharge). An assumption of this method was that streamflow was only a function of storage:

$$\frac{dS}{dt} = P - ET - Q \quad (4.1a)$$

where

$$Q = f(S) \quad (4.1b)$$

The streamflow sensitivity function $g(Q)$ used by *Kirchner* [2009] was defined by the change in streamflow per change in storage. We used only streamflow records from rainless nights and assumed that precipitation and evapotranspiration were small relative to streamflow during these time periods. Therefore, the streamflow sensitivity function was empirically estimated using only the streamflow record:

$$g(Q) = \frac{dQ}{dS} = \frac{dQ/dt}{dS/dt} = \frac{dQ/dt}{P - ET - Q} \approx \left. \frac{-dQ/dt}{Q} \right|_{P \ll Q, ET \ll Q} \quad (4.2)$$

Using the streamflow sensitivity function, the relationship between storage and streamflow was found by analytical integration:

$$S = \int \frac{dQ}{g(Q)} \quad (4.3a)$$

$$S(a) = \int_1^a \frac{1}{g(Q)} dQ \quad (4.3b)$$

We applied this method to three similarly-sized watersheds along an urban-to-rural gradient in the Baltimore Ecosystem Study Long Term Ecological Research (BES LTER) study area (Figure 4.2; Table 4.2) that are instrumented with USGS stream gages at their outlets. Dead Run (Dead Run at Franklinton, <http://waterdata.usgs.gov/md/nwis/uv/?01589330>) is a 14.1 sq. km. suburban watershed characterized by 45% impervious surface area that is a mixture of a mixture of residential, commercial, and transportation land use, with two major interstate highways bisecting its drainage area. Delight (Gwynns Falls Near Delight <http://waterdata.usgs.gov/usa/nwis/uv?01589197>) is a 10.6 sq. km. watershed composed of 19% impervious surface area, with largely residential suburban land use.

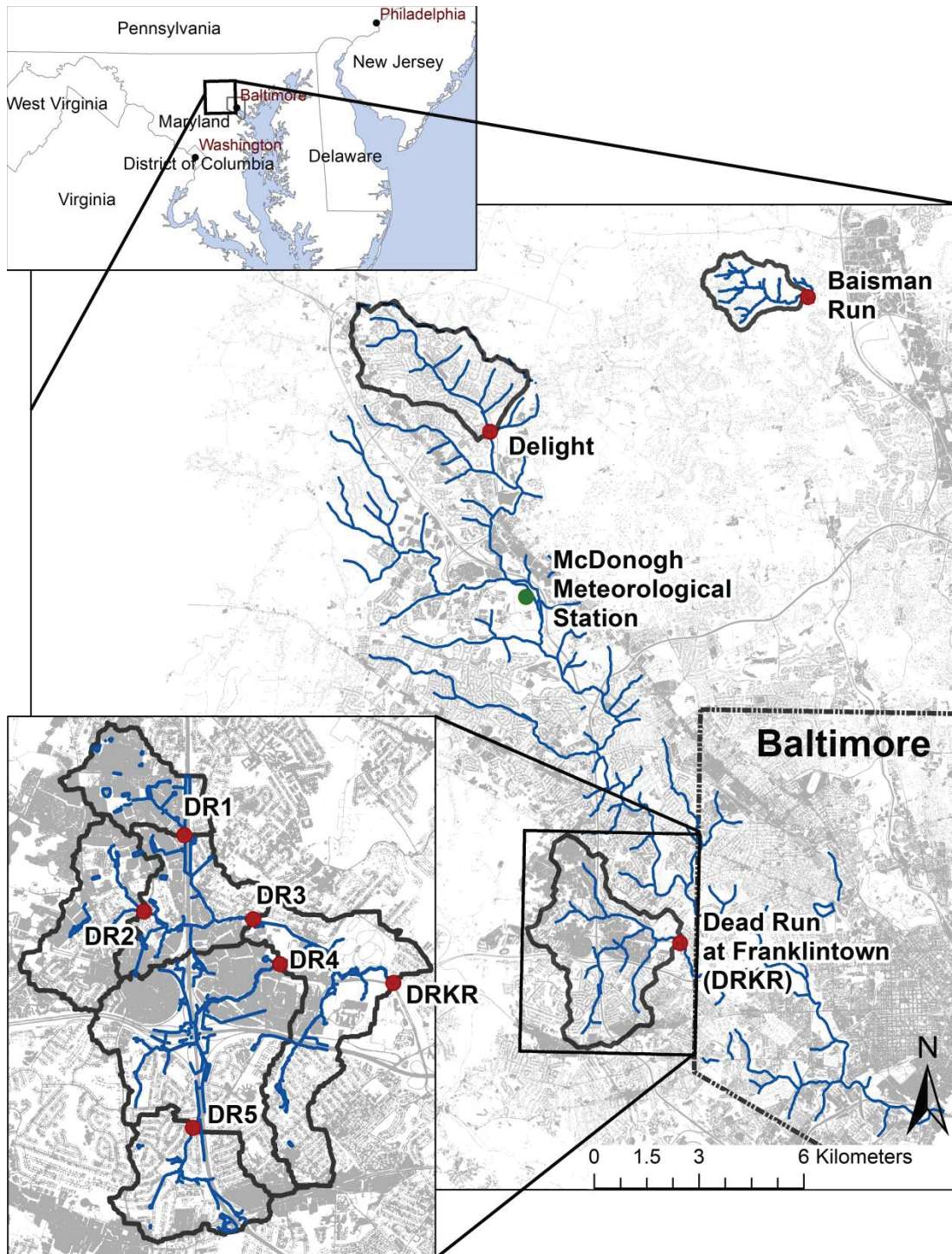


Figure 4.2. Map of watersheds used for simple dynamical systems analysis (Baisman Run, Delight, and Dead Run at Franklinton), and an inset showing the sub-watersheds of Dead Run that were used for the chemical hydrograph separation study (DRKR, DR1, DR2, DR3, DR4, and DR5). Red dots indicate stream gages, gray background indicates impervious surface cover, and blue lines represent hydrography (daylighted and buried streams).

Table 4.2. Watersheds used for chemical hydrograph separation and simple dynamical systems analysis, along with drainage area and impervious surface cover.

| Watershed | USGS Site Number | Drainage area (km²) | Percent impervious surface cover |
|--------------------------|-----------------------------|---|---|
| Baisman Run | 1583580 | 3.8 | 2.3 |
| Delight | 1589197 | 10.6 | 18.6 |
| DR Franklinton (DRKR) | 1589330 | 14.1 | 45.0 |
| DR1 | 1589317 | 1.3 | 51.1 |
| DR2 | 1589316 | 1.9 | 44.7 |
| DR3 | 1589320 | 5.0 | 48.2 |
| DR4 | 1589315 | 6.2 | 49.8 |
| DR5 | 1589312 | 1.53 | 44.9 |

Baisman Run (Baisman Run at Broadmoor, <http://waterdata.usgs.gov/usa/nwis/uv?01583580>) is 3.8 sq. km. in area, with only 2% impervious land cover and is largely forested with low-density residential land use. These three watersheds all lie within the Piedmont physiographic province.

We used USGS streamflow records from 2002-2008 at these three USGS stream gages, and standardized the time increments for hourly analysis. Streamflow was converted to units of mm/hour by scaling by watershed area (Table 4.3). The time period spanned extremes in dry (820 mm rain in 2002) and wet (1630 mm rain in 2003) years. Because of gaps in precipitation data, we used the average of two datasets: bias-corrected Hydro-NEXRAD and Stage IV radar-rainfall fields (M. L. Baeck and J. Smith, personal communication) [Smith *et al.*, 2012]. Any remaining time periods for which streamflow was rising but for which precipitation records were missing were manually excluded from analysis. Total solar irradiance was estimated with a LI-COR (Lincoln, NB) silicon pyranometer at the BES LTER meteorological station at McDonogh (Figure 4.2). Rainless time periods were defined as those with no precipitation for the previous six hours and the subsequent two hours. Night times were isolated by selecting times when the average solar irradiance over a three-hour time window was $< 1 \text{ W/m}^2$. These two criteria were combined to only use rainless night times for analysis, based on recommendations by *Kirchner* [2009]. The binning and fitting procedure used was similar to that in *Kirchner* [2009], in which bins had a standard error less than $\frac{1}{2}$ of the mean of $-dQ/dt$ values and contain at least 1% of the values. The exception was that a piecewise linear fit was used in logarithmic space in order to provide a better fit for our watersheds. The data from the BES LTER

Table 4.3. Parameter values for hillslope numerical experiments.

| Simulation | Hydraulic conductivity (m/s) | Total porosity (-) | Storm size (cm over 30 minutes) | Initial water table height (m) at up-gradient face (y=39.9 m) |
|-------------------|-------------------------------------|---------------------------|--|--|
| Base case | 10^{-4} | 0.4 | 1 cm / 30 minutes | 10.406 |
| Impervious | 10^{-7} | 0.05 | 1 cm / 30 minutes | 10.406 |
| Larger storm | 10^{-4} | 0.4 | 1.25 cm / 30 minutes | 10.406 |
| Smaller storm | 10^{-4} | 0.4 | 0.75 cm / 30 minutes | 10.406 |
| Initially wetter | 10^{-4} | 0.4 | 1 cm / 30 minutes | 10.9045 |

meteorological station at McDonogh was also used to calculate potential evapotranspiration using the Penman-Monteith formulation (G. Heisler, personal communication).

4.2.3 *Specific conductance measurements for use in chemical hydrograph separation*

YSI 600-LS conductivity/temperature sondes were deployed at USGS stream gaging stations at Dead Run Franklinton and its subwatersheds (Figure 4.2) [VerHoef *et al.*, 2011; VerHoef, 2012], with specific conductance data collected every 30 minutes beginning in October 2010. In this region, stream base flow has a specific conductance signal much greater than precipitation, owing to the accumulated road salt in the groundwater that is the source of streamflow. During storms, the specific conductance of stream flow is greatly diluted by precipitation. The disparate specific conductance signal in stream baseflow vs. precipitation and the co-location of the specific conductance and discharge measurements allows chemical storm hydrograph separation to be carried out.

4.2.4 *Question 1. Controls on pre-event water proportion*

4.2.4.1 Dead Run chemical hydrograph separation for pre-event water proportion

Chemical hydrograph separation was computed using a simple two-component model [Kendall and McDonnell, 1999]. Pre-event streamflow (discharge) was taken as the streamflow value occurring immediately before the onset of the rising limb of the stormflow hydrograph. The return to this pre-event streamflow value was used to define the end of the stormflow hydrograph. The pre-event solute concentration was taken as the value of streamflow specific conductance at the time

of the defined pre-event streamflow. Event concentration, or the specific conductance of precipitation, was based on data from the Beltsville, MD National Atmospheric Deposition Program (NADP) station and was taken to be constant at 0.025 mS/cm. Using this information along with recorded concentration and streamflow during the rain event, pre-event water proportion was calculated using:

$$\frac{Q_o}{Q_t} = \frac{C_n - C_t}{C_n - C_o} \quad (4.4)$$

where Q is streamflow (discharge), C is tracer concentration (specific conductance in our case), and the subscripts o , n , and t indicate old (pre-event) water, new (event) water, and total stream water, respectively. As the event water specific conductance was about two orders of magnitude smaller than pre-event water specific conductance, variations in event water specific conductance had little effect on resulting pre-event water proportion. Specific conductance (mS/cm) is linearly correlated to chloride concentration (mg/L) in these watersheds with an R^2 value of 1.

4.2.4.2 Numerical experiments of controls on pre-event water proportion

Two parameters were varied to investigate the sensitivity of pre-event water proportion: watershed imperviousness and storm size (precipitation amount). Watershed imperviousness was selected as a parameter of interest because of the potential importance of infiltration-excess overland flow for conditions with particularly high precipitation intensities or watershed impervious values. Impervious surfaces were represented by low saturated hydraulic conductivity, with a value of 1×10^{-7} m/s [Wiles and Sharp, 2008], and low porosity with a value of 0.05 [Liu and Guo, 2003]. Watershed imperviousness was set at 0% in the base case model, and 100% in the impervious surface cover model. At 100% impervious surface cover,

low hydraulic conductivity and porosity values representing imperviousness were specified for the entire hillslope.

Storm size was found to influence the pre-event water proportion in an analysis of Dead Run specific conductance records, and therefore this input was varied in the hillslope numerical experiments. Storm size was altered by changing precipitation amount from the base case value of 1 cm to values of 0.75 cm and 1.25 cm, while length of the rain event was constant at 30 minutes. Other temporally varying parameters, such as antecedent moisture or time between storms, were not considered because the effects of these were more broadly represented by initial storage conditions of the watershed (section 4.2.5.1).

4.2.5 *Question 2. Controls on storage-streamflow relationship*

4.2.5.1 Numerical experiments of controls on storage-streamflow relationship

Hillslope storage before the rain event was varied by changing the position of the water table at the beginning of the simulation (starting with the steady-state flow initialization). Initial water table elevation was varied between 10.406 m (base case) and 10.9045 m. The latter value corresponds to a 25% decrease in depth to water at the top of the hillslope. A 25% increase in depth to water was not possible because the hydraulic gradient would reverse from stream to hillslope. Subsurface storage could not be directly set in simulations, but was instead calculated after the simulation and was correlated to initial water table position. Subsurface storage was evaluated by calculating the volume of water present in every grid cell within the domain using a macro developed in Tecplot 360 to process the exported HydroGeoSphere files as follows:

$$\text{Subsurface Storage} = \text{Saturation} * \text{Specific Storage} * dx * dy * dz + \text{Saturation} * \text{Pressure Head} * \text{Porosity} * dx * dy * dz. \quad (4.5)$$

The resulting gridded subsurface storage was then summed over the entire subsurface to find the total subsurface storage in the domain.

Streamflow was also exported as a function of time. The effects of varying initial water table position, imperviousness, and storm size on the relationship between storage and streamflow were evaluated. Table 4.3 shows the parameter values for all hillslope numerical experiments for questions 1, 2 and 3.

4.2.5.2 Storage-streamflow relationships using simple dynamical systems analysis

Storage-streamflow relationships, developed as described in section 4.2.2 using the method of *Kirchner* [2009], were compared across three Baltimore watersheds having varying percentages of impervious surface coverage (2%, 19%, and 45%). We compared the derived relationships for these watersheds with those for the Severn and Wye Rivers, which are undeveloped watersheds of similar size in Plynlimon, Wales as well as for the undeveloped Rietholzbach watershed in the Swiss prealpine [*Teuling et al.*, 2010].

4.2.6 Question 3. Relationship between storage and pre-event water proportion

The relationship between pre-event water proportion and storage was investigated by using the output from the idealized simulations developed for questions (1) and (2). The pre-event water proportion was calculated in the idealized domain for various subsurface storage conditions. The relationship between pre-event water proportion and storage was thus developed for the idealized hillslope. Dead Run chemical hydrograph separation results were also used to compare storage

conditions during the time at which pre-event water proportion was calculated. Since watershed total storage conditions cannot be directly measured in the field, pre-event streamflow (baseflow) was used as a proxy for watershed storage, based on the assumption (e.g. used in the simple dynamical systems analysis), that storage and streamflow have 1:1 monotonic relationship.

4.3 *Results*

4.3.1 *Question 1. Controls on pre-event water proportion*

4.3.1.1 Dead Run chemical hydrograph separation

Table 4.4 shows the characteristics of each storm analyzed by chemical hydrograph separation. These storms are also presented in Figure 4.3. Storms with smaller precipitation amounts within the same watershed were found to be composed of a greater proportion of pre-event water. Across watersheds, smaller, headwater catchments were found to have greater pre-event water proportion than the downstream watersheds within which they were nested. As shown in Table 4.4, other variables explored, such as days since prior rainfall and pre-event streamflow (baseflow) were not found to have a clear relationship with pre-event water proportion. There was a close relationship between pre-event water proportion over the entire storm and the minimum pre-event water proportion (at peak streamflow).

4.3.1.2 Numerical experiments of controls on pre-event water proportion

Figure 4.4 shows the model domain to scale, with superimposed hydraulic head (m) contours. The background hydraulic gradient was defined by the boundary conditions applied throughout the simulation, where the highest head was specified at the $y = 39.9$ m face (hydraulic head = 10.406 m), and the lowest head was specified at

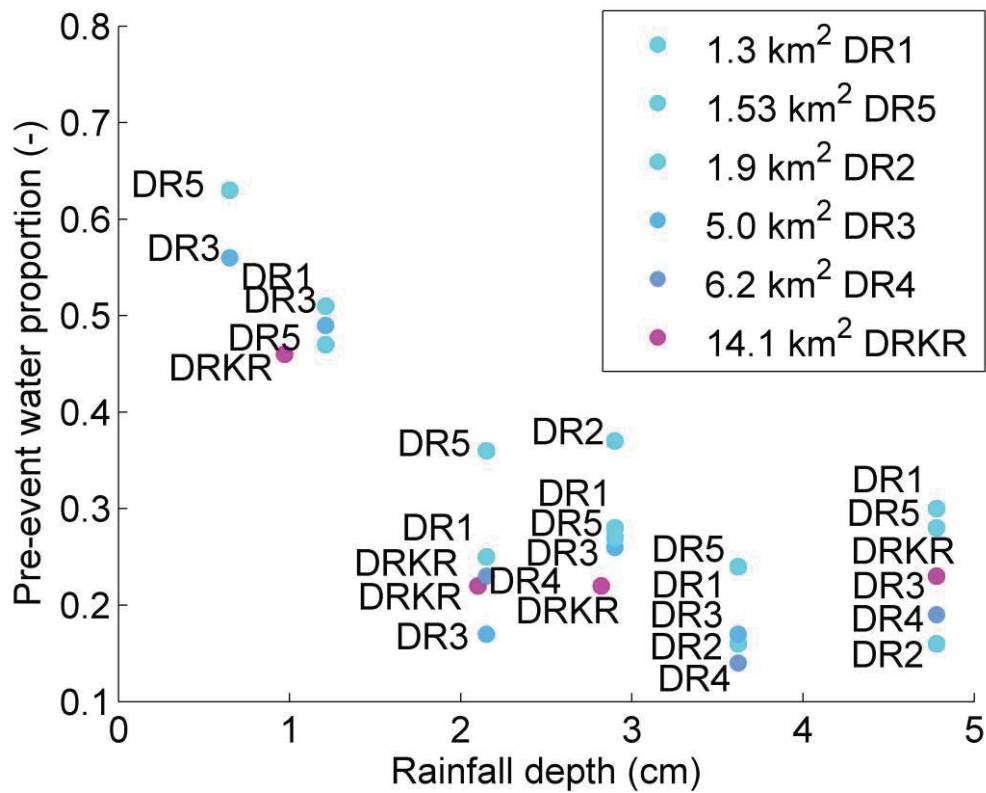


Figure 4.3. Pre-event water proportion based on Table 4.1 using chemical hydrograph separation from Dead Run sub-watersheds. Color of marker corresponds to drainage area, indicated in km² in legend. Label indicates station name abbreviation.

Table 4.4. Dead Run sub-watershed chemical hydrograph separation for storm events.

| Station | Storm start date (MM/DD/YYYY) | Rain-fall depth (cm) | Rain-fall duration (hr) | Time since last rain (days) | Baseflow (cfs) before storm | Q_t (cm) | Fracti on pre-event water (Q_0/Q_t) | Min Q_0/Q_t at peak storm flow |
|---------|-------------------------------|----------------------|-------------------------|-----------------------------|-----------------------------|------------|---|----------------------------------|
| DRKR | 10/19/2010 | 0.97 | 6.27 | 3.6 | 1.4 | 0.46 | 0.46 | 0.2 |
| DRKR | 10/14/2010 | 2.10 | 6.78 | 6.9 | 1.4 | 0.87 | 0.22 | 0.07 |
| DRKR | 11/30/2010 | 2.15 | 27.0 | 4.99 | 1.3 | 1.26 | 0.23 | 0.09 |
| DRKR | 11/3/2010 | 2.82 | 17.3 | 7.4 | 1.1 | 1.51 | 0.22 | 0.05 |
| DRKR | 5/11/2013 | 4.78 | 49.8 | 0.81 | 2.2 | 3.29 | 0.23 | 0.09 |
| DR5 | 4/19/2011 | 0.65 | 5.8 | 2.44 | 0.24 | 0.34 | 0.63 | 0.33 |
| DR5 | 4/8/2011 | 1.21 | 15 | 2.70 | 0.22 | 0.47 | 0.47 | 0.23 |
| DR5 | 11/30/2010 | 2.15 | 27.0 | 4.99 | 0.22 | 0.94 | 0.36 | 0.2 |
| DR5 | 4/16/2011 | 2.90 | 15.2 | 2.80 | 0.22 | 1.38 | 0.27 | 0.15 |
| DR5 | 8/21/2011 | 3.62 | 8.7 | 2.20 | 0.30 | 1.43 | 0.24 | 0.04 |
| DR5 | 5/11/2013 | 4.78 | 49.8 | 0.81 | 0.43 | 1.65 | 0.28 | 0.10 |
| DR4 | 11/30/2010 | 2.15 | 27.0 | 4.99 | 0.46 | 0.98 | 0.23 | 0.13 |
| DR4 | 8/21/2011 | 3.62 | 8.7 | 2.2 | 0.39 | 0.99 | 0.14 | 0.05 |
| DR4 | 5/11/2013 | 4.78 | 49.8 | 0.81 | 0.65 | 2.53 | 0.19 | 0.08 |
| DR3 | 4/19/2011 | 0.65 | 5.8 | 2.4 | 1.0 | 0.32 | 0.56 | 0.28 |
| DR3 | 4/8/2011 | 1.21 | 15 | 2.70 | 0.60 | 0.53 | 0.49 | 0.26 |
| DR3 | 11/30/2010 | 2.15 | 27.0 | 4.99 | 1.4 | 1.10 | 0.17 | 0.08 |
| DR3 | 4/16/2011 | 2.90 | 15.2 | 2.8 | 0.73 | 1.80 | 0.26 | 0.14 |
| DR3 | 8/21/2011 | 3.62 | 8.7 | 2.20 | 0.50 | 0.70 | 0.17 | 0.08 |
| DR3 | 5/11/2013 | 4.78 | 49.8 | 0.81 | 0.30 | 2.01 | 0.19 | 0.08 |
| DR2 | 4/16/2011 | 2.90 | 15.2 | 2.80 | 0.23 | 1.52 | 0.37 | 0.1 |
| DR2 | 8/21/2011 | 3.62 | 8.7 | 2.20 | 0.06 | 0.48 | 0.16 | 0.07 |
| DR2 | 5/11/2013 | 4.78 | 49.8 | 0.81 | 0.1 | 2.79 | 0.16 | 0.08 |
| DR1 | 4/8/2011 | 1.21 | 15 | 2.7 | 0.39 | 0.74 | 0.51 | 0.23 |
| DR1 | 11/30/2010 | 2.15 | 27.0 | 4.99 | 0.21 | 1.30 | 0.25 | 0.12 |
| DR1 | 4/16/2011 | 2.90 | 15.2 | 2.8 | 0.44 | 2.33 | 0.28 | 0.13 |
| DR1 | 8/21/2011 | 3.62 | 8.7 | 2.20 | 0.12 | 0.79 | 0.17 | 0.05 |
| DR1 | 5/11/2013 | 4.78 | 49.8 | 0.81 | 0.24 | 2.08 | 0.30 | 0.08 |

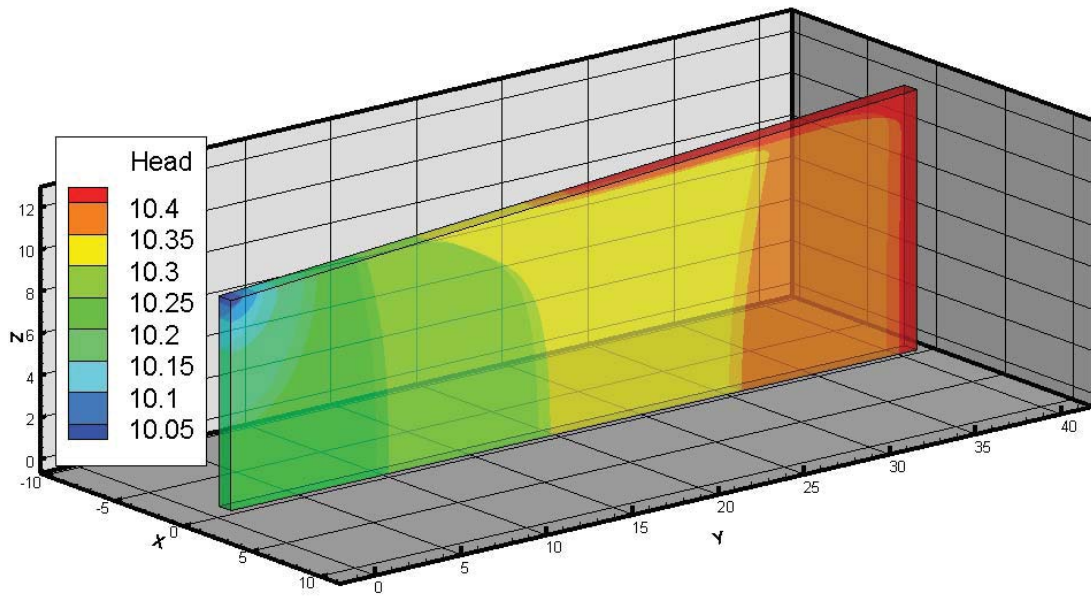


Figure 4.4. Model domain to scale of hillslope with base-case parameters. Colors indicate contours of head (m) at 14000 s (37 minutes after rain event ends).

the stream ($y = 0$ m with hydraulic head = 10.006 m). The storm event led to an increase in hydraulic head at the land surface, perturbing the background head gradient (Figure 4.4).

Figure 4.5a shows the total streamflow and the pre-event water over time for the simulations in Table 4.3. The simulations were run for 200,000 s or more at which point streamflow, subsurface storage, and chloride were all back to baseflow conditions. Figure 4.5 shows the beginning of the simulation focusing on the time period around the rain event. For the base-case model, streamflow reacted as expected with streamflow slightly decreasing before the storm event, increasing during the storm event, falling quickly after the rain stopped to near-baseflow levels, and then recessing more gradually to reach the baseflow value occurring before the rain event. The pre-event water proportion shown in Figure 4.5b was calculated using Equation 4.4. The chloride concentration, and therefore the pre-event water proportion had a drop that was longer in time duration but of a similar shape as the streamflow response in Figure 4.5a.

The streamflow response was much greater in magnitude for the impervious surface model, and the pre-event water proportion was lower (Figures 4.5a and 4.5b). The pre-event water proportion and subsurface storage took much longer to return to background levels in the impervious surface model because of the combination of low hydraulic conductivity which slowed flow and low porosity which led to less connected flow. The responses of the larger and smaller storm models were as expected. The larger storm had a higher streamflow peak and a greater decrease in pre-event water proportion, while the smaller storm showed the opposite compared to

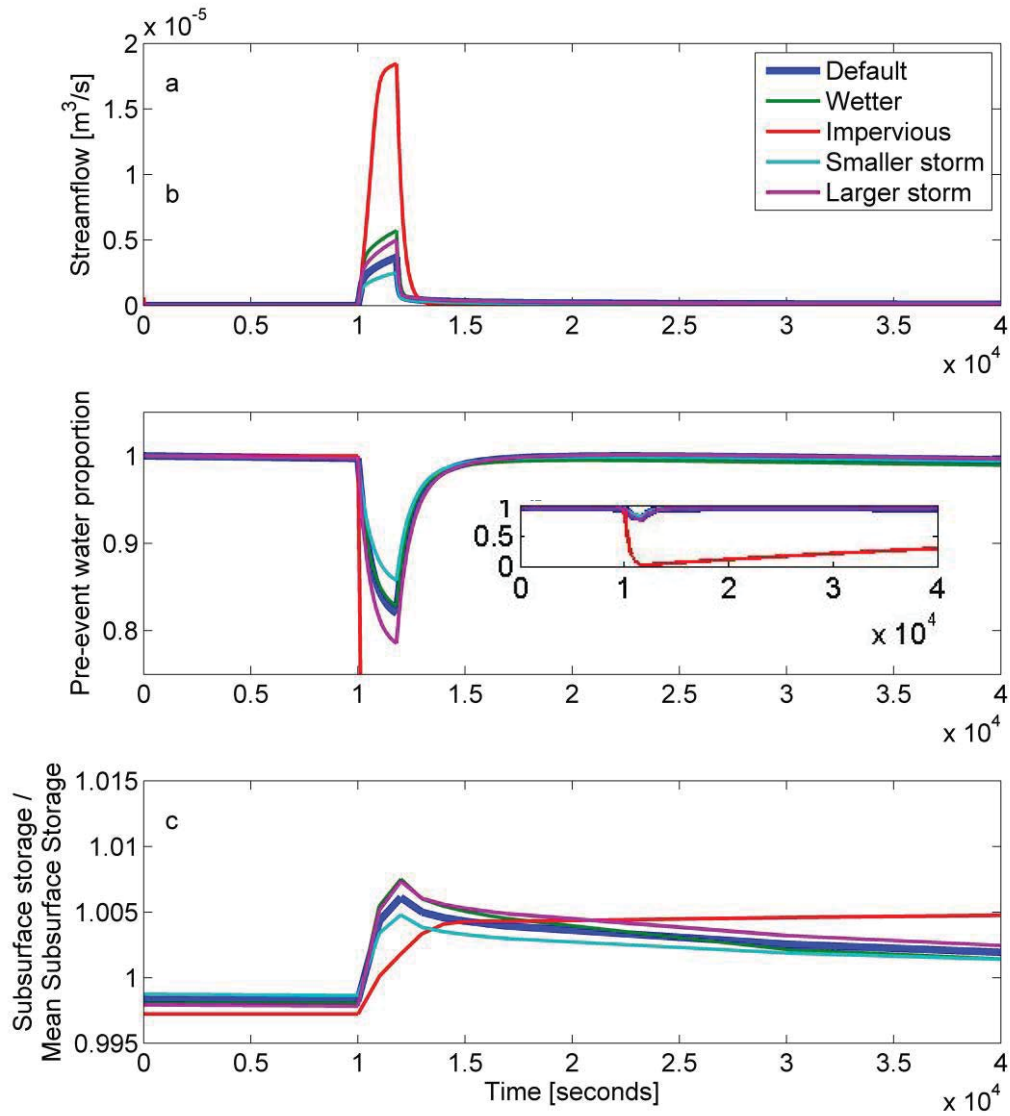


Figure 4.5. (a). Streamflow over time for model simulations given in Table 4.2. (b). Pre-event water proportion (Equation 4.4) for model simulations. Inset shows increased y-axis range of pre-event water proportion. (c). Subsurface storage calculated by Equation 4.5. Subsurface storage for each model is divided by its mean subsurface storage.

the base case model (Figure 4.5). The wetter initial condition had a larger streamflow than the base case, but a very similar pre-event water response to the base case.

4.3.2 *Question 2. Controls on storage-streamflow relationship*

4.3.2.1 Numerical experiments of controls on storage-streamflow relationship

Figure 4.5c shows subsurface storage as a function of time that occurred during the numerical experiments. Subsurface storage reached its pre-storm value after approximately 150,000 s in the base case model (it took more than double this time for the impervious surface simulation), but the entire simulation period is not shown so that the storm period can be illustrated more clearly in Figure 4.5. Figure 4.6 shows the relationship between streamflow (total and pre-event water) and subsurface storage for the base case model. This plot shows that the subsurface storage continued to increase slightly after the precipitation stopped and streamflow started to recede, with a hysteretic relationship between storage and both total and pre-event water streamflow. The rising limb had a higher streamflow for the same subsurface storage value as compared to the falling limb. The pre-event water did not reach the same peak as the total streamflow, but had a similar shape as total streamflow. The hydraulic head at the land surface before, during, and after the storm event is shown in Figure 4.7.

4.3.2.2 Storage-streamflow relationships using simple dynamical systems analysis

The hourly change in streamflow vs. streamflow for each watershed is shown in Figure 4.8, along with bin means, and fits to these bins. The linear plots in Figure 4.8 show that the three watersheds generally were characterized by quite different streamflow values. Dead Run had the highest streamflow values, whereas the

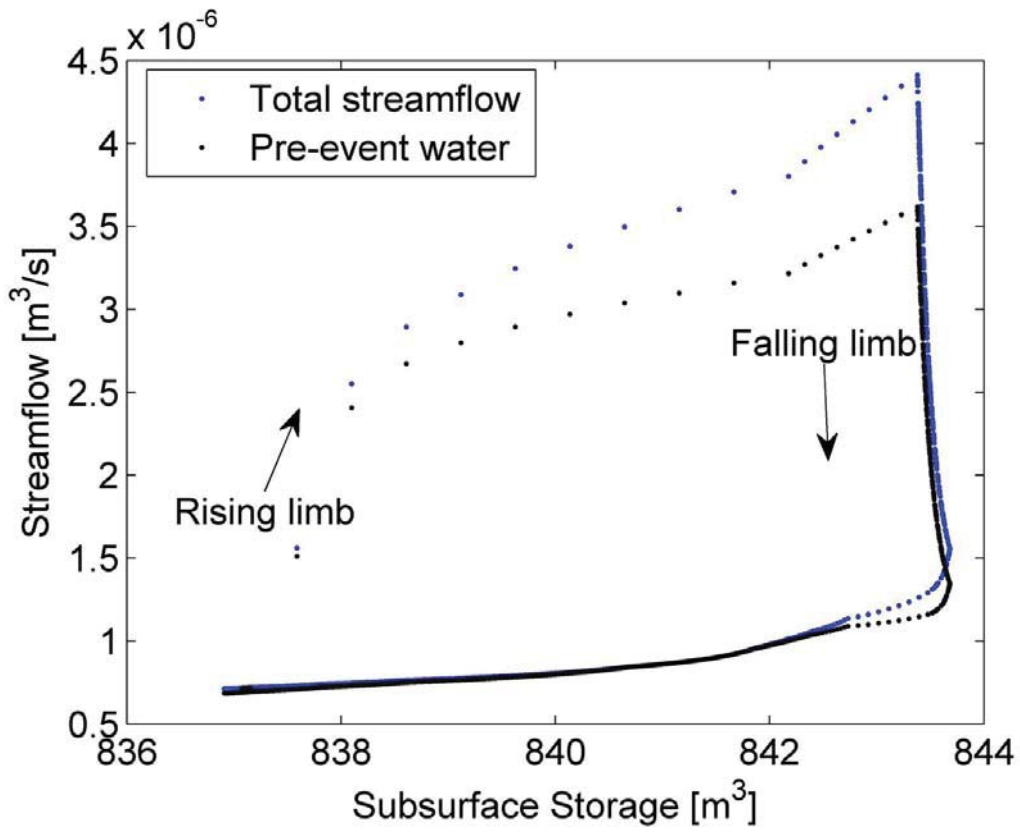


Figure 4.6. Subsurface storage vs. total and pre-event streamflow with base-case parameters in hillslope numerical experiments. Arrows indicate time, where rising limb indicates during the rain event, and falling limb indicates after the rain event.

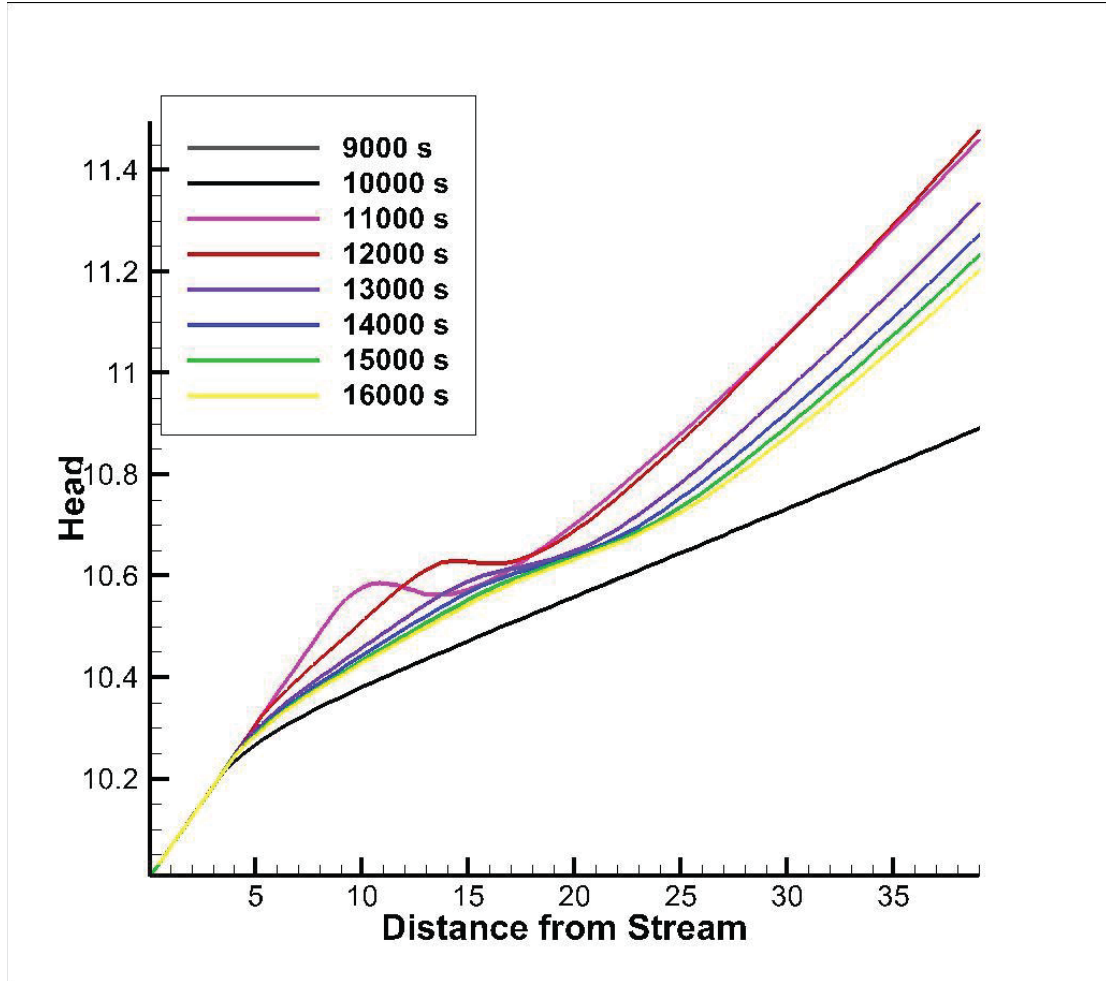


Figure 4.7. Hydraulic head (m) at the land surface vs. distance from stream (m), shown for multiple time points. Before the storm, the hydraulic head was relatively constant, so the curve for 9000 s is directly underneath the curve for 10,000 s.

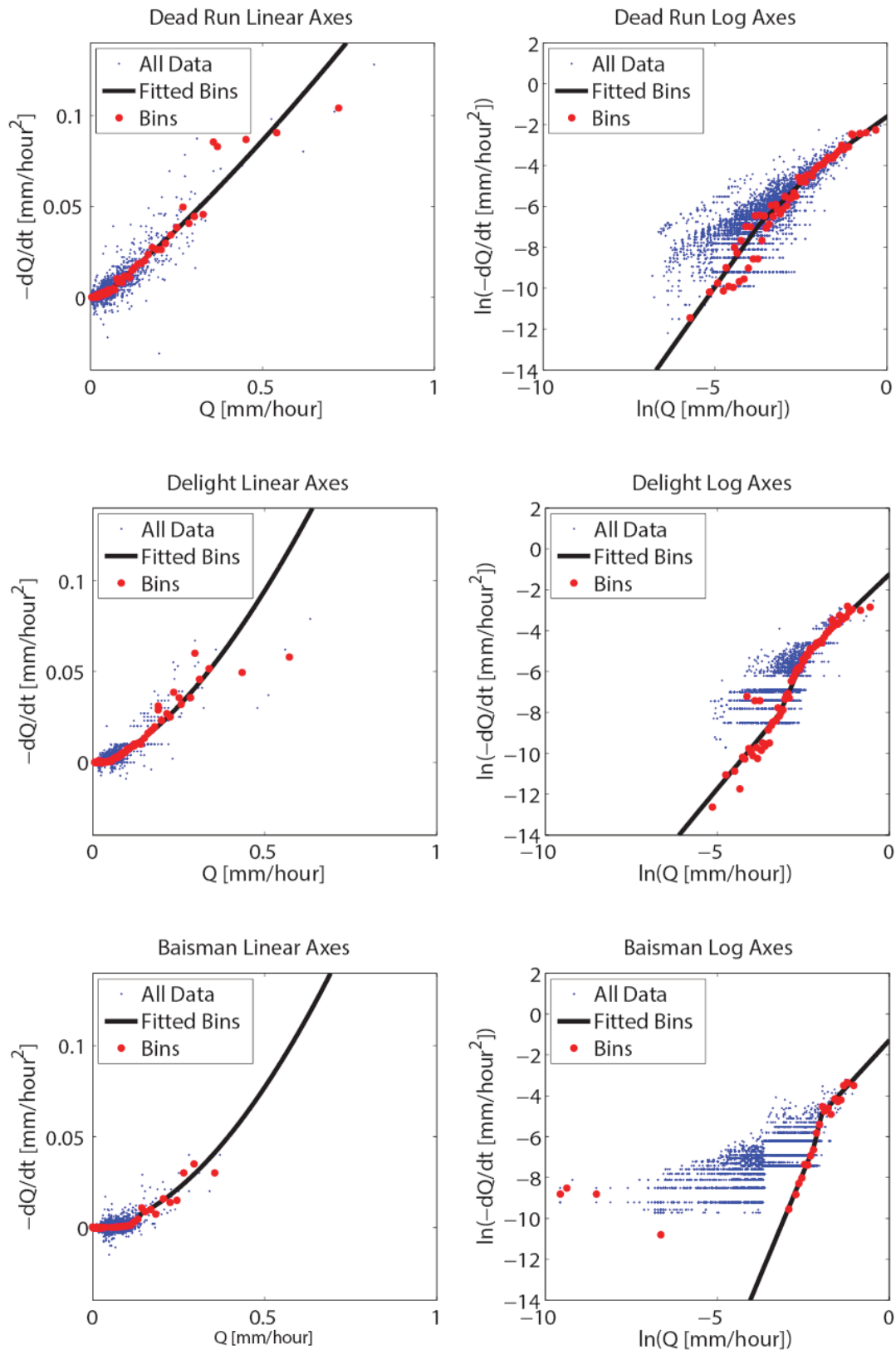


Figure 4.8. Hourly change in discharge vs. change in discharge on log and linear axes for the three study watersheds, along with bin means and bin fits.

streamflow values for Baisman Run were constrained to a narrow portion of the plot, and were always less than 0.5 mm/hour. In logarithmic space, the resolution of the data becomes evident in the plot for Baisman, as each 0.01-foot increment of stream stage represents a greater portion of the overall value as stage decreases. The resolution of the streamflow data, and multiples of this resolution, formed horizontal lines where finer changes of streamflow over an hour are irresolvable. This was somewhat apparent at Delight and Dead Run at low flows as well.

The time period of study included a drought year (2002) when Baisman Run went dry. This was not plotted on a logarithmic scale, but was included in the bins and the fits to the bins. Baisman Run had a strong diurnal cycle, which was particularly evident during dry summers. This led to some rainless night times that had increases in streamflow due to recovery from evapotranspiration pumping during the day. Therefore, there were bin means for which $-dQ/dt$ was negative for Baisman, which was why the bin fits appear to not match the logarithmic data as well as the linear data. At very low flows, $-dQ/dt$ is constrained to a narrow range around 0, and increased to positive values. These are the four outliers that can be seen in the logarithmic plot for Baisman Run that were not considered in the fit.

Figure 4.9 shows the fits of Figure 4.8 (transformed to streamflow sensitivity by dividing $-dQ/dt$ by Q), as well as the streamflow sensitivity functions reported in *Kirchner* [2009] and *Teuling et al.* [2010]. For most of the range of streamflow shown in the logarithmic plot, Dead Run, the most urban watershed, had the highest streamflow sensitivity, followed by Delight, the next most urban watershed as defined by percent impervious area. A high streamflow sensitivity at a given streamflow

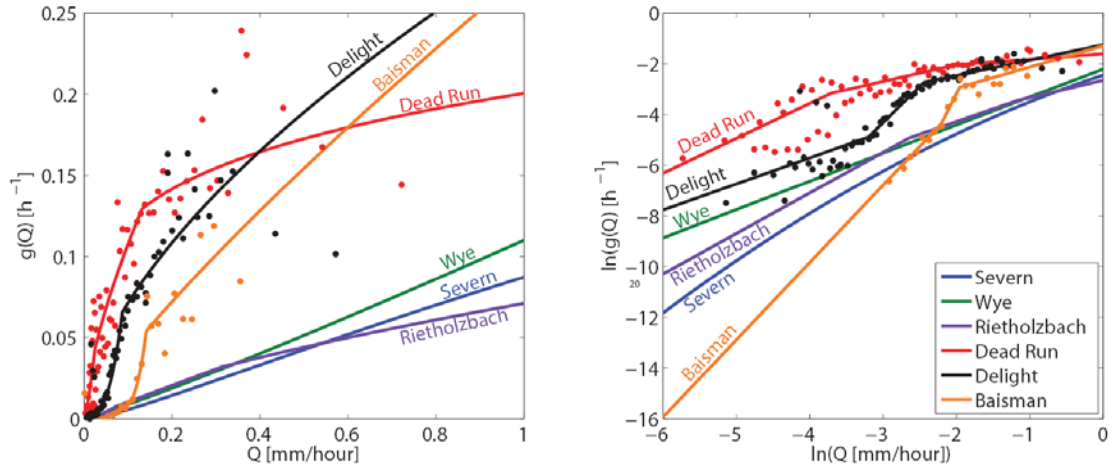


Figure 4.9. Discharge sensitivity functions vs. discharge in linear (left) and logarithmic (right) axes, along with bins for three study watersheds and previously published work [Kirchner, 2009; Teuling et al., 2010].

value means that the watershed has a high rate of change of streamflow for a given change in storage. The streamflow sensitivity of Baisman Run crossed above the streamflow sensitivity of the other watersheds at the highest streamflow values, above where we had observed data. The observed data is limited here by the method used, where we considered only the falling limb during rainless night times, meaning that the streamflow sensitivity function is calculated over a streamflow range that is limited compared to the entire range of values present in the streamflow record.

Figure 4.10 uses the integration of the streamflow sensitivity function to find the relationship between streamflow and storage for each watershed. This was derived through integration up to an additive constant (constant of integration), and therefore the relative x-position of these watersheds is arbitrary, but the relative slopes can be compared. Based on the higher streamflow sensitivity functions found in Figure 4.9, all three study watersheds had steeper storage – streamflow relationships compared to those presented in the literature for which this analysis had been carried out previously.

Lastly, we completed short streamflow simulations using the streamflow sensitivity function, spatially-variable precipitation records, and estimated evapotranspiration from the McDonogh meteorological station (shown in Figure 4.2). The overall differences in streamflow response among the three watersheds are captured by the simulated streamflow, although the streamflow of Dead Run and Baisman Run were overestimated and Delight was underestimated by the simulation (Figure 4.11).

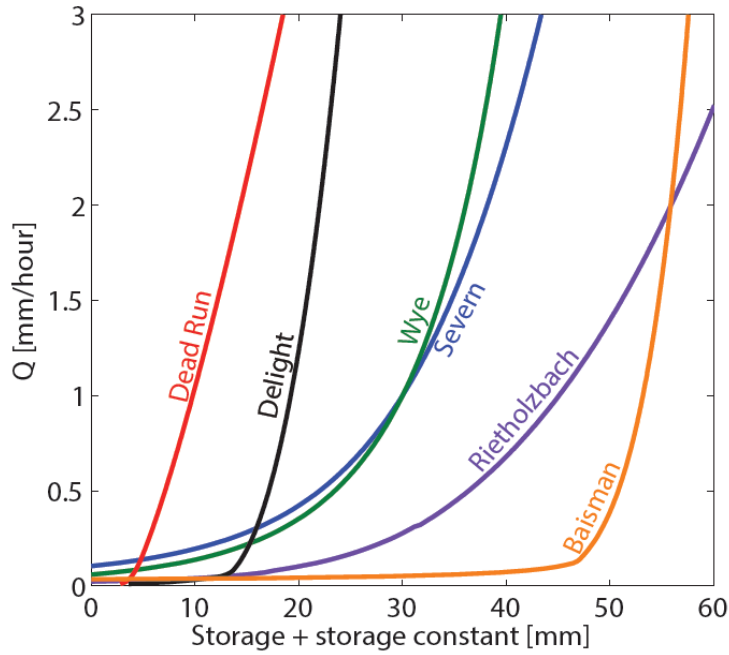


Figure 4.10. Streamflow vs. watershed storage using the simple dynamical systems analysis, where storage is determined by integration, and therefore includes an unknown constant of integration (Equation 4.3).

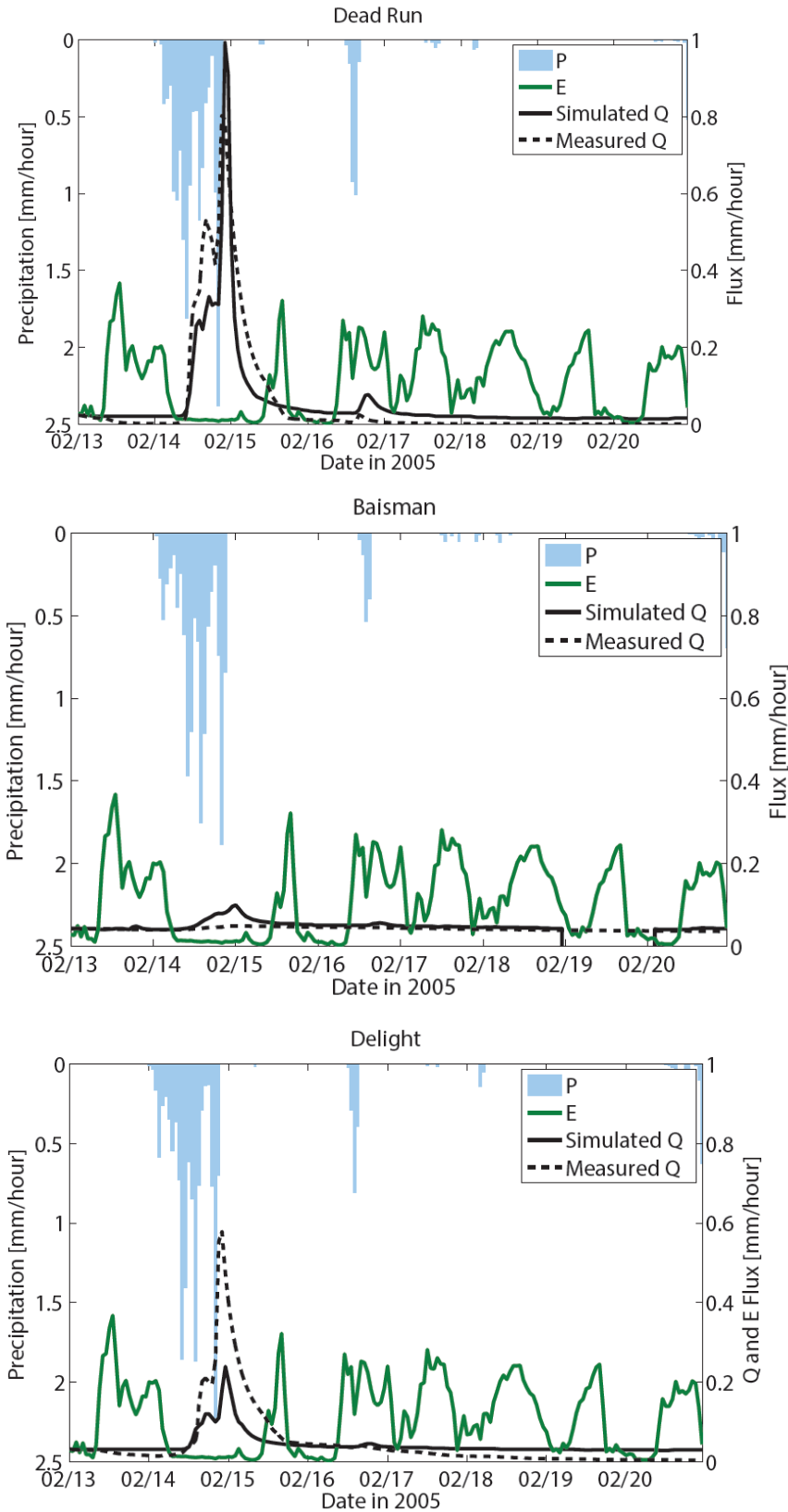


Figure 4.11. Streamflow simulation for Dead Run, Delight, and Baisman during an 8-day period in February 2005 using simple dynamical systems approach.

4.3.3 *Question 3. Relationship between storage and pre-event water proportion*

Based on Table 4.4, there was little relationship between pre-event water proportion determined using chemical hydrograph separation in Dead Run sub-watersheds and storage, which was assessed using pre-event baseflow. Figure 4.12 shows the relationship between pre-event water proportion and subsurface storage based on the hillslope numerical experiments. Just as there was a hysteretic relationship found between storage and streamflow in the hillslope model (Figure 4.6), there was a hysteric relationship found between subsurface storage and pre-event water proportion. Before the rain event began, and long after the rain event ended, the relationship between storage and pre-event water proportion had a positive slope, as less storage over time led to falling chloride values. During and directly after the rain event, the slope between storage and pre-event water proportion was negative meaning that greater storage led to lower chloride values with the influx of low chloride rain.

4.4 *Discussion*

4.4.1 *Precipitation amount as the primary control on pre-event water proportion*

Both methods used to address Question 1 indicate that precipitation volume played a primary role in controlling pre-event water proportion within a single watershed. Table 4.4 and Figure 4.3 show that out of the factors investigated, precipitation volume had the closest relationship to pre-event water proportion. Hillslope experiments also demonstrated that the variation in precipitation volume led to a greater change in pre-event water proportion compared to changes in initial storage conditions (represented by initial water table position).

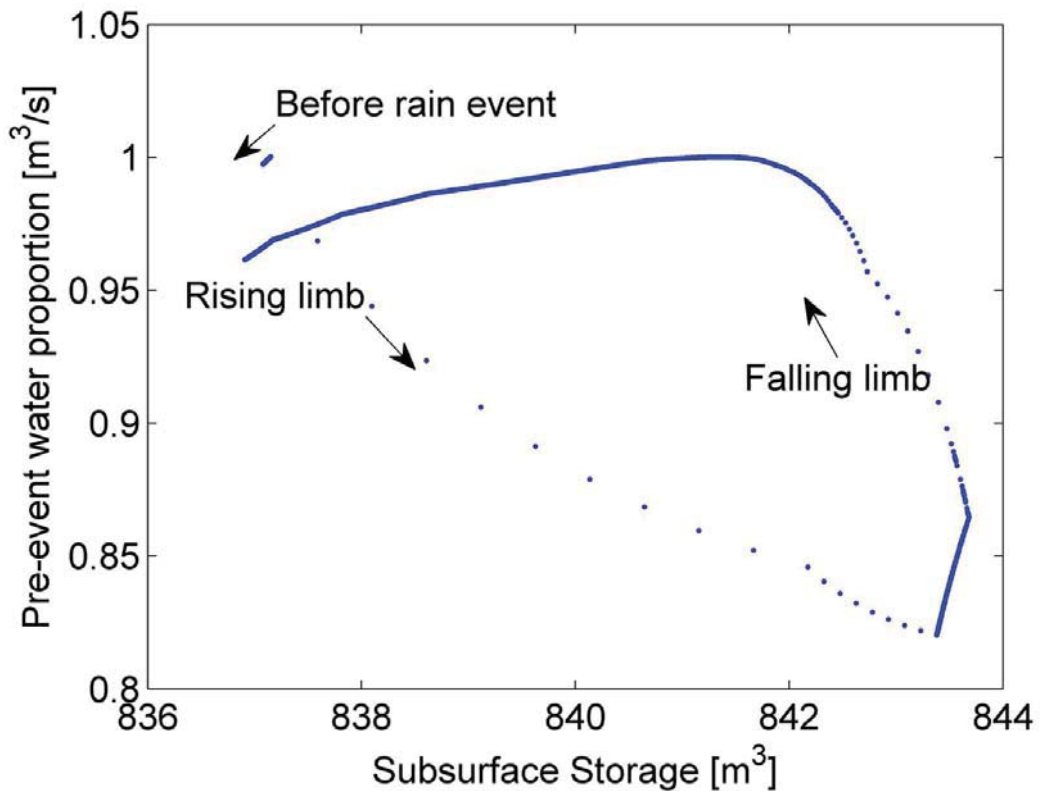


Figure 4.12. Pre-event water proportion and subsurface storage using base-case parameters in hillslope numerical experiments. Arrows indicate time, where before rain event indicates baseflow, rising limb indicates during the rain event, and falling limb indicates after the rain event.

Hillslope numerical experiments also indicated that increased impervious surface (represented by decreased hydraulic conductivity and porosity) led to greater event water in streamflow, which was expected with greater infiltration-excess overland flow directly carrying low-chloride rainwater to the stream. Chemical hydrograph separation in Dead Run also indicated that watershed position played a role in determining pre-event water proportion. Small, headwater streams generally had greater pre-event water proportion compared to larger watersheds. The variation in impervious surface cover between the watersheds was small (Table 4.2), and therefore this factor that was explored in the numerical experiments did not explain the change observed in pre-event water across watersheds. The greater contribution of pre-event water is likely explained by smaller total streamflow in headwater streams.

4.4.2 Controls on the storage-streamflow relationship

Comparing the storage-streamflow relationship (Figure 4.10) and the streamflow sensitivity functions (Figure 4.9) between the study watersheds, it appears that urban development leads to greater discharge sensitivity. The higher streamflow sensitivity in urban watersheds produced a feedback where increased storage due to precipitation events led to much larger increased streamflow, which further led to large changes in streamflow.

We found that Dead Run simulated streamflow during a relatively small storm event corresponded surprisingly well to the measured streamflow for most of the hydrograph (Figure 4.11) considering there was no calibration done beyond that presented in Figure 4.8. Furthermore, only rainless night times were used and the

data in Figure 4.8 used to make fits were from baseflow or falling limb time periods. We expected the rising limbs in urban areas, where there may be significant contributions from infiltration-excess overland flow from impervious surfaces bypassing storage reservoirs, would not be well predicted by this method. For Delight, the simple dynamical systems method overestimated streamflow, whereas for Baisman Run, this method underestimated streamflow (Figure 4.11). This method was able to reproduce the general obvious differences among watershed responses, where Baisman Run had a much more muted streamflow response to a similar precipitation event compared to Delight and Dead Run.

The storage-streamflow relationship developed using the simple dynamical systems approach did not capture the hysteretic behavior observed in the modeled hillslope experiments. As seen by comparing Figures 4.5a and 4.5c, subsurface storage responded on a much longer time scale than did streamflow. Streamflow returned to baseflow levels while subsurface storage was still high. The hysteresis between streamflow and storage may be a combination of two factors, the fast response of saturation-excess overland flow to the stream and the slow and temporally-variable groundwater contributions as a result of the formation of a groundwater mound near the stream. The hydraulic head in the shallow subsurface showed a groundwater mound that developed and dissipated as a response to the storm event (Figure 4.7). This groundwater mound led to an increase in hydraulic gradient near the stream in early storm response with increased groundwater contributions to the stream. Later, when the mound dissipated and the hydraulic gradient returned to a constant value along the hillslope, the decreased hydraulic

gradient led to smaller groundwater contributions to the stream. Both the dissipation of the groundwater mound and the cessation of overland flow contribute to the phenomenon observed where streamflow returns to baseflow values more quickly than overall hillslope subsurface storage, leading to hysteretic relationship. Previous researchers have also observed a clockwise hysteretic relationship between storage and streamflow [Kendall *et al.*, 1999; Sayama *et al.*, 2011; Xu *et al.*, 2012], where streamflow values during wetting are greater than those during drying for the same storage conditions. Investigators have called for a better understanding and representation of the hysteresis in the storage-streamflow relationship [Beven, 2006; Spence, 2010], but this hysteresis complicates the monotonic simple dynamical systems approach by Kirchner [2009] as explored by Xu *et al.* [2012].

4.4.3 Storage as a secondary control on pre-event water proportion

Both chemical hydrograph separation in small, urban watersheds (Figure 4.3) and hillslope numerical experiments (Figure 4.5), indicate that pre-storm storage conditions play a secondary role in determining pre-event water proportion in small, urban watersheds and in hillslope numerical experiments. A similar conclusion can be drawn from Figure 4.13, which shows precipitation vs. stormflow at Dead Run at Franklinton. Other studies have observed a threshold between precipitation and storm response or between storage and storm response [Evetts and Dutt, 1985; Sidle *et al.*, 2000; Li and Gong, 2002; Rezaei *et al.*, 2003; Tromp-van Meerveld and McDonnell, 2006; Zehe *et al.*, 2007; Hood *et al.*, 2007; Spence, 2007; Detty and McGuire, 2010; Graham and McDonnell, 2010; McGuire and McDonnell, 2010; Seibert *et al.*, 2011]. In contrast, in this watershed such threshold was not observed.

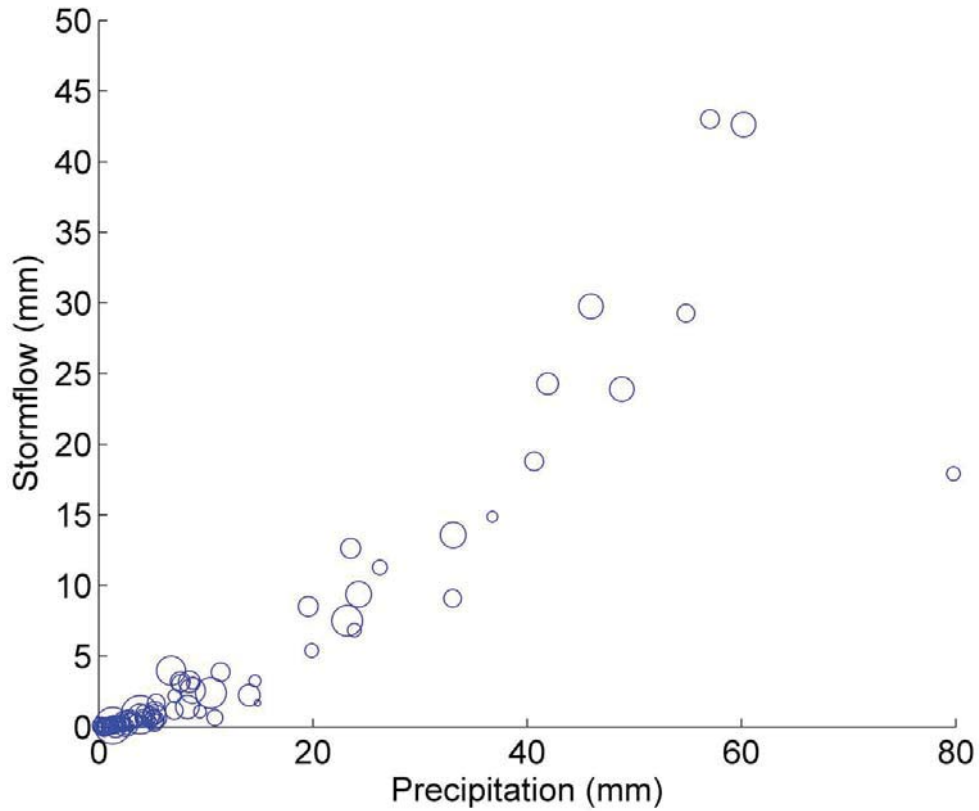


Figure 4.13. Precipitation and stormflow during storm events in Dead Run at Franklinton (DRKR). Circle size is proportional to pre-event streamflow (baseflow). Stormflow was calculated from USGS streamflow records using the straight-line method for hydrograph separation, while maintaining equal pre- and post-storm baseflow values. Precipitation values were averaged over the watershed from bias-corrected Hydro-NEXRAD radar rainfall values [Smith et al., 2012]. Only isolated storm events were used, such that a direct response between a specific precipitation event and storm response could be manually identified.

Almost every storm event produced a storm response, although the slope between precipitation and stormflow was nonlinear and became greater at high precipitation amounts. The magnitude of baseflow (size of markers in Figure 4.13) also did not seem to have an effect on the stormflow response. Precipitation volume had a tight relationship with stormflow in Dead Run at Franklinton, as it was found to be the primary control on pre-event water proportion in chemical hydrograph separation in this watershed and in hillslope numerical experiments.

There was a directional change in the relationship between storage and pre-event water proportion that was observed between recession and event periods (Figure 4.12). This was likely due to a number of factors, such as the streamflow-storage relationship being hysteretic (Figure 4.6) and the concentration of chloride in groundwater not being constant during baseflow as well as storm periods. This can be seen during baseflow (Figure 4.5b), but is not clearly observable during the storm period because the chloride signal solely from groundwater is not visible. While this phenomenon may not be commonly observed in urban groundwater systems of a much larger scale, the hillslope model here was small enough that chloride in groundwater could become depleted. There was chloride entering the hillslope model from 'regional flow' (up-gradient third-type transport boundary condition; Figure 4.1), but the chloride entering the system, even at the same concentration as the initial concentration (0.2 kg/m^3), does not completely replenish the chloride leaving through streamflow. This might be analogous to larger urban aquifers over longer periods of time. For example, during periods when road salt is not being applied, chloride leaves through groundwater contributions through streamflow, but is not being added

to the system at the same rate. Therefore, the chloride mass in the overall reservoir will decrease over time although since the reservoir is very large and is usually replenished every winter, it may not be observable in streamflow. Also, low-chloride rainwater that enters the system that remains relatively shallow may set up a concentration gradient where chloride concentration is related to flow path travel time. This did not affect our chemical hydrograph separation during the storm because the chloride concentration just before the rain event was used for the separation. Nonetheless, this non-constant pre-event tracer concentration complicates the chemical hydrograph separation method, as others have pointed out [*Gremillion et al.*, 2000; *Kirchner*, 2003].

4.4.4 Limitations of water balance based approach in an urban setting

As indicated in *Bhaskar and Welty* [2012b], the water balances of Baltimore watersheds are considerably altered compared to their nearby rural counterparts. Watershed inflows and outflows, in particular, infiltration and inflow (I&I) of groundwater and stormwater into wastewater pipes, play an important role in the Baltimore water balance. I&I and other aspects of the water balance related to urban infrastructure are not available at spatio-temporal scales similar to streamflow and precipitation. For example, monthly I&I data were provided to us by municipal governments, but I&I is commonly known to vary dramatically during storm events. Therefore, the simple dynamical systems analysis for the study watersheds was carried out in the form presented by *Kirchner* [2009], in which the water balance (Equation 4.1) was composed of precipitation, evapotranspiration, and streamflow and no urban components. The urban water balance terms that were neglected in

Equation 4.1, in particular I&I, may have affected the results that were generated using this method. If contributions of I&I were significant compared to streamflow, as was found in *Bhaskar and Welty* [2012] for two Baltimore City streams, the recession (change in streamflow for a given change in storage) may have been interpreted to be faster than was really the case due to the confounding factor of infiltration into wastewater pipes (or vice versa for exfiltration into wastewater pipes during a storm). The effect of this omission may be similar to previously researched effects of anthropogenic factors on recession constants [*Wang and Cai*, 2010].

4.5 Summary and implications

Our findings can be summarized as follows:

1. Chemical hydrograph separation using small, nested urban watersheds indicated that precipitation amount is the primary control on pre-event water proportion (Figure 4.3). Watershed position also played a role across watersheds, where smaller, headwater watersheds had greater pre-event water proportion compared to larger watersheds. The storage condition before the storm event appeared to play little role in affecting pre-event water proportion (Table 4.4) or streamflow response (Figure 4.13).
2. Hillslope numerical experiments also indicated that precipitation amount played a primary role in determining pre-event water proportion and streamflow response. Imperviousness also reduced pre-event water proportion to a value of 0.02 at the peak streamflow. Numerical experiments indicated that the relationship between storage and streamflow (Figure 4.6) was clockwise hysteretic and the

relationship between storage and pre-event water proportion (Figure 4.12) was hysteretic and not monotonic.

3. The simple dynamical systems analysis based on *Kirchner* [2009] showed that streamflow sensitivity was greater in urban watersheds characterized by a greater degree of urbanization (Figure 9). This meant that the change in streamflow for a given change in storage was larger in more urban watersheds. Simulations based on the storage-streamflow relationship developed using the simple dynamical systems analysis captured characteristics of observed streamflow (Figure 4.11).

Based on these points, we found that precipitation amount and not storage is the primary control on pre-event water proportion in urban watersheds and in the hillslope numerical experiments, in contrast to previous studies [*Burns et al.*, 2001; *Pellerin et al.*, 2008]. This leaves open the question regarding the old water paradox [*Kirchner*, 2003], in which the streamflow generation mechanism giving rise to pre-event water is unknown. The large proportion of pre-event water is particularly surprising in urban watersheds, in which the interaction between groundwater and surface-water is commonly assumed to be more limited than in other settings with more permeable surface cover. The “fill and spill” streamflow generation mechanism [*Tromp-van Meerveld and McDonnell*, 2006], also called the bedrock detention storage mechanism [*Graham and McDonnell*, 2010], proposes that the available storage reservoir needs to first be filled before subsurface saturation can become connected. After this threshold where the storage has been filled by initial precipitation, subsequent precipitation leads to spilling, and stormflow is generated. This model does not seem to apply well to the urban watersheds studied here. There

is little if any threshold in the relationship between precipitation and stormflow in Dead Run (Figure 4.13). Furthermore, this hypothesized mechanism would imply that initial storage conditions, i.e., how filled storage reservoirs are before the rain event, would play a major role in either determining the threshold or the amount of stormflow generated for the same precipitation amount; this also did not seem to be the case here (Figure 4.13).

Pre-event water largely resides in the subsurface before a rain event. The contribution of pre-event water to stormflow and the maintenance of baseflow show the presence of interaction between subsurface and surface water during both stormflow and baseflow. Pre-event water in watersheds around 50% impervious can account for more than 50% of the stormflow (Table 4.4). Here we propose a few possible reasons that groundwater and surface water are observed to be interacting in these urban watersheds, yet groundwater level (or subsurface storage) appears to play a secondary role in storm response. The storage reservoir in Dead Run may be small and therefore is almost always filled by any precipitation event, before spilling occurs. This cannot mean that the watershed soils are always near saturation, since they are not, but the reservoir of storage that contributes to streamflow may be a small portion of the watershed. Another reason may be that the conditions studied here were of relatively similar storage, whereas more variation in storage may have a larger effect on stormflow response. There may be a discrepancy between the subsurface storage that our metrics are quantifying and the subsurface storage that is affecting stormflow response. Lastly, it is possible that the interactions between groundwater and surface water are important but are unaffected by changes in storage

condition. There is some evidence for this last possibility based on the streamflow sensitivity function (Figure 4.9). Dead Run has the highest streamflow sensitivity of the watersheds studied, but that streamflow sensitivity is relatively constant over the range of observed streamflow. In comparison to the other watersheds, in Dead Run the streamflow response to an increase in storage due to precipitation is not affected much by the initial storage (or streamflow) conditions in the watershed. All the possibilities listed here are opportunities for future research.

4.6 Acknowledgements

This work benefitted from bias-corrected Hydro-NEXRAD radar-rainfall fields provided by Mary Lynn Baeck and Jim Smith (Princeton University), and meteorological data from the McDonogh station provided by Gordon Heisler and Emma Noonan Powell (USFS). We are grateful for assistance in data processing by Joshua Cole, Roxanne Sanderson, Kelsey Weaver, and Phillip Larson (UMBC CUERE). This research was supported by National Science Foundation (NSF) Grants DGE-0549469, EF-0709659, DEB-0948944, and CBET-1058038 and NOAA Grant NA10OAR431220. In addition, this work builds upon field and data infrastructure supported by the NSF Long-Term Ecological Research (LTER) Program (Baltimore Ecosystem Study) under NSF Grants DEB-0423476 and DEB-1027188.

Chapter 5: Conclusions

5.1 *Summary*

Urban development has led and continues to lead to alterations in hydrologic systems of metropolitan areas. Management of urban development such that cities retain ecosystem services provided by undeveloped landscapes requires that alteration due to urban development be well understood and quantified. Some effects on the hydrologic cycle caused by urban development are not generally known, such as the impacts on the whole water balance of urban areas, groundwater flow systems, and streamflow generation. This research addresses these gaps in knowledge. In this Chapter, I summarize the work presented in Chapters 2, 3, and 4 addressing the research questions presented in Chapter 1.

1. How does the water balance change along the urban-to-rural gradient, both in the forms and relative amounts of watershed inflows and outflows?

The forms of inflows and outflows varied between urban and rural watersheds in the Baltimore region because urban development has introduced leakage from supply pipes, lawn irrigation, and infiltration and inflow into wastewater collection pipes. Whereas natural water balance components in both rural and urban watersheds always include precipitation, evapotranspiration, and streamflow, I found that there was a greater volume of water exiting urban watersheds by wastewater pipes (565 mm/year) or streamflow (465 mm/year) as compared to evapotranspiration in urban watersheds (360 mm/year), whereas rural watersheds were evapotranspiration-dominated (830 mm/year). Precipitation was the largest inflow to urban watersheds

(1160 mm/year), although lawn irrigation (25 mm/year) and water supply pipe leakage (159 mm/year) both contributed additional water.

2. How do the magnitudes of human-induced (“urban”) water fluxes (water supply pipe leakage, wastewater infiltration and inflow, and lawn irrigation) compare to natural inflows (precipitation) and outflows (streamflow and evapotranspiration)? Which urban fluxes are most significant?

I compared the magnitudes of piped urban water balance components to natural water balance components. For two Baltimore City watersheds I&I was 131% and 110% of mean annual streamflow. Lawn irrigation and water supply pipe leakage together accounted for 11 – 21% of monthly precipitation inputs over 2001-2009. Annually, for the average of two Baltimore City watersheds, lawn irrigation and pipe leakage were 14% of total watershed inflows and I&I was 41% of total watershed outflows. Reservoir withdrawals upstream of gages were 64% (Liberty Reservoir) and 100% (T. Howard Duckett Reservoir) of annual streamflow in reservoir-containing watersheds. On average, the most significant urban component was I&I, but urban water balance components were extremely spatially heterogeneous.

3. How do urban and rural water balances vary as a function of time, both seasonally and interannually?

I observed that net inflow into urban areas was greater than that in rural areas for dry years, whereas the urban and rural net inflow converged in the wet year of 2003. The wet year behavior could be attributed to urban streamflow increases relative to rural streamflow while the evapotranspiration difference stayed about the

same compared to other years. Rural areas showed more seasonal variability in evapotranspiration than urban areas. On average, there were some modest variations in precipitation and streamflow by season, but evapotranspiration was by far the largest control of seasonal variations in the water balance, leading to corresponding seasonal storage cycles.

4. How can spatially-and temporally-variable urban input data be best discovered, processed, and synthesized for incorporation into an integrated (surface-subsurface-land-atmosphere) hydrologic model?

Synthesis of input data for distributed hydrologic modeling of undeveloped areas is already a challenging task, and is made much more complicated when evaluating urban areas. Chapter 3 provides a framework for finding potential data sources, processing urban-related data, and synthesizing with hydrogeologic data for incorporation into a coupled groundwater-surface water model. The data sets that were derived are hydrogeologic material properties, upscaled soil hydraulic conductivity, land surface slopes, representation of impervious surfaces, lawn irrigation, water supply pipe leakage, residential and municipal well withdrawals, surface water reservoir withdrawals, and infiltration and inflow into wastewater pipes. These data were derived from a range of sources, including reanalysis of data provided by municipal governments, national and local elevation, soil, and land cover datasets, state well and tax permit databases, coastal aquifer extents and thicknesses based on well borings, and previously published studies on hydraulic conductivity of various media.

5. How do reduced urban evapotranspiration, urban hardscapes, infiltration of groundwater into wastewater pipes, and other anthropogenic recharges and discharges affect subsurface storage on a regional scale?

I isolated the effect of four urban features on subsurface storage using the coupled subsurface-surface-land surface hydrologic model, ParFlow.CLM, applied to the Baltimore metropolitan area. The urban features considered, in order of increasing magnitude of change to subsurface storage, were: infiltration and inflow (I&I) of groundwater into wastewater pipes, anthropogenic recharges (water supply pipe leakage and lawn irrigation), reduced vegetative cover, and impervious surface coverage. After six months of simulation, removing I&I led to 5.1% greater total subsurface storage, removing all anthropogenic fluxes led to 3.7% greater subsurface storage, the vegetated city scenario had a 0.13% decrease in subsurface storage, and the pervious city scenario had a 0.0004% increase in subsurface storage, all referenced to precipitation minus evapotranspiration. The spatial extent and magnitude of the effects of alteration in urban features did not always correspond to the area over which these features applied. For example, we applied I&I over only 6.6% of the model domain, yet this urban feature was found to have the largest magnitude of effect on total model subsurface storage.

6. What controls the pre-event water proportion of stormflow in urbanizing areas?

Chemical hydrograph separation using six small, nested urban watersheds in the Baltimore area indicated that precipitation amount is the primary control on pre-event proportion, with greater pre-event water proportion in storms with greater

precipitation. Watershed position also played a role among watersheds, where smaller, headwater catchments had greater pre-event water proportion compared to larger watersheds. Numerical experiments using the coupled groundwater-surface water flow and transport model HydroGeoSphere applied to an idealized hillslope also indicated that precipitation amount played a primary role in determining pre-event water proportion and streamflow response. Additionally, imperviousness as quantified by low permeability of the surface model layer was found to reduce pre-event water proportion in the numerical experiments.

7. What controls the relationship between storage and streamflow along an urban-to-rural gradient?

I applied the simple dynamical systems analysis based on *Kirchner* [2009] to urban watersheds for the first time. I showed that the streamflow sensitivity function was greater in watersheds characterized by a greater degree of urbanization as defined by percent impervious surface coverage, and that simulations based on this relationship were able to represent characteristics of observed streamflow. The most urban watershed investigated (Dead Run, Baltimore, at 45% impervious surface coverage) was found to have the highest streamflow sensitivity function (greatest change in streamflow for an equal change in storage), but this value of streamflow sensitivity was more constant over the range of streamflow compared to other watersheds. This implies that the streamflow response is relatively constant across levels of initial baseflow for this watershed, and that streamflow responds strongly in Dead Run to precipitation regardless of pre-event storage. The numerical experiments indicated that the relationship between storage and streamflow was

clockwise hysteretic. Subsurface storage was found to take much longer to return to pre-storm levels compared to streamflow. Therefore, subsurface storage remained high even when streamflow had returned to baseflow levels during the falling limb, whereas on the rising limb both storage and streamflow rose together. This indicates that the dynamical systems analysis, which assumes a singular relationship between storage and streamflow, does not represent the complexity of the hysteretic relationship between storage and streamflow.

8. What is the relationship between pre-event water proportion of stormflow and watershed storage in urban areas?

Using chemical hydrograph separation, watershed storage condition was approximated by pre-event baseflow and was found to have little relationship with pre-event water proportion during the storm event. During a given event, hillslope numerical experiments indicated that the relationship between pre-event water proportion and subsurface storage was hysteretic and not monotonic. Pre-event water proportion and storage had a positive relation before and long after the storm event. In contrast, during and directly following precipitation, pre-event water proportion and storage had a negative relation.

5.2 Contributions

The above summarizes the findings from my work. These findings represent fundamental new contributions to scientific knowledge. The urban water balance has not been computed previously for Baltimore, and in general, as demonstrated in my literature review, there has been little urban water balance work carried out that quantifies each water balance component separately (as opposed to calculation by

subtraction), and there has been no work that has used the spatially-variable data sources that were used here. The work presented in Chapter 3 using ParFlow is the first application of such a complex integrated hydrologic model to an urban area, and also the first coupled groundwater-surface water study to isolate individual features of urban development through modeling. The methodology required for synthesis of disparate datasets for use in urban groundwater modeling has not been presented previously in the literature.

The few previous numerical experiments examining the relationship between pre-event water proportion and hillslope stormflow response in the literature have only considered undeveloped areas, and none have compared their results to a simple dynamical systems analysis and observed results from chemical hydrograph separation. No previous modeling studies have investigated the relationship among storage, stormflow, and pre-event water proportion.

5.3 *Recommendations for future work*

5.3.1 *Application to other cities*

Through this research, a number of avenues for future work were revealed. Both Chapter 2 and 3 focus on the Baltimore metropolitan region. The water balance and effects of urban features on storage will likely vary among cities, providing an opportunity for a fruitful cross-site comparison of urban water balances and comparisons of impact on subsurface storage of various urban features. The impact of urban development depends on the natural climate, hydrogeologic setting, as well as the form of urban development and associated infrastructure leakage, but through

cross-site comparisons there is a potential for categorizing how these features lead to varied urban effects.

5.3.2 *Implications for water quality*

The work presented here demonstrates that water mixes between the natural (un-piped) hydrologic system and the piped drinking water and wastewater systems. There is leakage out of pressurized drinking water supply pipes and significant groundwater infiltration into wastewater pipes. In this research, I have quantified the water quantity effect of the interactions between the piped, infrastructure systems and the natural system, in terms of the effects on water balance and subsurface storage. What I have not explored are the potentially considerable implications that this interaction has for water quality in urban areas. If increased infiltration of groundwater into wastewater pipes leads to less groundwater storage and lower water tables, this could mean that there is a reduction in the magnitude of fluxes between groundwater and surface water and therefore less potential for denitrification and nutrient processing. High levels of I&I also mean that wastewater pipes are more susceptible to being surcharged when a storm event occurs, leading to wastewater exfiltration and groundwater contamination. On the other hand, leakage out of pressurized drinking water pipes is contributing clean water to the urban subsurface. Overall, greater knowledge of the fluxes between groundwater and surface water and the impacts of urban development on these fluxes can aid in urban water quality management. The present work can be extended to include transport of solutes of interest, but quantifying the water fluxes is a necessary first step to quantification of the potential pollutants this water is carrying into urban water bodies.

5.3.3 *Consideration of infrastructure condition for urban water management*

Both Chapters 2 and 3 demonstrate the importance of the effect of urban infrastructure on the hydrologic system, and the close connection between groundwater and the wastewater system in Baltimore. This connection impacts the capacity of wastewater treatment facilities, as I&I makes up about 68% of wastewater volume. The connection also affects groundwater recharge and the urban water balance, and therefore efforts to mimic natural groundwater recharge or pre-development water balance conditions through local stormwater management need to consider gray infrastructure of wastewater, water, and stormwater systems. Currently, in managing urban water resources much focus is on reducing the coverage of impervious surfaces directly connected to streams. While this is critical to mitigate surface flow regime alteration, research presented in Chapter 3 shows that infrastructure such as groundwater leaking into wastewater pipes, is more significant than impervious surfaces for groundwater systems. Future research on alteration due to urban development to the hydrologic cycle should consider leakage into and out of urban infrastructure on par with the impacts of impervious surfaces. Since leakage from urban infrastructure is underground and there are at present few tools to estimate this aspect of urban development, the leakage is not as easily quantifiable as imperviousness in urban watersheds, but future research should focus on ways to better estimate leakage from/to urban infrastructure and incorporate this into hydrologic studies.

5.3.4 *Need for improved urban water and evapotranspiration data*

The water balance work presented in Chapter 2 underscored the need for better spatio-temporal quantification of evapotranspiration, and in particular for fine-scale evapotranspiration data in urban areas, as this is a large contributor to uncertainty in the water balance of both urban and rural watersheds. The piped or infrastructure components of the urban water balance were also subject to uncertainties, as well as data synthesis issues discussed below.

5.3.5 *Data access and synthesis*

The input data sets used in Chapter 2 and especially Chapter 3 required a large amount of effort to obtain and process. For example, acquiring municipal well pumping data from some municipalities necessitated public information requests and these data were often received in paper form requiring digitization. Even data sets characterizing the natural system can be difficult to assemble. Hydrogeologic data (e.g., hydraulic conductivity, porosity, and specific storage) have not been compiled nationally but rather are available piecemeal in technical reports (e.g., USGS Regional Aquifer-System Analysis (RASA) studies [*Sun et al.*, 1997]), although some efforts have been made towards compilation [*Gleeson et al.*, 2011; Maryland Coastal Plain Aquifer Information System (J. Raffensperger, USGS, personal communication, 2012)]. These data access challenges are likely to face researchers implementing hydrologic models in other cities.

In general, the discovery and synthesis of input data sets is a major hurdle in the application of hydrologic models. Data access has not kept pace with advances in other aspects of hydrologic modeling, such as increases in computer speed and

memory, improvement of codes for parallel processing, and complex coupling across components of the hydrologic cycle with the goal of earth-system simulation. The mismatch of space and time scales of readily accessible data for use in hydrologic models has been widely acknowledged [e.g., *NRC*, 1998; *CUAHSI*, 2002; *Jacobs et al.*, 2006]; however, few systems have been put in place to address this problem. The Consortium of Universities for the Advancement of Hydrologic Science, Inc. (CUAHSI) has made great strides in facilitating hydrologic data storage, access, and discovery in an integrated way [*Tarboton et al.*, 2011; *Ames et al.*, 2012], but these tools have so far focused on hydrologic time-series data typically used for calibration, not model input data such as hydrogeologic data. An additional challenge lies in obtaining legacy or “dark” data [*Heidorn*, 2008] that may be unpublished or unavailable in publicly-served electronic format. Despite difficulties in preparing model input data, hydrologic problem solving still needs to move forward using models as tools for analysis. Streamlining the synthesis of model input data will allow for time to be spent on scientific inquiry, and therefore a commitment to overcoming the data access problem is a worthy goal for the hydrologic science community.

The synthesis and processing of these disparate data sets serves as an example of the need for national compilation of existing hydrologic model input data. Although creation of national databases for hydrogeologic and urban model input data sets is a daunting task that will require investment of significant resources to achieve, the result will foster scientific advancement by allowing researchers to focus

on hydrologic questions rather than being hindered by data discovery and processing challenges.

Symbols

| | |
|-----|---|
| ET | Evapotranspiration |
| I | Irrigation of lawns within publicly served area |
| I&I | Infiltration and inflow of groundwater and stormwater into wastewater pipes through cracks and improper connections |
| L | Leakage from water supply pipes |
| P | Precipitation |
| Q | Streamflow |
| W | Well withdrawals |

Bibliography

- Achmad, G. (1991), *Simulated hydrologic effects of the development of the Patapsco aquifer system in Glen Burnie, Anne Arundel County, Maryland*, Report of investigation No. 54, Maryland Geological Survey Report of Investigation No. 54, Baltimore, Maryland.
- American Public Works Association (1971), *Excerpts from Control of Infiltration and Inflow into Sewer Systems and Prevention and Correction of Excessive Infiltration and Inflow into Sewer Systems: A Manual of Practice*, Environmental Protection Agency, Water Quality Office, Cincinnati, Ohio.
- Ames, D. P., J. S. Horsburgh, Y. Cao, J. Kadlec, T. Whiteaker, and D. Valentine (2012), HydroDesktop: Web services-based software for hydrologic data discovery, download, visualization, and analysis, *Environ. Model. Softw.*, 37, 146–156, doi:10.1016/j.envsoft.2012.03.013.
- Amoozegar, A., P. J. Schoeneberger, and M. J. Vepraskas (1991), *Characterization of Soils and Saprolites from the Piedmont Region for Waste Disposal Purposes*, Water Resources Research Institute of the University of North Carolina, Raleigh, North Carolina.
- Andreasen, D. (1999), *The geohydrology and water-supply potential of the lower Patapsco aquifer and Patuxent aquifers in the Indian Head-Bryans road area, Charles County, Maryland*, Report of investigation No. 69, Maryland Geological Survey Report of Investigation No. 69, Baltimore, Maryland.
- Andreasen, D., and T. B. Fewster (2001), *Estimation of areas contributing recharge to selected public-supply wells in designated metro core areas of upper*

Wicomico River and Rockawalking Creek Basins, Maryland, Open File Report No. 2001-02-14, Maryland Geological Survey Open File Report No. 2001-02-14, Baltimore, Maryland.

Andreasen, D., and W. Fleck (1996), *Geohydrologic framework, ground-water quality and flow, and brackish-water intrusion in east-central Anne Arundel County, Maryland*, Report of investigation No. 62, Maryland Geological Survey Report of Investigation No. 62, Baltimore, Maryland.

Andreasen, D. C. (2007), *Optimization of groundwater withdrawals in Anne Arundel County, Maryland, from the Upper Patapsco, Lower, Patapsco, and Patuxent Aquifers projected through 2044*, Report of Investigations No. 77, 107 pp, Report of Investigations, Maryland Geological Survey Report of Investigations No. 77.

Appleyard, S. (1995), The Impact Of Urban Development On Recharge And Groundwater Quality In A Coastal Aquifer Near Perth, Western Australia, *Hydrogeol. J.*, 3(2), 65–75, doi:10.1007/s100400050072.

Ashby, S. F., and R. D. Falgout (1996), A Parallel Multigrid Preconditioned Conjugate Gradient Algorithm for Groundwater Flow Simulations, *Nucl. Sci. Eng.*, 124, 145–159.

Aston, A. (1977), Water resources and consumption in Hong Kong, *Urban Ecol.*, 2(4), 327–353, doi:10.1016/0304-4009(77)90002-X.

Barnes, M., J. Cole, A. J. Miller, and C. Welty (2013), Effects of incorporating the urban stormwater drainage system in an integrated groundwater-surface water

model, 2013 CUAHSI Conference on Hydroinformatics and Modeling, July 17-19, 2013, Logan UT.

Barnes, M. C., C. Welty, and A. J. Miller (2012), Distributed Modeling with Parflow using High Resolution LIDAR Data, in *Abstract H51J-1489. Fall 2012 Meeting of the American Geophysical Union, December 3-7, 2012, San Francisco, CA.*

Barringer, T. H., R. G. Reiser, and C. V. Price (1994), Potential Effects of Development on Flow Characteristics of Two New Jersey Streams¹, *J. Am. Water Resour. Assoc.*, 30(2), 283–295, doi:10.1111/j.1752-1688.1994.tb03291.x.

Beighley, R. E., and G. E. Moglen (2002), Trend Assessment in Rainfall-Runoff Behavior in Urbanizing Watersheds, *J. Hydrol. Eng.*, 7(1), 27, doi:10.1061/(ASCE)1084-0699(2002)7:1(27).

Beven, K. (2006), Searching for the Holy Grail of scientific hydrology: $Q_{sub\ t} = H(S, R, \Delta t) A$ as closure, *Hydrol. Earth Syst. Sci.*, 10(5), 609–618.

Bhaskar, A. S., and C. Welty (2012a), Water Balances Along an Urban-to-Rural Gradient of Metropolitan Baltimore, 2001–2009, *Environ. Eng. Geosci.*, 18(1), 37–50, doi:10.2113/gseegeosci.18.1.37.

Bhaskar, A. S., and C. Welty (2012b), Water Balances Along an Urban-to-Rural Gradient of Metropolitan Baltimore, 2001–2009, *Environ. Eng. Geosci.*, 18(1), 37–50, doi:10.2113/gseegeosci.18.1.37.

- Binder, C., R. Schertenleib, J. Diaz, H.-P. Bader, and P. Baccini (1997), Regional Water Balance as a Tool for Water Management in Developing Countries, *Int. J. Water Resour. Dev.*, 13(1), 5.
- Birkle, P., V. T. Rodríguez, and E. G. Partida (1998), The water balance for the Basin of the Valley of Mexico and implications for future water consumption, *Hydrogeol. J.*, 6(4), 500–517.
- Brandes, D., G. J. Cavallo, and M. L. Nilson (2005), Base flow trends in urbanizing watersheds of the Delaware River Basin, *J. Am. Water Resour. Assoc.*, 41(6), 1377–1391.
- Burns, D., T. Vitvar, J. McDonnell, J. Hassett, J. Duncan, and C. Kendall (2005), Effects of suburban development on runoff generation in the Croton River basin, New York, USA, *J. Hydrol.*, 311(1-4), 266–281.
- Burns, D. A. (2002), Stormflow-hydrograph separation based on isotopes: the thrill is gone — what's next?, *Hydrol. Process.*, 16(7), 1515–1517, doi:10.1002/hyp.5008.
- Burns, D. A., J. J. McDonnell, R. P. Hooper, N. E. Peters, J. E. Freer, C. Kendall, and K. Beven (2001), Quantifying contributions to storm runoff through end-member mixing analysis and hydrologic measurements at the Panola Mountain Research Watershed (Georgia, USA), *Hydrol. Process.*, 15(10), 1903–1924, doi:10.1002/hyp.246.
- Buttle, J. M. (1994), Isotope hydrograph separations and rapid delivery of pre-event water from drainage basins, *Prog. Phys. Geogr.*, 18(1), 16–41, doi:10.1177/030913339401800102.

- Buttle, J. M., A. M. Vonk, and C. H. Taylor (1995), Applicability of isotopic hydrograph separation in a suburban basin during snowmelt, *Hydrol. Process.*, 9(2), 197–211, doi:10.1002/hyp.3360090206.
- Carlsson, L., and J. Falk (1977), Urban Hydrology in Sweden--An Inventory of the Problems and Their Costs, *IAHS-AISH Publ.*, 123, 478–487.
- Carroll County (2009), *Hampstead Sewer System: Preliminary Infiltration & Inflow Study*.
- Carroll County Government (2009), *Carroll County Water Demands and Availability*.
- Chapelle, F. H. (1986), A Solute-Transport Simulation of Brackish-Water Intrusion Near Baltimore, Maryland, *Ground Water*, 24(3), 304–311, doi:10.1111/j.1745-6584.1986.tb01006.x.
- City of Baltimore (2006), *Comprehensive Water and Wastewater Plan*, Department of Public Works.
- Claessens, L., C. Hopkinson, E. Rastetter, and J. Vallino (2006a), Effect of historical changes in land use and climate on the water budget of an urbanizing watershed, *Water Resour. Res.*, 42(3), doi:10.1029/2005WR004131.
- Claessens, L., C. Hopkinson, E. Rastetter, and J. Vallino (2006b), Effect of historical changes in land use and climate on the water budget of an urbanizing watershed, *Water Resour. Res.*, 42(3), doi:10.1029/2005WR004131.
- CUAHSI, H. S. S. C. (2002), *A Vision for Hydrologic Science Research*, CUAHSI Technical Report Number 1, Washington, D.C. [online] Available from: <http://www.cuahsi.org/docs/doi/CUAHSI-TR1.pdf>

- Dai, Y. et al. (2003), The Common Land Model, *Bull. Am. Meteorol. Soc.*, 84(8), 1013–1023, doi:10.1175/BAMS-84-8-1013.
- Daniel, III, C. C., D. G. Smith, and J. L. Eimers (1997), *Hydrogeology and simulation of ground-water flow in the thick regolith-fractured crystalline rock aquifer system of Indian Creek Basin, North Carolina*, U.S. Geological Survey Water-Supply Paper 2341–C, Denver, Colorado.
- DeSimone, L. A. (2004), *Simulation of Ground-Water Flow and Evaluation of Water-Management Alternatives in the Assabet River Basin, Eastern Massachusetts*, US Geological Survey SIR 2004-5114.
- Detty, J. M., and K. J. McGuire (2010), Threshold changes in storm runoff generation at a till-mantled headwater catchment, *Water Resour. Res.*, 46(7), doi:10.1029/2009WR008102.
- Deutsch, C. V., and A. G. Journel (1998), *GSLIB: Geostatistical Software Library and User's Guide*, 2nd ed., Oxford University Press, USA.
- Eiswirth, M. (2001), Hydrogeological Factors for Sustainable Urban Water Systems, in *Current problems of Hydrogeology in Urban Areas*, edited by K. Howard and R. Israfilov, pp. 159–183.
- Eiswirth, M., L. Wolf, and H. Hötzl (2004), Balancing the contaminant input into urban water resources, *Environ. Geol.*, 46(2), 246–256.
- Ek, M. B., K. E. Mitchell, Y. Lin, E. Rogers, P. Grunmann, V. Koren, G. Gayno, and J. D. Tarpley (2003), Implementation of Noah land surface model advances in the National Centers for Environmental Prediction operational mesoscale Eta model, *J. Geophys. Res.*, 108, 16 PP., doi:200310.1029/2002JD003296.

- Eshleman, K. N., J. S. Pollard, and A. K. O'Brien (1993), Determination of contributing areas for saturation overland flow from chemical hydrograph separations, *Water Resour. Res.*, 29(10), 3577–3587, doi:10.1029/93WR01811.
- Espinosa, C. A., and G. Wyatt (2007), Comprehensive Flow Monitoring Program - The Baltimore City Approach, in *Proceedings of the Water Environment Federation Session 81 through Session 90*, vol. Session 81 through Session 90, pp. 6941–6954.
- Evelt, S. R., and G. R. Dutt (1985), Effect of Slope and Rainfall Intensity on Erosion from Sodium Dispersed, Compacted Earth Microcatchments¹, *Soil Sci. Soc. Am. J.*, 49(1), 202, doi:10.2136/sssaj1985.03615995004900010040x.
- Ferguson, B. K., and P. W. Suckling (1990), Changing rainfall-runoff relationships in the urbanizing Peachtree Creek watershed, Atlanta, Georgia, *J. Am. Water Resour. Assoc.*, 26(2), 313–322, doi:10.1111/j.1752-1688.1990.tb01374.x.
- Ferguson, I. M., and R. M. Maxwell (2010), Role of groundwater in watershed response and land surface feedbacks under climate change, *Water Resour. Res.*, 46(10), n/a–n/a, doi:10.1029/2009WR008616.
- Fleck, W., and D. Vroblesky (1996), *Simulation of ground-water flow of the coastal plain aquifers in parts of Maryland, Delaware, and the District of Columbia*, Regional aquifer-system analysis, U.S. Geological Survey Professional Paper 1404-J, Washington, D.C.
- Freeze, A. R., and J. A. Cherry (1979), *Groundwater*, 1st ed., Prentice Hall.

- Freeze, R. A. (1974), Streamflow generation, *Rev. Geophys.*, 12(4), PP. 627–647, doi:197410.1029/RG012i004p00627.
- Fry, J. A., G. Xian, S. Jin, J. A. Dewitz, C. G. Homer, L. Yang, C. A. Barnes, N. D. Herold, and J. D. Wickham (2011), Completion of the 2006 national land cover database for the conterminous United States, *Photogramm. Eng. Remote Sens.*, 77, 858–864.
- Garcia-Fresca, B. (2006), Urban-enhanced groundwater recharge: review and case study of Austin, Texas, USA, in *Urban Groundwater, Meeting the Challenge. International Association of Hydrogeologists Selected Papers*, edited by K. W. F. Howard, pp. 3–18, Taylor & Francis, London, UK.
- Garcia-Fresca, B., and J. M. Sharp Jr (2005), Hydrogeologic considerations of urban development: Urban-induced recharge, *Geol. Soc. Am. Rev. Eng. Geol.*, XVI, 123–126.
- Gelhar, L. W., and C. L. Axness (1983), Three-dimensional stochastic analysis of macrodispersion in aquifers, *Water Resour. Res.*, 19(1), 161–180, doi:198310.1029/WR019i001p00161.
- Gelhar, L. W., and J. L. Wilson (1974), Ground-Water Quality Modeling, *Ground Water*, 12(6), 399–408, doi:10.1111/j.1745-6584.1974.tb03050.x.
- Genereux, D. P., and R. P. Hooper (1999), Oxygen and Hydrogen Isotopes in Rainfall-Runoff Studies, in *Isotope Tracers in Catchment Hydrology*, edited by C. Kendall and J. J. McDonnell, Elsevier Science.

- Gleeson, T., L. Smith, N. Moosdorf, J. Hartmann, H. H. Dürr, A. H. Manning, L. P. H. van Beek, and A. M. Jellinek (2011), Mapping permeability over the surface of the Earth, *Geophys. Res. Lett.*, 38(2), doi:10.1029/2010GL045565.
- Göbel, P. et al. (2004), Near-natural stormwater management and its effects on the water budget and groundwater surface in urban areas taking account of the hydrogeological conditions, *J. Hydrol.*, 299(3-4), 267–283.
- Graham, C. B., and J. J. McDonnell (2010), Hillslope threshold response to rainfall: (2) Development and use of a macroscale model, *J. Hydrol.*, 393, 77–93, doi:10.1016/j.jhydrol.2010.03.008.
- Gremillion, P., A. Gonyeau, and M. Wanielista (2000), Application of alternative hydrograph separation models to detect changes in flow paths in a watershed undergoing urban development, *Hydrol. Process.*, 14(8), 1485–1501, doi:10.1002/1099-1085(20000615)14:8<1485::AID-HYP988>3.0.CO;2-1.
- Grimm, N. B., S. H. Faeth, N. E. Golubiewski, C. L. Redman, J. Wu, X. Bai, and J. M. Briggs (2008), Global Change and the Ecology of Cities, *Science*, 319, 756–760, doi:10.1126/science.1150195.
- Grimmond, C. S. B., and T. R. Oke (1986), Urban Water Balance: 2. Results From a Suburb of Vancouver, British Columbia, *Water Resour. Res.*, 22(10), 1404, doi:10.1029/WR022i010p01404.
- Grimmond, C. S. B., and T. R. Oke (1999), Evapotranspiration rates in urban areas, *Impacts Urban Growth Surf. Water Groundw. Qual. Proc. IUGG 99 Symp. HS5, IAHS Publ. No. 259*, 235–243.

- Groffman, P. M., N. J. Boulware, W. C. Zipperer, R. V. Pouyat, L. E. Band, and M. F. Colosimo (2002), Soil Nitrogen Cycle Processes in Urban Riparian Zones, *Environ. Sci. Technol.*, 36(21), 4547–4552, doi:10.1021/es020649z.
- Hamel, P., E. Daly, and T. D. Fletcher (2013), Source-control stormwater management for mitigating the impacts of urbanisation on baseflow: A review, *J. Hydrol.*, 485, 201–211, doi:10.1016/j.jhydrol.2013.01.001.
- Hardison, E. C., M. A. O’Driscoll, J. P. DeLoatch, R. J. Howard, and M. M. Brinson (2009), Urban Land Use, Channel Incision, and Water Table Decline Along Coastal Plain Streams, North Carolina, *J. Am. Water Resour. Assoc.*, 45(4), 1032–1046, doi:10.1111/j.1752-1688.2009.00345.x.
- Harford County Department of Public Works (2007), *Harford County Water and Sewer Master Plan*.
- Heaney, J. P., R. Pitt, and R. Field (2000), *Innovative Urban Wet-weather Flow Management Systems*, CRC Press.
- Heath, R. C. (1984a), *Groundwater Regions of the United States*, U.S. Geological Survey Water Supply Paper 2242, U.S. Government Printing Office, Washington, D.C., 78 pp.
- Heath, R. C. (1984b), *Groundwater Regions of the United States*, U.S. Geological Survey Water Supply Paper 2242, U.S. Government Printing Office, Washington, D.C., 78 pp., U.S. Geological Survey Water Supply Paper 2242, U.S. Government Printing Office, Washington, D.C., 78 pp.
- Heidorn, P. B. (2008), Shedding light on the dark data in the long tail of science, *Libr. Trends*, 57(2), 280–299.

- Hess, K. M., S. H. Wolf, and M. A. Celia (1992), Large-scale natural gradient tracer test in sand and gravel, Cape Cod, Massachusetts: 3. Hydraulic conductivity variability and calculated macrodispersivities, *Water Resour. Res.*, 28(8), 2011–2027, doi:199210.1029/92WR00668.
- Hogan, D., T. Jarnagin, J. Loperfido, and K. Van Ness (2013), Mitigating the Effects of Landscape Development on Streams in Urbanizing Watersheds, *J. Am. Water Resour. Assoc.*, doi:10.1111/jawr.12123.
- Hood, M. J., J. C. Clausen, and G. S. Warner (2007), Comparison of Stormwater Lag Times for Low Impact and Traditional Residential Development, *J. Am. Water Resour. Assoc.*, 43(4), 1036–1046, doi:10.1111/j.1752-1688.2007.00085.x.
- Hopp, L., and J. J. McDonnell (2009), Connectivity at the hillslope scale: Identifying interactions between storm size, bedrock permeability, slope angle and soil depth, *J. Hydrol.*, 376(3-4), 378–391.
- Howard County (2005), *Sewer System Evaluation Survey Report: Little Patuxent Parallel Sewer Phase II-A, Howard County Capital Project S-6175*, Department of Public Works.
- Jacobs, J., W. Krajewski, H. Loescher, R. Mason, K. McGuire, B. Mohanty, A. Texas, M. G. Poulos, N. P. Reed, and J. Shanley (2006), Enhanced Water Cycle Measurements for Watershed Hydrologic Sciences Research, *Rep. Consort. Univ. Adv. Hydrol. Sci. Inc.* [online] Available from: <http://www.cuahsi.org/docs/doi/CUAHSI-HMF-WC-May2006.pdf>

- James, A. L., J. J. McDonnell, I. Tromp-van Meerveld, and N. E. Peters (2010), Gypsies in the palace: experimentalist's view on the use of 3-D physics-based simulation of hillslope hydrological response, *Hydrol. Process.*, 24(26), 3878–3893, doi:10.1002/hyp.7819.
- Jia, Y., G. Ni, J. Yoshitani, Y. Kawahara, and T. Kinouchi (2002), Coupling simulation of water and energy budgets and analysis of urban development impact, *J. Hydrol. Eng.*, 7, 302.
- Jones, J. E., and C. S. Woodward (2001), Newton-Krylov-multigrid solvers for large-scale, highly heterogeneous, variably saturated flow problems, *Adv. Water Resour.*, 24(7), 763–774, doi:16/S0309-1708(00)00075-0.
- Jones, J. P., E. A. Sudicky, A. E. Brookfield, and Y.-J. Park (2006), An assessment of the tracer-based approach to quantifying groundwater contributions to streamflow, *Water Resour. Res.*, 42, 15 PP., doi:200610.1029/2005WR004130.
- Journel, A. G., and C. J. Huijbregts (1978), *Mining Geostatistics*, Academic Press Inc.
- Kaushal, S. S., and K. T. Belt (2012), The urban watershed continuum: evolving spatial and temporal dimensions, *Urban Ecosyst.*, 15(2), 409–435, doi:10.1007/s11252-012-0226-7.
- Kaushal, S. S., P. M. Groffman, G. E. Likens, K. T. Belt, W. P. Stack, V. R. Kelly, L. E. Band, and G. T. Fisher (2005), Increased salinization of fresh water in the northeastern United States, *Proc. Natl. Acad. Sci. U. S. A.*, 102(38), 13517–13520, doi:10.1073/pnas.0506414102.

- Kendall, C., and J. J. McDonnell (1999), *Isotope Tracers in Catchment Hydrology (Developments in Water Science)*, Elsevier Science.
- Kendall, K. ., J. . Shanley, and J. . McDonnell (1999), A hydrometric and geochemical approach to test the transmissivity feedback hypothesis during snowmelt, *J. Hydrol.*, 219(3-4), 188–205, doi:10.1016/S0022-1694(99)00059-1.
- Kenny, J. F., N. L. Barber, S. S. Hutson, K. S. Linsey, J. K. Lovelace, and M. A. Maupin (2009), *Estimated Use of Water in the United States in 2005*, US Geological Survey Circular 1344. [online] Available from: <http://pubs.usgs.gov/circ/1344/>
- Kienzler, P. M., and F. Naef (2008), Subsurface storm flow formation at different hillslopes and implications for the “old water paradox,” *Hydrol. Process.*, 22(1), 104–116, doi:10.1002/hyp.6687.
- Kim, Y. Y., K. K. Lee, and I. Sung (2001), Urbanization and the groundwater budget, metropolitan Seoul area, Korea, *Hydrogeol. J.*, 9(4), 401–412.
- Kirchner, J. W. (2003), A double paradox in catchment hydrology and geochemistry, *Hydrol. Process.*, 17(4), 871–874, doi:10.1002/hyp.5108.
- Kirchner, J. W. (2009), Catchments as simple dynamical systems: Catchment characterization, rainfall-runoff modeling, and doing hydrology backward, *Water Resour. Res.*, 45(2), W02429.
- Kollet, S. J., and R. M. Maxwell (2006), Integrated surface-groundwater flow modeling: A free-surface overland flow boundary condition in a parallel

groundwater flow model, *Adv. Water Resour.*, 29(7), 945–958,
doi:16/j.advwatres.2005.08.006.

Kollet, S. J., and R. M. Maxwell (2008), Capturing the influence of groundwater dynamics on land surface processes using an integrated, distributed watershed model, *Water Resour. Res.*, 44, doi:200810.1029/2007WR006004.

Konrad, C. P., D. B. Booth, and S. J. Burges (2005), Effects of urban development in the Puget Lowland, Washington, on interannual streamflow patterns: Consequences for channel form and streambed disturbance, *Water Resour. Res.*, 41(7), doi:10.1029/2005WR004097.

Ku, H. F. H., N. W. Hagelin, and H. T. Buxton (1992), Effects of Urban Storm-Runoff Control on Ground-Water Recharge in Nassau County, New York, *Ground Water*, 30(4), 507–514, doi:10.1111/j.1745-6584.1992.tb01526.x.

Law, N., L. Band, and M. Grove (2004a), Nitrogen input from residential lawn care practices in suburban watersheds in Baltimore county, MD, *J Env Plan. Man*, 737–755, doi:10.1080/0964056042000274452.

Law, N., L. Band, and M. Grove (2004b), Nitrogen input from residential lawn care practices in suburban watersheds in Baltimore County, MD, *J. Environ. Plan. Manag.*, 47(5), 737–755, doi:10.1080/0964056042000274452.

Leopold, L. B. (1968), *Hydrology for urban land planning--A guidebook on the hydrologic effects of urban land use*, Circular 554, U.S. Geological Survey, Washington D.C.

Lerner, D. (2002), Identifying and quantifying urban recharge: a review, *Hydrogeol. J.*, 10(1), 143–152, doi:10.1007/s10040-001-0177-1.

- Li, X.-Y., and J.-D. Gong (2002), Compacted microcatchments with local earth materials for rainwater harvesting in the semiarid region of China, *J. Hydrol.*, 257(1–4), 134–144, doi:10.1016/S0022-1694(01)00550-9.
- Liu, L., and T. Guo (2003), Determining the Condition of Hot Mix Asphalt Specimens in Dry, Water-Saturated, and Frozen Conditions Using GPR, *J. Environ. Eng. Geophys.*, 8(2), 143, doi:10.4133/JEEG8.2.143.
- Low, D. J., D. J. Hippe, and D. Yannacci (2002), *Geohydrology of Southeastern Pennsylvania*, US Geological Survey Water-Resources Investigations Report 00-4166.
- Lull, H. W., and W. E. Sopper (1969), *Hydrologic effects from urbanization of forested watersheds in the northeast*, Upper Darby, PA. [online] Available from: <http://www.treesearch.fs.fed.us/pubs/23740>
- Mack, F., and R. Mandle (1977), *Digital simulation and prediction of water levels in the Magothy aquifer in southern Maryland*, Report of investigation No. 28, Maryland Geological Survey Report of investigation No. 28, Baltimore, Maryland.
- Martinez, S. E., O. Escolero, and L. Wolf (2011), Total Urban Water Cycle Models in Semiarid Environments—Quantitative Scenario Analysis at the Area of San Luis Potosi, Mexico, *Water Resour. Manag.*, 25(1), 239–263, doi:10.1007/s11269-010-9697-6.
- Maxwell, R. M., and N. L. Miller (2005), Development of a Coupled Land Surface and Groundwater Model, *J. Hydrometeorol.*, 6(3), 233–247, doi:10.1175/JHM422.1.

- Mayer, P. M., P. M. Groffman, E. A. Striz, and S. S. Kaushal (2010), Nitrogen Dynamics at the Groundwater–Surface Water Interface of a Degraded Urban Stream, *J. Environ. Qual.*, 39(3), 810, doi:10.2134/jeq2009.0012.
- McCord, J. (2009a), Aging Pipes Hamper Water Delivery, *WYPR* 881.
- McCord, J. (2009b), Aging Pipes Hamper Water Delivery, *WYPR* 881.
- McDonnell, J. J. (2003), Where does water go when it rains? Moving beyond the variable source area concept of rainfall-runoff response, *Hydrol. Process.*, 17, 1869–1875, doi:10.1002/hyp.5132.
- McDonnell, J. J., and R. Woods (2004), On the need for catchment classification, *J. Hydrol.*, 299(1-2), 2–3, doi:10.1016/j.jhydrol.2004.09.003.
- McFarland, E. R. (1997), *Ground-water flow, geochemistry, and effects of agricultural practices on nitrogen transport at study sites in the piedmont and the coastal plain physiographic provinces, Patuxent River Basin, Maryland*, US Geology Survey Water Supply Paper 2449.
- McGuire, K. J., and J. J. McDonnell (2010), Hydrological connectivity of hillslopes and streams: Characteristic time scales and nonlinearities, *Water Resour. Res.*, 46, doi:10.1029/2010WR009341.
- McNamara, J. P., D. Tetzlaff, K. Bishop, C. Soulsby, M. Seyfried, N. E. Peters, B. T. Aulenbach, and R. Hooper (2011), Storage as a Metric of Catchment Comparison, *Hydrol. Process.*, 25, 3364–3371, doi:10.1002/hyp.8113.
- Meierdiercks, K. L., J. A. Smith, M. L. Baeck, and A. J. Miller (2010), Heterogeneity of Hydrologic Response in Urban Watersheds, *J. Am. Water Resour. Assoc.*, 46(6), 1221–1237, doi:10.1111/j.1752-1688.2010.00487.x.

- Meriano, M., K. W. F. Howard, and N. Eyles (2011), The role of midsummer urban aquifer recharge in stormflow generation using isotopic and chemical hydrograph separation techniques, *J. Hydrol.*, 396(1-2), 82–93, doi:10.1016/j.jhydrol.2010.10.041.
- Meyer, S. C. (2005), Analysis of base flow trends in urban streams, northeastern Illinois, USA, *Hydrogeol. J.*, 13(5-6), 871–885, doi:10.1007/s10040-004-0383-8.
- Milesi, C., S. W. Running, C. D. Elvidge, J. B. Dietz, B. T. Tuttle, and R. R. Nemani (2005a), Mapping and Modeling the Biogeochemical Cycling of Turf Grasses in the United States, *Environ. Manage.*, 36(3), 426–438, doi:10.1007/s00267-004-0316-2.
- Milesi, C., S. W. Running, C. D. Elvidge, J. B. Dietz, B. T. Tuttle, and R. R. Nemani (2005b), Mapping and Modeling the Biogeochemical Cycling of Turf Grasses in the United States, *Environ. Manage.*, 36(3), 426–438, doi:10.1007/s00267-004-0316-2.
- Milly, P. C. D., J. Betancourt, M. Falkenmark, R. M. Hirsch, Z. W. Kundzewicz, D. P. Lettenmaier, and R. J. Stouffer (2008), Stationarity Is Dead: Whither Water Management?, *Science*, 319(5863), 573–574, doi:10.1126/science.1151915.
- Mitchell (2006), Applying Integrated Urban Water Management Concepts: A Review of Australian Experience, *Environ. Manage.*, 37(5), 589–605, doi:10.1007/s00267-004-0252-1.

- Mitchell, T. A. McMahon, and R. G. Mein (2003), Components of the Total Water Balance of an Urban Catchment, *Environ. Manage.*, 32(6), 735–746, doi:10.1007/s00267-003-2062-2.
- Morris, B., J. Rueedi, A. A. Cronin, C. Diaper, and D. DeSilva (2007), Using linked process models to improve urban groundwater management: an example from Doncaster England, *Water Environ. J.*, 21(4), 229–240.
- Mu, Q., M. Zhao, and S. W. Running (2011), Improvements to a MODIS global terrestrial evapotranspiration algorithm, *Remote Sens. Environ.*, 115(8), 1781–1800, doi:10.1016/j.rse.2011.02.019.
- Mueller, B. et al. (2011), Evaluation of global observations-based evapotranspiration datasets and IPCC AR4 simulations, *Geophys. Res. Lett.*, 38(6), doi:10.1029/2010GL046230. [online] Available from: <http://www.agu.org/pubs/crossref/2011/2010GL046230.shtml>
- Niemczynowicz,, J. (1990), A detailed water budget for the city of Lund as a basis for the simulation of different future scenarios, *Hydrol. Process. Water Manag. Urban Areas Proc. Duisberg Symp., IAHS Publ. no. 198*, 51–58.
- Nolan, K. M., and B. R. Hill (1990), Storm-runoff generation in the Permanente Creek drainage basin, west central California -- An example of flood-wave effects on runoff composition, *J. Hydrol.*, 113(1-4), 343–367, doi:10.1016/0022-1694(90)90183-X.
- NRC (1998), *Proceedings of the 1997 Abel Wolman Distinguished Lecture and Symposium on the Hydrologic Sciences, Water Science and Technology*

Board, National Research Council, *Hydrologic Sciences: Taking Stock and Looking Ahead*, The National Academies Press, Washington, D.C.

Nutter, L. J., and E. G. Otton (1969), *Ground-Water Occurrence in the Maryland Piedmont*, Report of Investigations, Maryland Geological Survey Report of Investigations 10.

O'Brien, E. L., and S. W. Buol (1984), Physical Transformations in a Vertical Soil-Saprolite Sequence, *Soil Sci. Soc. Am. J.*, 48(2), 354–357.

Park, Y.-J., E. A. Sudicky, A. E. Brookfield, and J. P. Jones (2011), Hydrologic response of catchments to precipitation: Quantification of mechanical carriers and origins of water, *Water Resour. Res.*, 47, 11 PP., doi:201110.1029/2010WR010075.

Pataki, D. E., C. G. Boone, T. S. Hogue, G. D. Jenerette, J. P. McFadden, and S. Pincetl (2011), Socio-ecohydrology and the urban water challenge, *Ecohydrology*, 4(2), 341–347, doi:10.1002/eco.209.

Paul, M. J., and J. L. Meyer (2001), Streams in the Urban Landscape, *Annu. Rev. Ecol. Syst.*, 32(1), 333–365, doi:10.1146/annurev.ecolsys.32.081501.114040.

Pellerin, B. A., W. M. Wollheim, X. Feng, and C. J. Vörösmarty (2008), The application of electrical conductivity as a tracer for hydrograph separation in urban catchments, *Hydrol. Process.*, 22(12), 1810–1818, doi:10.1002/hyp.6786.

Pickett, S. T., M. L. Cadenasso, J. M. Grove, C. H. Nilon, R. V. Pouyat, W. C. Zipperer, and R. Costanza (2001), Urban ecological systems: linking

terrestrial ecological, physical, and socioeconomic components of metropolitan areas, *Annu. Rev. Ecol. Syst.*, 127–157.

Pluhowski, E. J., and A. G. Spinello (1978), Impact of sewerage systems on stream base flow and ground-water recharge on Long Island, New York, *US Geol. Surv. J. Res.*, 6(2), 263–271.

Price, K. (2011), Effects of watershed topography, soils, land use, and climate on baseflow hydrology in humid regions: A review, *Prog. Phys. Geogr.*, 35(4), 465–492, doi:10.1177/0309133311402714.

Prince George's County (2008), *Adopted 2008 Water and Sewer Plan: Ten-Year Plan for Water Supply and Sewerage Systems*.

Rasmussen, T. C., R. H. Baldwin Jr, J. F. Dowd, and A. G. Williams (2000), Tracer vs. pressure wave velocities through unsaturated saprolite, *Soil Sci. Soc. Am. J.*, 64(1), 75–85.

Rezaur, R., H. Rahardjo, E. Leong, and T. Lee (2003), Hydrologic Behavior of Residual Soil Slopes in Singapore, *J. Hydrol. Eng.*, 8(3), 133–144, doi:10.1061/(ASCE)1084-0699(2003)8:3(133).

Roach, W. J., J. B. Heffernan, N. B. Grimm, J. R. Arrowsmith, C. Eisinger, and T. Rychener (2008), Unintended Consequences of Urbanization for Aquatic Ecosystems: A Case Study from the Arizona Desert, *BioScience*, 58(8), 715, doi:10.1641/B580808.

Rodell, M., J. S. Famiglietti, J. Chen, S. I. Seneviratne, P. Viterbo, S. Holl, and C. R. Wilson (2004a), Basin scale estimates of evapotranspiration using GRACE and other observations, *Geophys Res Lett*, 31, L20504.

- Rodell, M. et al. (2004b), The Global Land Data Assimilation System, *Bull. Am. Meteorol. Soc.*, 85(3), 381–394, doi:10.1175/BAMS-85-3-381.
- Rodriguez, F., H. Andrieu, and F. Morena (2008), A distributed hydrological model for urbanized areas-Model development and application to case studies, *J. Hydrol.*, 351(3-4), 268–287.
- Rose, S., and N. E. Peters (2001), Effects of urbanization on streamflow in the Atlanta area (Georgia, USA): a comparative hydrological approach, *Hydrol. Process.*, 15(8), 1441–1457, doi:10.1002/hyp.218.
- Roy, A. H., M. C. Freeman, B. J. Freeman, S. J. Wenger, W. E. Ensign, and J. L. Meyer (2005), Investigating hydrologic alteration as a mechanism of fish assemblage shifts in urbanizing streams, *Soc. Freshw. Sci.*
- Saar, M. O., and M. Manga (2004), Depth dependence of permeability in the Oregon Cascades inferred from hydrogeologic, thermal, seismic, and magmatic modeling constraints, *J. Geophys. Res.*, 109, 19 PP., doi:200410.1029/2003JB002855.
- Sayama, T., J. J. McDonnell, A. Dhakal, and K. Sullivan (2011), How much water can a watershed store?, *Hydrol. Process.*, doi:10.1002/hyp.8288.
- Schoeneberger, P. J., and A. Amoozegar (1990), Directional Saturated Hydraulic Conductivity and Macropore Morphology of a Soil-Saprolite Sequence, *Geoderma*, 46(1-3), 31–49.
- Seibert, J., K. Bishop, L. Nyberg, and A. Rodhe (2011), Water storage in a till catchment. I: Distributed modelling and relationship to runoff, *Hydrol. Process.*, 25(25), 3937–3949, doi:10.1002/hyp.8309.

- Semádeni-Davies, A. F., and L. Bengtsson (1999), The water balance of a sub-Arctic town, *Hydrol. Process.*, *13*(12-13), 1871–1885, doi:10.1002/(SICI)1099-1085(199909)13:12/13<1871::AID-HYP878>3.0.CO;2-M.
- Shepherd, J. M. (2005), A Review of Current Investigations of Urban-Induced Rainfall and Recommendations for the Future, *Earth Interact.*, *9*, 1–27.
- Sidle, R. C., Y. Tsuboyama, S. Noguchi, I. Hosoda, M. Fujieda, and T. Shimizu (2000), Stormflow generation in steep forested headwaters: a linked hydrogeomorphic paradigm, *Hydrol. Process.*, *14*, 369–385, doi:10.1002/(SICI)1099-1085(20000228)14:3<369::AID-HYP943>3.0.CO;2-P.
- Sidle, W. C., and P. Y. Lee (1999), Urban Stormwater Tracing with the Naturally Occurring Deuterium Isotope, *Water Environ. Res.*, *71*, 1251–1256, doi:10.2175/106143096X122357.
- Simmons, D. L., and R. J. Reynolds (1982), Effects of urbanization on base flow of selected south-shore streams, Long Island, New York, *J. Am. Water Resour. Assoc.*, *18*(5), 797–805, doi:10.1111/j.1752-1688.1982.tb00075.x.
- Simpson, G. G. (1986), Hydraulic Characteristics of Soil-Saprolite Profiles from the North Carolina Piedmont, in *Twenty-Ninth Annual Meeting Vol. XXIX*, pp. 147–154, Soil Science Society of North Carolina.
- Sklash, M. G., and R. N. Farvolden (1979), The role of groundwater in storm runoff, *J. Hydrol.*, *43*(1-4), 45–65, doi:16/0022-1694(79)90164-1.
- Smith, J. A., M. L. Baeck, G. Villarini, C. Welty, A. J. Miller, and W. F. Krajewski (2012), Analyses of a long-term, high-resolution radar rainfall data set for the

Baltimore metropolitan region, *Water Resour. Res.*, 48(4),
doi:10.1029/2011WR010641. [online] Available from:
<http://onlinelibrary.wiley.com/doi/10.1029/2011WR010641/abstract>
(Accessed 19 September 2013)

Spence, C. (2007), On the relation between dynamic storage and runoff: A discussion on thresholds, efficiency, and function, *Water Resour. Res.*, 43,
doi:10.1029/2006WR005645.

Spence, C. (2010), A Paradigm Shift in Hydrology: Storage Thresholds Across Scales Influence Catchment Runoff Generation, *Geogr. Compass*, 4, 819–833,
doi:10.1111/j.1749-8198.2010.00341.x.

Stephens, D. B., M. Miller, S. J. Moore, T. Umstot, and D. J. Salvato (2012),
Decentralized Groundwater Recharge Systems Using Roofwater and
Stormwater Runoff, *J. Am. Water Resour. Assoc.*, 48(1), 134–144,
doi:10.1111/j.1752-1688.2011.00600.x.

Stephenson, D. (1994), Comparison of the water balance for an undeveloped and a
suburban catchment, *Hydrol. Sci. J.*, 39(4), 295–307,
doi:10.1080/02626669409492751.

Stewart, J. W. (1962), *Water-yielding potential of weathered crystalline rocks at the
Georgia Nuclear Laboratory*, U.S. Geological Survey Professional Paper 450-
B, Atlanta, Georgia.

Sudicky, E. A. (1986), A natural gradient experiment on solute transport in a sand
aquifer: Spatial variability of hydraulic conductivity and its role in the

dispersion process, *Water Resour. Res.*, 22(13), 2069–2082,
doi:10.1029/WR022i013p02069.

Sudicky, E. A., W. A. Illman, I. K. Goltz, J. J. Adams, and R. G. McLaren (2010), Heterogeneity in hydraulic conductivity and its role on the macroscale transport of a solute plume: From measurements to a practical application of stochastic flow and transport theory, *Water Resour. Res.*, 46(W01508), doi:10.1029/2008WR007558.

Sun, R. J., J. B. Weeks, and H. F. Grubb (1997), *Bibliography of the Regional Aquifer-System Analysis (RASA) Program of the U.S. Geological Survey, 1978-96*, U.S. Geological Survey Water-Resources Investigation Report 97-4074, Austin, Texas. [online] Available from:
<http://water.usgs.gov/ogw/rasa/html/introduction.html>

Swenson, S., and J. Wahr (2006), Post-processing removal of correlated errors in GRACE data, *Geophys Res Lett*, 33, L08402.

Tapley, B. D. (2004), GRACE Measurements of Mass Variability in the Earth System, *Science*, 305(5683), 503–505, doi:10.1126/science.1099192.

Tarboton, D. G., D. Maidment, I. Zaslavsky, D. P. Ames, J. Goodall, R. P. Hooper, J. Horsburgh, D. Valentine, T. Whiteaker, and K. Schreuders (2011), Data Interoperability in the Hydrologic Sciences, in *Proceedings of the Environmental Information Management Conference*, pp. 132–137. [online] Available from: http://gsl.geology.isu.edu/sites/default/files/EIM-manuscript-HIS_rev3.pdf

- Teuling, A., I. Lehner, J. Kirchner, and S. Seneviratne (2010), Catchments as simple dynamical systems: Experience from a Swiss prealpine catchment, *Water Resour. Res.*, 46(10).
- Theis, C. V., R. H. Brown, and R. R. Meyer (1963), *Estimating the transmissibility of aquifers from the specific capacity of wells in Methods of determining permeability, transmissivity, and drawdown, compiled by R Bentall*, Methods of determining permeability, transmissibility, and drawdown, U.S. Geological Survey Water-Supply Paper 1536-I, Washington, D.C.
- Therrien, R., R. G. McLaren, E. A. Sudicky, and S. M. Panday (2010), *HydroGeoSphere A Three-dimensional Numerical Model Describing Fully-integrated Subsurface and Surface Flow and Solute Transport*, Groundwater Simulation Group, University of Waterloo, Waterloo, Ontario, Canada.
[online] Available from: <http://hydrogeosphere.org/hydrosphere.pdf>
- Townsend-Small, A., D. E. Pataki, H. Liu, Z. Li, Q. Wu, and B. Thomas (2013), Increasing summer river discharge in southern California, USA linked to urbanization, *Geophys. Res. Lett.*, n/a–n/a, doi:10.1002/grl.50921.
- Trapp, H., Jr., and M. A. Horn (1997), *Ground Water Atlas of the United States: Delaware, Maryland, New Jersey, North Carolina, Pennsylvania, Virginia, West Virginia*, U.S. Geological Survey Water HA 730-L.
- Tromp-van Meerveld, H. J., and J. J. McDonnell (2006), Threshold relations in subsurface stormflow: 2. The fill and spill hypothesis, *Water Resour. Res.*, 42(2), doi:10.1029/2004WR003800.

- Tromp-van Meerveld, I., and M. Weiler (2008), Hillslope dynamics modeled with increasing complexity, *J. Hydrol.*, 361, 24–40, doi:10.1016/j.jhydrol.2008.07.019.
- Trowsdale, S. A., and D. N. Lerner (2003), Implications of flow patterns in the sandstone aquifer beneath the mature conurbation of Nottingham (UK) for source protection, *Q. J. Eng. Geol. Hydrogeol.*, 36(3), 197–206, doi:10.1144/1470-9236/02-017.
- United States Census Bureau (2007), Census 2000 Summary File 1,
- Vázquez-Suñé, E., X. Sánchez-Vila, and J. Carrera (2005), Introductory review of specific factors influencing urban groundwater, an emerging branch of hydrogeology, with reference to Barcelona, Spain, *Hydrogeol. J.*, 13(3), 522–533, doi:10.1007/s10040-004-0360-2.
- Van de Ven, F. H. M. (1990), Water Balances of Urban Areas, *Hydrol. Process. Water Manag. Urban Areas Proc. Duisberg Symp.*, 21–33.
- Vepraskas, M. J., and J. P. Williams (1995), Hydraulic Conductivity of Saprolite as a Function of Sample Dimensions and Measurement Technique, *Soil Sci. Soc. Am. J.*, 59, 975–981.
- VerHoef, J., C. Welty, J. Miller, Melissa Grese, Michael P. McGuire, Roxanne Sanderson, Sujay Kaushal, and Andrew J. Miller (2011), *Preliminary Assessment of Real-Time Sensor Deployment in Baltimore Urban Watersheds*, CUERE Technical Report 2011/001, Center for Urban Environmental Research and Education, UMBC, Baltimore, MD. [online] Available from: <http://www.umbc.edu/cuere/BaltimoreWTB/>

- VerHoef, J. R. (2012), Spectral analysis of weekly and high-frequency stream chemistry data in urban watersheds, Master's thesis, University of Maryland, Baltimore County, September. [online] Available from:
<http://gradworks.umi.com/15/19/1519129.html>
- Vizintin, G., P. Souvent, M. Veselic, and B. Cencur Curk (2009), Determination of urban groundwater pollution in alluvial aquifer using linked process models considering urban water cycle, *J. Hydrol.*, 377(3-4), 261–273.
- Wagener, T., M. Sivapalan, P. Troch, and R. Woods (2007), Catchment Classification and Hydrologic Similarity, *Geogr. Compass*, 1, 901–931, doi:10.1111/j.1749-8198.2007.00039.x.
- Wagener, T., M. Sivapalan, P. A. Troch, B. L. McGlynn, C. J. Harman, H. V. Gupta, P. Kumar, P. S. C. Rao, N. B. Basu, and J. S. Wilson (2010), The future of hydrology: An evolving science for a changing world, *Water Resour. Res.*, 46(5), doi:10.1029/2009WR008906.
- Walsh, C. J. (2004), Protection of in-stream biota from urban impacts: minimise catchment imperviousness or improve drainage design?, *Mar. Freshw. Res.*, 55(3), 317–326.
- Walsh, C. J., A. H. Roy, J. W. Feminella, P. D. Cottingham, P. M. Groffman, and R. P. Morgan II (2005), The urban stream syndrome: current knowledge and the search for a cure, *J. North Am. Benthol. Soc.*, 24(3), 706–723.
- Wang, D., and X. Cai (2010), Comparative study of climate and human impacts on seasonal baseflow in urban and agricultural watersheds, *Geophys. Res. Lett.*, 37(6), doi:10.1029/2009GL041879.

- Weiler, M., and J. McDonnell (2004), Virtual experiments: a new approach for improving process conceptualization in hillslope hydrology, *J. Hydrol.*, 285(1-4), 3–18.
- Welty, C. et al. (2007), Design of an environmental field observatory for quantifying the urban water budget, in *Cities of the future: Towards integrated sustainable water and landscape management*, edited by V. Novotny and P. Brown, pp. 72–88, International Water Association, London. [online] Available from: <http://www.treesearch.fs.fed.us/pubs/18857> (Accessed 27 March 2013)
- Wiles, T. J., and J. M. Sharp (2008), The Secondary Permeability of Impervious Cover, *Environ. Eng. Geosci.*, 14(4), 251 –265, doi:10.2113/gsegeosci.14.4.251.
- Winter, T. C., J. W. Harvey, O. L. Franke, and W. M. Alley (1998), *Ground Water and Surface Water: A Single Resource*, Circular 1139, U.S. Geological Survey, Denver, Colorado.
- Wolf, L., J. Klinger, H. Hoetzl, and U. Mohrlök (2007), Quantifying Mass Fluxes from Urban Drainage Systems to the Urban Soil-Aquifer System (11 pp), *J. Soils Sediments*, 7(2), 85–95, doi:10.1065/jss2007.02.207.
- Xian, G., C. Homer, and J. A. Fry (2009), Updating the 2001 National Land Cover Database land cover classification to 2006 by using Landsat imagery change detection methods, *Remote Sens. Environ.*, 113(6), 1133–1147.
- Xu, N., J. E. Saiers, H. F. Wilson, and P. A. Raymond (2012), Simulating streamflow and dissolved organic matter export from a forested watershed, *Water Resour.*

Res., 48(5), doi:10.1029/2011WR011423. [online] Available from:

<http://doi.wiley.com/10.1029/2011WR011423> (Accessed 30 September 2013)

Yang, Y., D. N. Lerner, M. H. Barrett, and J. H. Tellam (1999), Quantification of groundwater recharge in the city of Nottingham, UK, *Environ. Geol.*, 38(3), 183–198, doi:10.1007/s002540050414.

Zehe, E., H. Elsenbeer, F. Lindenmaier, K. Schulz, and G. Blöschl (2007), Patterns of predictability in hydrological threshold systems, *Water Resour. Res.*, 43(7), doi:10.1029/2006WR005589.

Bou-Zeid, E., J. Overney, B. D. Rogers, and M. B. Parlange (2009), The Effects of Building Representation and Clustering in Large-Eddy Simulations of Flows in Urban Canopies, *Bound.-Layer Meteorol.*, 132(3), 415–436, doi:10.1007/s10546-009-9410-6.

